IMPAIRMENT-CONSTRAINED NETWORK DESIGN IN MIXED LINE RATE AND FLEXIBLE-GRID OPTICAL NETWORKS

by

Weisheng Xie

APPROVED BY SUPERVISORY COMMITTEE:

Dr. Jason P. Jue, Chair

Dr. Jorge A. Cobb

Dr. András Faragó

Dr. Andrea Fumagalli

Copyright © 2014

Weisheng Xie

All rights reserved

To my parents and family

IMPAIRMENT-CONSTRAINED NETWORK DESIGN IN MIXED LINE RATE AND FLEXIBLE-GRID OPTICAL NETWORKS

by

WEISHENG XIE, BS, MS

DISSERTATION

Presented to the Faculty of

The University of Texas at Dallas

in Partial Fulfillment

of the Requirements

for the Degree of

DOCTOR OF PHILOSOPHY IN

TELECOMMUNICATIONS ENGINEERING

THE UNIVERSITY OF TEXAS AT DALLAS

August 2014

UMI Number: 3634652

All rights reserved

INFORMATION TO ALL USERS
The quality of this reproduction is dependent upon the quality of the copy submitted.

In the unlikely event that the author did not send a complete manuscript
and there are missing pages, these will be noted. Also, if material had to be removed,
a note will indicate the deletion.

UMI 3634652

Published by ProQuest LLC (2014). Copyright in the Dissertation held by the Author.

Microform Edition © ProQuest LLC.
All rights reserved. This work is protected against
unauthorized copying under Title 17, United States Code

ProQuest LLC.
789 East Eisenhower Parkway
P.O. Box 1346
Ann Arbor, MI 48106 - 1346

ACKNOWLEDGMENTS

I would like to express the deepest appreciation to my advisor, Dr. Jason P. Jue. He is the best advisor I could ever ask for. He has given me the freedom to pursue various research projects, since the first day I entered the lab. He is one of the most creative and smartest people I know. He can always quickly capture the main points and tradeoffs in my research problems, and give constructive advice accordingly. In the past four years, I have witnessed his great patience in discussing every detail of my research topics and reviewing every word of my manuscripts. I have received his constant financial support, which helped me only to focus on my study. Without him, this dissertation would not have been possible.

I would like to convey my gratitude to Dr. Jorge A. Cobb, Dr. András Faragó, and Dr. Andrea Fumagalli for serving on my supervisory committee and for their valuable advice.

I am also grateful to my collaborators Dr. Xi Wang, Dr. Qiong Zhang, Dr. Qingya She, Dr. Paparao Palacharla, and Motoyoshi Sekiya from Fujitsu, for their insightful comments and continuous help.

My sincere thanks also go to all members in the Advanced Networks Research Lab for their cooperation and constructive suggestions during our group meetings, seminars, and discussions. In particular, I owe gratitude to Dr. Yi Zhu, Fahim Khandaker, Dr. Ankitkumar Patel, Dr. Chengyi Gao, Dr. Nipatjakorn Kannasoot, Dr. Saket Varma, Sangjin Hong, and Nannan Wang.

I want to thank my fiancée Leese for always understanding me and staying beside me.

Most importantly, I would like to thank my parents for their unconditional love, support, and sacrifice over the years. Without their support, I would not be able to achieve my goals.

June 2014

PREFACE

This dissertation was produced in accordance with guidelines which permit the inclusion as part of the dissertation the text of an original paper or papers submitted for publication. The dissertation must still conform to all other requirements explained in the "Guide for the Preparation of Master's Theses and Doctoral Dissertations at The University of Texas at Dallas." It must include a comprehensive abstract, a full introduction and literature review, and a final overall conclusion. Additional material (procedural and design data as well as descriptions of equipment) must be provided in sufficient detail to allow a clear and precise judgment to be made of the importance and originality of the research reported.

It is acceptable for this dissertation to include as chapters authentic copies of papers already published, provided these meet type size, margin, and legibility requirements. In such cases, connecting texts which provide logical bridges between different manuscripts are mandatory. Where the student is not the sole author of a manuscript, the student is required to make an explicit statement in the introductory material to that manuscript describing the student's contribution to the work and acknowledging the contribution of the other author(s). The signatures of the Supervising Committee which precede all other material in the dissertation attest to the accuracy of this statement.

IMPAIRMENT-CONSTRAINED NETWORK DESIGN IN MIXED LINE RATE AND FLEXIBLE-GRID OPTICAL NETWORKS

Publication No. _____

Weisheng Xie, PhD
The University of Texas at Dallas, 2014

Supervising Professor: Dr. Jason P. Jue

Mixed line rate (MLR) and flexible-grid optical networks are two promising network paradigms for next generation optical networks. In MLR optical networks, different optical channels may operate at different line rates and use the same amount of spectrum. In flexible-grid optical networks, besides different line rates, different optical channels can use different amount of spectrum. In both MLR and flexible-grid optical networks, the physical layer impairments will impact the signal reachability and will require regenerator placement to restore the signal quality. Different line rates and modulation formats suffer from different levels of impairments, and thus have different reachabilities. In this dissertation, we study multiple network design problems with impairment constraints for both MLR and flexible-grid optical networks.

We first study regenerator site (RS) selection problems in MLR optical networks. Given a network topology, set of requests, and different line rates' reachabilities, the problem is to select the minimum number of nodes in the network as RSs. We divide the topic into two separate research problems depending on whether routing is fixed or flexible.

Energy efficiency is an important factor that will impact the operational expenditure of a telecom network. When designing the routing and wavelength assignment approach for a set of connection requests, the placement of regenerators needs to be considered in order to increase energy efficiency. In this work, we study how to place the minimum number of regenerators in MLR optical networks, while satisfying all the requests.

Virtual optical network (VON) mapping plays a vital role in optical network virtualization. When mapping VONs, it is necessary to provision backup resources to guarantee survivability. Thus, we consider how to map VONs that can survive single link failures in flexible-grid optical networks. The objective is to minimize network equipment cost, including regenerators.

We also study the problem of cost-optimized design of flexible-grid optical networks with RS concentration. Besides transponder, regenerator, and shared infrastructure cost, the cost of RSs is also taken into consideration. The problem is to find the routing, regenerator placement, line rate and modulation format selection for each connection request with the minimum cost.

TABLE OF CONTENTS

LIST OF FIGURES

LIST OF TABLES

CHAPTER 1

INTRODUCTION

In this chapter, we first introduce the evolution of optical networks from fixed grid mixed line rate to flexible-grid optical networks. Then, we give an overview of physical impairments and optical network virtualization. We also suggest the research challenges in impairment-constrained network design. An outline of the dissertation is given in the end of this chapter.

1.1 Optical Network Evolution

1.1.1 Mixed Line Rate Optical Networks

The emergence of high-bandwidth applications and services, such as multimedia content delivery, cloud computing, data centers, and scientific computing, has led to an increased demand for higher network capacity. In order to satisfy these demands, wavelength division multiplexing (WDM) transmission systems have continued to evolve to provide higher line rates. Current core backbone networks operate primarily at line rates of 10 Gbps and 40 Gbps, while 100 Gbps systems are being deployed [2]. Emerging transmission technologies based on advanced modulation formats promise even higher rates up to hundreds of Tbps [3]. When combined with optical switching equipment, these transmission systems can be used to establish high-rate connections, or lightpaths, end-to-end across a network.

Although 100 Gbps wavelengths provide higher capacity and lower cost-per-bit in optical transponders, it may not be cost-effective to deploy only 100 Gbps wavelengths in an optical network. First, not all the connections require 100 Gbps line rate. If we use a 100 Gbps wavelength to accommodate a 10 Gbps request, then 90 Gbps of capacity is wasted. Also, the physical impairments of such high line rate are severe and limit the signal

reachabilities. Expensive regeneration equipment is needed to restore the signal quality of 100 Gbps wavelengths. For some long-distance connection requests, it is more cost-effective to use lower rate wavelengths with longer reachabilities in order to eliminate the expensive regeneration. Thus, mixed line rate (MLR) optical networks [4, 5, 6, 7, 8], in which different line rates co-exist in the same optical network infrastructure, are required to achieve high cost-efficiency.

1.1.2 Flexible-Grid Optical Networks

In MLR optical networks, all the line rates (10 Gbps, 40 Gbps, and 100 Gbps) follow the rigid ITU-T standard, in which each channel is allocated 50 GHz of spectral bandwidth [9]. However, the ITU-T fixed grid may not be sufficient to support emerging super-channels [10] that operates at line rates higher than 100 Gbps. Also, a fixed grid can lead to inefficient utilization of spectrum for low line rate channels that require less than 50 GHz of spectrum. These issues have motivated a flexible-grid paradigm that provides flexible channel spacing and flexible center frequency to each channel [11, 12, 13, 14].

Figure 1.1 shows the comparison of fixed-grid MLR optical networks and flexible-grid optical networks. In contrast to the rigid 50 GHz channel spacing in the fixed-grid optical networks, the flexible-grid optical networks utilize flexible (or elastic) spectral bandwidth for each channel. This flexible-grid paradigm promises: (a) to achieve high spectral efficiency by eliminating stranded spectrum between the fixed-grid bandwidths, (b) to support both subchannel and superchannel traffic, (c) to provide multiple line rates and modulation formats.

Optical Orthogonal Frequency-Division Multiplexing (O-OFDM) [15] is an enabling technology for flexible-grid optical networks. In O-OFDM, orthogonal optical subcarriers, which have a frequency spacing equal to the inverse of the symbol duration, are multiplexed. The bandwidth of an optical channel can be adjusted by varying number of subcarriers, and

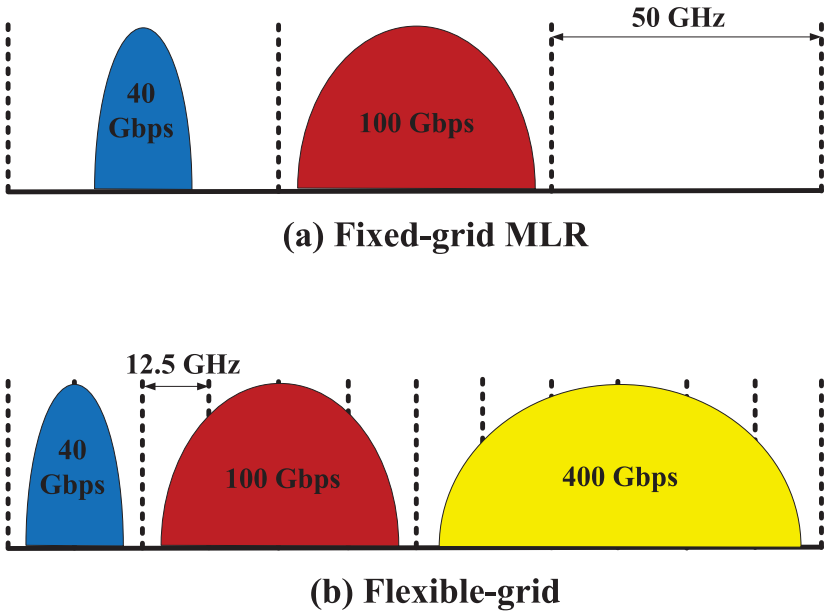

Figure 1.1. Fixed-grid MLR vs Flexible-grid

thus achieving flexible rate. To realize flexible-grid optical networks, bandwidth-agnostic wavelength crossconnects (WXCs) and bandwidth-agnostic reconfigurable optical add/drop multiplexers (ROADMs) can be equipped in the network core, while rate/modulation-format flexible transponders can be deployed at the network edge [13, 16].

1.2 Physical Layer Impairments

1.2.1 Categories of Physical Layer Impairments

In optical networks, physical layer impairments cause the signal quality to degrade as the signal propagates through the network [17, 18, 19]. Figure 1.2 shows the categories of physical layer impairments. The physical layer impairments can be generally classified into two categories: linear impairments and non linear impairments. Linear impairments affect each optical channel independently, while non linear impairments not only affect each optical channel, but also cause interferences between them. Thus, non linear impairments strongly depend on the routing and wavelength assignment (RWA) or routing and spectrum

assignment (RSA). The existing lightpaths in the network can cause interferences to a new lightpath, while a new lightpath can also degrade the signal quality of the existing lightpaths.

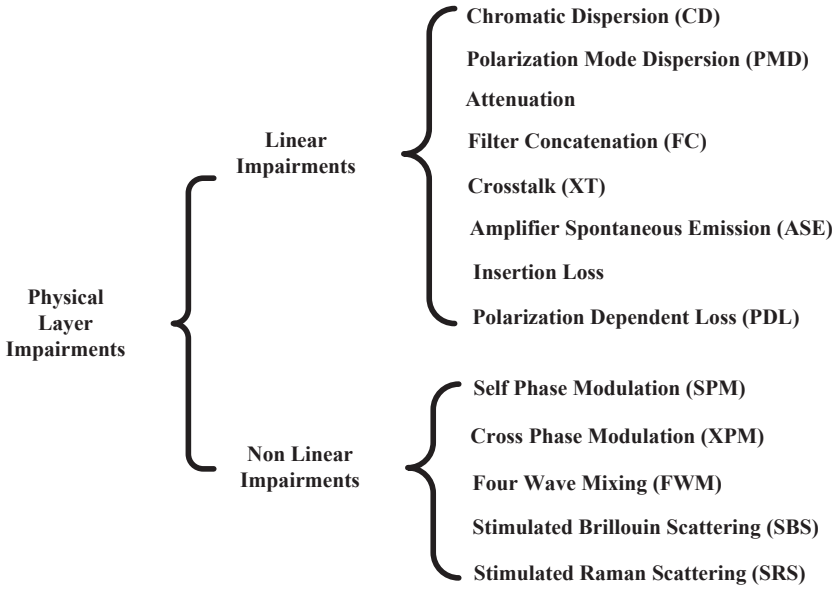

Figure 1.2. Categories of physical layer impairments

In MLR or flexible-grid optical networks, higher line rates tend to suffer greater impairments than lower line rates [4]. The distance that an optical signal can travel before its quality and the bit error rate degrade to an unacceptable level is called the *reachability*. When the receiving optical signal-to-noise ratio (OSNR) is below a certain threshold, the receiver cannot receive the data correctly. In order to guarantee successful transmission, 3R regenerators (reamplification, retiming, and reshaping) can be used in the optical network to restore the optical signal quality before the distance of the reachability.

1.2.2 Regenerator Placement

Regenerators are usually deployed in reconfigurable optical add drop multiplexers (ROADMs). Besides the function of wavelength switching, ROADMs are also capable of adding or dropping wavelengths. A certain wavelength can be dropped from an aggregate of wavelengths in

a single fiber, and the incoming traffic is re-added back to the same wavelength in the same fiber. However, in traditional ROADMs, each add/drop port is pre-assigned a fixed color (wavelength) and a fixed direction. Each add/drop port is only able to add/drop a certain color to/from a certain direction. Thus, traditional ROADMs require pre-plan of network colors and port assignments, which limit the flexibility of ROADMs. To overcome the disadvantages of traditional ROADMs, colorless and directionless ROADMs (CD ROADMs) were proposed [20]. Figure 1.3 [20] shows an example of the CD ROADM architecture. The "colorless" feature is realized by using the colorless multiplexers and de-multiplexers before the add/drop ports. The power splitters are able to broadcast the entire aggregate of wavelengths in a single fiber to all directions, and thus realizing the "directionless" feature.

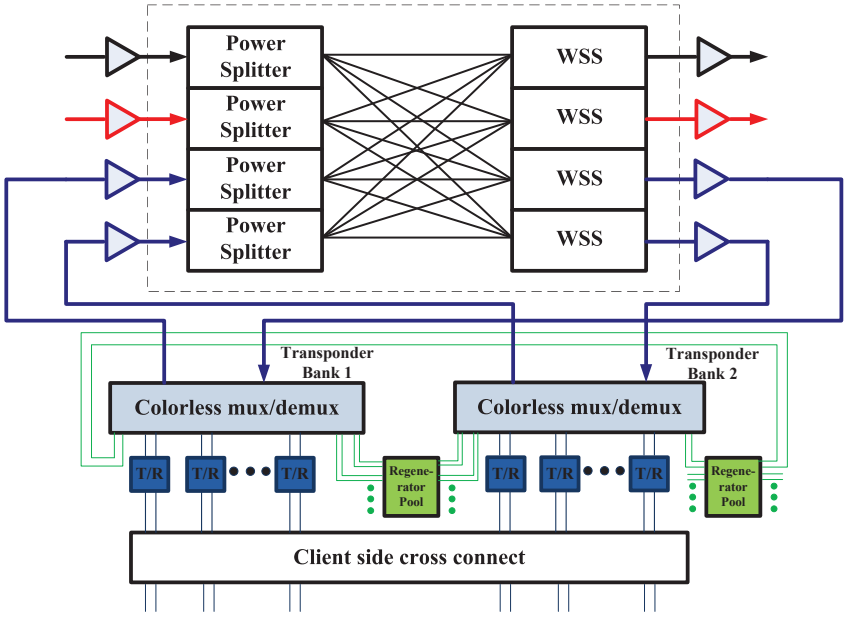

Figure 1.3. CD ROADM architecture with regenerator pools

The introduction of CD ROADMs enables the regenerators to be pre-deployed, since the regenerators are able to serve any wavelengths from any directions. Pre-deployed regenerators allow connection requests to quickly establish lightpaths, rather than requiring on-site technicians to deploy regenerators on demand. This approach greatly increases the service

deployment efficiency, which is essential in a dynamic optical network where lightpaths need to be established and torn down rapidly. Also, when a failure occurs in the network, a working path can quickly switch to its backup path, where the regenerators are pre-deployed, and thus the recovery time is shortened.

There are generally two approaches to pre-deploy regenerators in optical networks: placing regenerators in a limited number of ROADMs, which then become regenerator sites (RSs), or placing regenerators anywhere without concentration of RSs. It is shown that properly selecting a small number of RSs can potentially reduce capital expenditure (CAPEX) and operational expenditure (OPEX) compared to placing regenerators anywhere [21]. If regenerators are placed at the concentrated RSs, they are available to be used by a large number of source-destination pairs, and the number of idle regenerators will be reduced. CAPEX will then reduce due to fewer regenerators that need to be deployed. OPEX will also reduce because a small number of RSs save the management cost. Also, technicians need fewer truck rolls to deploy regenerators or maintain RSs. However, if we limit the number of RSs too much, some connection requests may have to choose long paths in order to reuse the limited number of RSs. On the contrary, if we place regenerators anywhere without concentration of RSs, each connection request can simply choose its shortest path and use regenerators only when its path distance reaches the optical signal's reachability limit.

1.3 Optical Network Virtualization

The emergence of cloud-based services coupled with big data has motivated the need for a dynamic computing and networking infrastructure that is capable of supporting a wide range of high-bandwidth heterogeneous applications. A key concept in the realization of such an infrastructure is the virtualization of computing and networking resources with the ability to provision resources on-demand to create application-specific virtual networks [22, 23]. The process of allocating the physical network's resources to the virtual networks is called virtual

network mapping or virtual network embedding [24], in which each virtual node is mapped to a physical node, while each virtual link is mapped to one or more paths in the physical network.

Optical networks will play a vital role in next-generation virtual network infrastructures to meet the challenges imposed by bandwidth intensive applications and services, such as cloud-based services, content distribution, and large-scale distributed scientific computing. In virtual optical networking, virtual optical networks (VONs) are composed through the partitioning or aggregation of physical optical network resources, such as ROADMs, transponders, regenerators, fiber links, wavelengths, and spectrum slices [25, 26]. In optical network virtualization, VON mapping is to assign the required resources of a VON to the physical optical network components. A VON node is mapped to a node in the physical optical network, while a VON link is mapped to an optical path in the physical optical network. Note that a VON node may have multiple candidate physical nodes, because multiple nodes in the physical network may provide the same applications or services. Figure 1.4 shows an example of VON mapping over the physical optical network, where the optical network serves the IP traffic.

Network virtualization can be supported in a network through the use of appropriate control and management mechanisms. Examples of such mechanisms include multiprotocol label switching (MPLS), generalized multiprotocol label switching (GMPLS), and OpenFlow [27]. MPLS operates between layer 2 and layer 3, and it enables the establishment of virtual circuits, also known as label switched paths (LSPs), over a packet-switched network. MPLS can be used in the establishment and deployment of virtual private networks (VPNs). GMPLS extends MPLS to support the establishment of circuits over circuit-switched networks and can be used to establish lightpaths for a virtual topology in a wavelength-routed optical network. OpenFlow is a mechanism that enables programmability of the forwarding plane in switches or routers. This programmability allows for the separation of the control

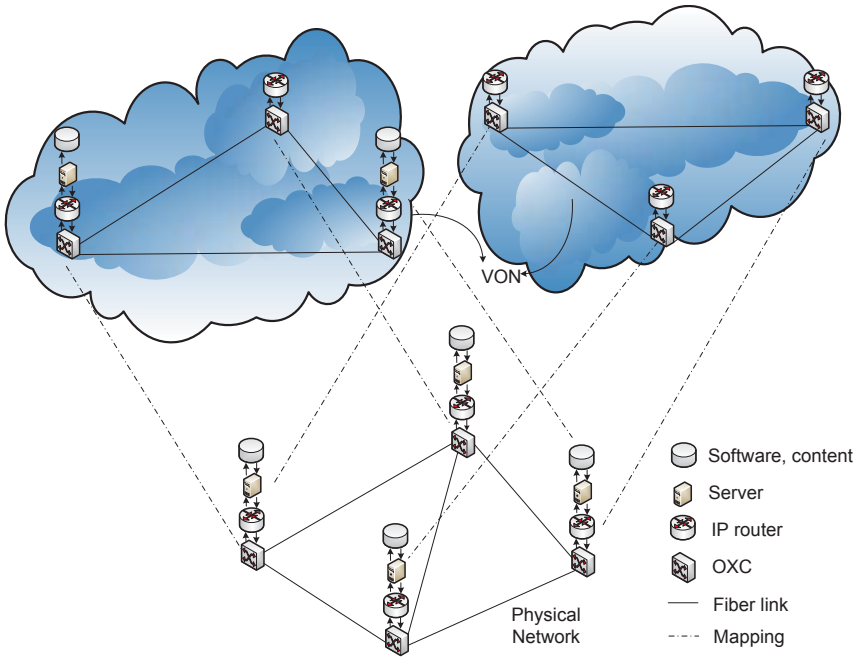

Figure 1.4. VON mapping over physical optical network

plane and data plane in a switch and also provides a mechanism for slicing and isolating traffic in packet-switched networks. The OpenFlow concept can also be extended to the optical network layer as a mechanism to provision virtual optical paths [28, 29]. OpenFlow is viewed by many as a key enabler for software defined networking (SDN) [30].

An important issue in VON design is that of survivability. Since a single failure in the physical infrastructure may disrupt multiple virtual links or nodes, it is important that appropriate measures be taken to protect the virtual network against such failures. Existing optical network protection mechanisms typically involve the provisioning of backup resources along paths, segments, or links that are disjoint from the path of the working connection. Both the working lightpaths and the backup lightpaths suffer from physical layer impairments, and thus regenerators may be needed to restore the signal quality. The mapping of VONs over a physical optical network that is subject to failures of optical equipment and various physical layer impairments thus introduces additional constraints compared to traditional virtual network mapping problems.

1.4 Research Problems

In this section, we briefly introduce the research problems in impairment-constrained network design. A set of the research problems are studied under MLR optical networks, and the other set of research problems are studied under flexible-grid optical networks. In each of these two network paradigms, we either concentrate the regenerators into RSs or place regenerators anywhere without concentrating RSs. Figure 1.5 shows a categorization of the research problems in this dissertation.

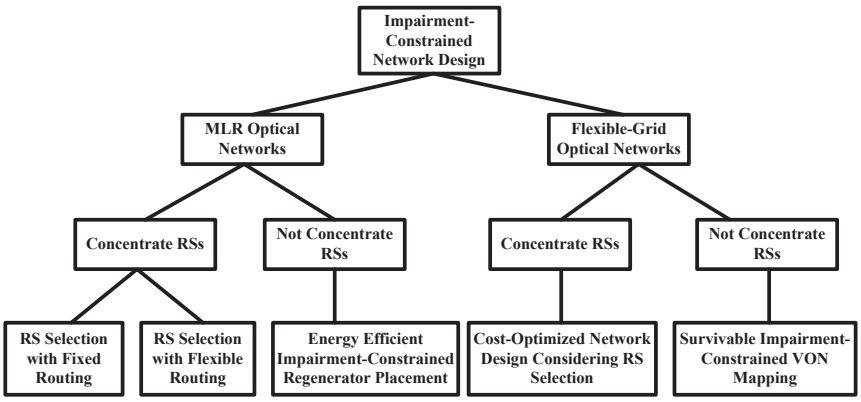

Figure 1.5. Categories of research problems in this dissertation

1.4.1 RS Selection for MLR Optical Networks with Fixed Routing

In the first research problem, we study how to select RSs in MLR optical networks, when routing is given with each connection request. Since concentrating RSs may reduce CAPEX and OPEX, our design objective is to minimize the number of RSs while satisfying all the connection requests.

In this research problem, a set of connection requests are given, and for each request, we know the source, destination, required line rate, and routing. The reachability is measured in terms of the maximum hop counts the optical signal can travel without regeneration, and different line rates have different reachabilities. We need to find the minimum number of

network nodes to serve as RSs, such that: 1) all the requests are assigned their requested line rate; and 2) along any path, the distance without regeneration cannot exceed the corresponding line rate's reachability.

The RS selection for single line rate (SLR) optical networks with fixed routing has been proved to be NP-hard in [31]. Since SLR is a special case of MLR when only a single line rate is available, our problem is also NP-hard. Thus, instead of finding an optimal algorithm, we design approximation and heuristic algorithms to solve the problem. An integer linear programming (ILP) model can also be formulated to solve the problem on small-scale networks.

Besides designing algorithms and an ILP to find minimum number of RSs, another problem is to study how the RSs are distributed in the network. We show the probability of each node being chosen as a RS, under large number of experiments, and then suggest a way to select RSs in MLR optical networks.

1.4.2 RS Selection for MLR Optical Networks with Flexible Routing

In the second research problem, we study the RS selection problem in MLR optical networks, when routing is not given with each connection request. Compared with fixed routing, the number of RSs may be further reduced when routing is flexible.

In this research problem, for each connection request, we know its source, destination, required line rate, and the number of required line rate's wavelengths. We are also given a set of reachabilities of different line rates. Reachability is measured as the maximum distance the optical signal can travel without regeneration. We have two different problems based on two different design objectives.

The first objective is to minimize the number of RSs in the network. However, the number of regenerators may increase when the RSs are concentrated, since some requests have to choose longer paths in order to reuse the existing RSs. If the cost of a regenerator is

comparable to the cost of a RS, then we cannot neglect the increasing number of regenerators. Thus, we have the second problem whose objective is to minimize the combined cost of RSs and regenerators. For this objective, we assume the cost of a RS and the cost of different line rate's regenerators are given. In [31], the RS selection problem for SLR optical networks with flexible routing is proven NP-hard, which implies that our problems are also NP-hard. Thus, we design heuristic approaches and formulate ILPs to solve the problems.

1.4.3 Energy-Efficient Impairment-Constrained Regenerator Placement in MLR Optical Networks

Recent studies have shown that communication networks account for up to 10% of the world-wide power consumption [32], and that the power usage of the US network infrastructure (mostly optical networks) is between 5 to 24 TWh/year or \$0.5-2.4B/year [33]. Thus, energy efficiency has to be taken into consideration when designing an optical network. Regenerators and transponders consume a large portion of the total energy in an optical network. Therefore, we wish to place as few regenerators as possible and choose proper line rates for lightpaths in order to minimize the energy consumption.

In the third research problem, we aim at minimizing the energy consumption of transponders and regenerators in MLR optical networks. We are given a graph representing the optical network. The transponders and regenerators are placed at the nodes of the graph. Each link of the graph represents a fiber, which contains certain number of wavelengths. We are also given a set of connection requests. For each connection request, we know the source, destination, and the required traffic demand. A set of available line rates is given. For each line rate, we know the energy consumption of a transponder and a regenerator of this line rate's wavelength.

We need to find a set of wavelengths to accommodate each connection request, and the proper line rate for each wavelength. We also need to find the RWA for each connection

request, and place regenerators along the path if needed. There are several constraints we need to guarantee. The first constraint is traffic constraint. The combined traffic of the wavelengths that are assigned to a connection request can not be smaller than the required traffic demand. The second constraint is the wavelength constraint, which means the total number of occupied wavelengths on any link cannot exceed this link's wavelength capacity. The third constraint is the rate constraint. The total traffic which goes through one wavelength cannot exceed the line rate for this wavelength. The last constraint is the impairment constraint, which specifies that along any path, the length of each segment without regenerators should not exceed the reachability limit.

1.4.4 Survivable Impairment-Constrained VON Mapping in Flexible-Grid Optical Networks

The fourth research problem we consider is survivable VON mapping in flexible-grid optical networks with impairment constraints. Survivability is a critical issue in optical network virtualization, especially when the VONs are running critical applications. Unlike virtual network mapping in Layer 2/3 networks, VON mapping needs to consider the placement of regenerators under impairment constraints. Thus, how to map VONs in flexible-grid optical networks under survivability and impairment constraints becomes an important research problem.

In this research problem, we are given a physical optical network. Each physical node is a ROADM which can be deployed with transponders and regenerators, and each physical link is a fiber with certain distance. A VON is given. Each virtual node is given a set of candidate physical nodes, where the applications or services are located, and each virtual node has to be mapped to one of its candidate physical nodes. Each virtual link is given with an aggregated traffic amount. In this work, we assume the VON can survive single link failures in the physical optical network. Thus, for each virtual link, we need to find two link-disjoint paths, based on the assumption that dedicated protection is provided.

The design objective is to minimize the total equipment cost for the VON. The equipment cost includes the transponder cost, regenerator cost, and shared infrastructure cost. The shared infrastructure includes fiber, spectrum, amplifiers, etc. Thus, we are also given the unit costs of transponders and regenerators of different line rates and modulation formats, and the unit cost of infrastructure. The reachabilities under different line rates and modulation formats are given, which are measured as the maximum distances the optical signal can travel without regeneration.

To solve the problem, we need to find the node mapping and link mapping for the given VON. We also need to find a set of optical channels and determine the line rate and modulation format for each optical channel to satisfy the traffic demand of each virtual link. There are some constraints we need to guarantee when mapping the VON. The first constraint is the node mapping constraint. We assume that each virtual node can only be mapped to a physical node specified in its set of candidate nodes, and that no two virtual nodes can be mapped to the same physical node. The second constraint is the survivability constraint. Each virtual link is mapped to two link-disjoint paths. Also, each path has enough equipment and bandwidth to support the required capacity of the virtual link. The last constraint is the impairment constraint, which specifies that the optical signal cannot travel the distance longer than its reachability without regeneration.

1.4.5 Cost-Optimized Design of Flexible-Grid Optical Networks Considering RS Selection

Cost-optimized network design is a critical research problem in flexible-grid optical networks. Traditionally, network cost mainly includes transponder cost, regenerator cost, and shared infrastructure cost. However, the selection of RSs may effect the total network cost, since concentrating RSs may decrease CAPEX and OPEX. Thus, in the fifth research problem, we study how to design a flexible-grid optical network to satisfy a set of connection requests with minimum cost, when the cost of RSs is considered.

We are given a ROADM network, where each node can be placed with transponders and regenerators, while each link is a fiber with certain distance. For each connection request, we know its source, destination, and the required traffic demand. We are also given with a set of line rates, their corresponding reachabilities, transponder costs, regenerator costs, and channel widths. The cost of a RS and the unit infrastructure cost are also given.

The design objective is to minimize the network cost, which includes transponder cost, regenerator cost, RS cost, and shared infrastructure cost. We need to find: (1) the line rate selection for each connection request; (2) the routing for each optical channel; (3) the regenerator placement and RS selection. There are two constraints we cannot violate. One is the traffic constraint, which means, for each connection request, the combined traffic of the assigned optical channels can not be smaller than the required traffic demand. The other constraint is the impairment constraint, which specifies that the length of each segment without regenerators does not exceed the corresponding line rate's reachability limit.

1.5 Outline of the Dissertation

The rest of this dissertation is organized as follows. In Chapter 2, a detailed review of related works and motivations of our problems are discussed. In Chapter 3, the RS selection problem is studied in MLR optical networks with fixed routing. In Chapter 4, we present the work on RS selection in MLR optical networks with flexible routing. In Chapter 5, the energy-efficient MLR optical network design is described. In Chapter 6, we focus on the VON mapping in flexible-grid optical networks with impairment constraints. In Chapter 7, we discuss the cost-optimized design of flexible-grid optical network considering RS selection. In Chapter 8, conclusive remarks of the full dissertation are given.

CHAPTER 2

LITERATURE SURVEY AND MOTIVATIONS

In this chapter, we review contemporary research related to impairment-constrained optical network design. To the end of each problem space, we provide the necessary motivations behind our research problems.

2.1 Research in Impairment-Constrained Regenerator Placement

The work on impairment-constrained regenerator placement can be categorized as: regenerator placement without concentration of the RSs and regenerator placement with concentration of the RSs.

A group of papers considers regenerator placement under different objectives without concentrating RSs. Among these papers, a group of papers [34, 35, 36, 37, 38, 39, 40] considers placing O/E/O 3R regenerators only. The work in [34] studies how to place regenerators to satisfy multiple sets of requests, such that different sets of requests can share a set of regenerators. The work in [35] and [36] jointly consider the placement of regenerators with RWA, with the objective of minimizing the number of required regenerators and satisfying as many connection requests as possible, given a limited number of wavelengths. In [37], the authors study the problem of establishing a light-tree and assigning wavelengths with the objective of minimizing the number of regenerators. In [38], Shen *et al.* explore the physical layer heterogeneity of optical networks and develop heuristic to minimize the number of regenerators under physical layer heterogeneity. The work in [39] studies how to place regenerators and grooming equipment to minimize the total equipment cost under both dedicated and shared connection-level protection. In [40], the authors study the 3R regenerator placement in MLR

optical networks with the objective of minimizing the total energy consumption. Another group of papers [41, 42, 43] considers mixed regenerator placement, where all-optical 2R (reamplification and reshaping) regenerators are used to partially replace 3R regenerators. In [41], Zhu *et al.* show that using the 2R regenerators can greatly save the energy cost in offline network planning scenarios. They also compare the performance of their proposed algorithms in terms of blocking probability in online provisioning. Their work is extended in [42], where the authors study the mixed regenerator placement problem with survivability constraint. In [43], the authors address the 2R/3R regenerator placement problem with the objective of minimizing the network cost.

Another group of previous works attempts to concentrate the RSs when placing regenerators in SLR optical networks. In [44], it is proved that the RS selection problem is NP-complete when routes are not given with each source-destination pair, and some heuristic approaches are proposed. In [31], the RS selection problem is considered under four scenarios, depending on whether or not route is given with the request, and whether or not there is a limit on the number of regenerators at each node. It proves that the RS selection problem is NP-complete even if routes are given with each source-destination pair, and that the problem is not approximable when there is a given bound on the number of regenerators that can be placed in a single node. In [45, 46], the RSs are concentrated subject to a constraint that every source-destination pair doesn't use more than the minimum number of regenerators of this s-d pair. A greedy heuristic approach is proposed to solve the problem. The work in [47] studies how to select RSs for providing any-to-any optical connectivity when each node pair has only one path to choose; in [48], the work is extended to consider multiple paths, that is, every node pair can choose a path from multiple path candidates. In [49], protection requirements are considered when selecting RSs. The authors try to minimize the number of RSs, subject to the constraint that every s-d pair has two disjoint paths. In [50] and [51], the authors try to minimize the number of required regenerators and concentrate them in a limited number of RSs.

There are very limited works studying RS selection in MLR optical networks. In [52], the authors address the problem of minimizing the combined cost of RSs, optical switch ports, and regenerators in MLR waveband optical networks.

Different from the papers on regenerator placement without concentrating RSs, we consider how to concentrate the RSs in MLR optical networks. We will show that the number of RSs can be greatly reduced while hardly increasing the number of regenerators. For the research work on RS selection in SLR optical networks, their proposed approaches either cannot be applied to the MLR optical network directly, or cannot achieve good performance under MLR optical networks. In our work, we design approaches for MLR optical networks with different reachabilities, which makes the problem more complex. For the existing research work on RS selection in MLR optical networks [52], their work is specifically for waveband optical networks. Also, they only propose heuristic approaches without performance guarantees. In our work, besides heuristics, we give approximation algorithms to solve the RS selection problem in general MLR optical networks.

2.2 Research in Energy-Efficient Optical Networks

A group of previous works attempts to minimize energy cost by routing requests and provisioning resources in a manner that maximizes idle network components, which can be switched off or placed in a low-power mode [53, 54, 55, 32, 56]. In [53], the authors try to maximize the number of idle line cards in low demand scenarios to save energy in IP-over-WDM networks. In [54], an approximate traffic model is formulated, and the power consumption exactly follows the traffic demand. In [55], Wu *et al.* aim to minimize the power consumption when solving the RWA problem by making maximum usage of powered-on devices. [32] and [56] study switching off the idle routers or links, so that the total power consumption is minimized.

Another group of works considers energy-aware traffic grooming under a static traffic scenario [57, 58, 59]. In [57], the authors assume that switches are modular in terms of power management and operations, and develop two heuristic approaches. In [58], ILP is formulated to solve the energy-aware traffic grooming problem. In [59], the authors try to minimize the number of interfaces of lightpaths, in order to minimize the energy consumption.

A third group of works focuses on static energy-efficient network design problems that consider the placement of network equipment [60, 61, 62]. The authors in [60] design an IP over optical network with the goal of minimizing the total power consumed by routers, transponders, and amplifiers. In [61], the authors consider how to provision each node in order to minimize network-wide power consumption. Two aspects are considered. One is how many chassis should be allocated on each node, and the other is how many line cards should be allocated. In [62], the authors demonstrate that a network with multiple line rates consumes less energy than a network with a single line rate.

In our work, we do not consider traffic grooming at intermediate nodes since electronic processing is proved to be energy consuming [63]. We do not switch off idle equipment either, since we study a static network design problem in which we need to decide how many equipment to allocate for a set of requests. The existing works do not take impairments into consideration, which is a major focus in our work.

2.3 Research in Virtual Network Mapping

The virtual network mapping problem has been extensively studied in layer 2/3 networks. A group of papers [64, 65, 66] study the virtual network mapping problem without survivability constraints. Another group of papers [67, 68, 69, 70] investigate the virtual network mapping problem with various survivability requirements. In [67], the virtual networks can survive single link failure by changing the node mapping. [68] also uses the node migration approach to protect against single link failures, but virtual nodes are only allowed to migrate among

their primary locations in order to save reserved resources. In [69], the authors study how to protect against both a physical node and a physical link failure. In [70], Yu *et al.* study the survivable virtual network mapping problem under single regional failures, where a single regional failure may destroy one or more physical nodes.

Some current works study the VON mapping problem in fixed-grid WDM networks. In [71], Peng *et al.* proposed an impairment-aware VON mapping scheme in SLR WDM networks. In [72], the work is extended to include the consideration of MLR WDM networks, and the authors further extend the work to WDM networks with multiple modulation formats in [73]. In [74], an overview of the challenges in VON mapping is presented, and the authors formulate an ILP model to solve the VON mapping problem in WDM networks. In [75], the authors further propose a heuristic algorithm and consider both transparent VONs and opaque VONs. These papers focus on the link mapping problem only, assuming that the node mapping is fixed. Also, they do not take the survivability constraint into consideration. In [76], Zhang *et al.* propose various algorithms to solve the node mapping, routing, and wavelength assignment problems in VON mapping. In [77], a VON consists both transparent and translucent virtual links. A transparent virtual link needs to be allocated one or more continuous wavelengths along the lightpath, while a translucent virtual link can accept regeneration at intermediate nodes. A heuristic is proposed to solve the problem. [78] studies how to minimize the total network cost when mapping a VON in MLR WDM networks. These works differ from our work in that they do not consider the survivability requirement or flexible-grid optical networks. In [79], the authors study the disaster-resilient and post-disaster-survivable VON mapping problem in fixed-grid WDM networks.

Another group of papers studies how to map VONs in flexible-grid optical networks. In [80], the authors attempt to maximize the number of successfully mapped VONs to a resource-limited physical optical network with the consideration of reachability constraint. The paper assumes that the node mapping is fixed and no regeneration is allowed. In [81],

Zhang *et al.* formulate ILP models and propose heuristic algorithms for both WDM and flexible-grid optical networks. Pages *et al.* focus on the link mapping problem in flexible-grid optical networks in [82], under the assumption that node mapping is given. The authors in [83] study the VON mapping problem in flexible-grid optical networks under both static and dynamic traffic, with an ILP model and two heuristic algorithms presented. In [84], Gong *et al.* address the problem of transparent VON mapping in flexible-grid optical networks under dynamic traffic. This work is extended in [85] by including the opaque VON mapping problem. In [86], Ye *et al.* compare two heuristic algorithms which differ in the sequence of allocating the VON's computing and network resources. Allocating the network resources first is shown to be more effective than allocating the computing resources first, in terms of the request blocking probability. These papers do not consider the survivability constraint. In [87], the authors investigate how to choose a subset of data centers with minimum delay among the data centers, while guaranteeing k-connected survivability.

The existing approaches for virtual network mapping over layer 2/3 networks cannot be applied to VON mapping, because they do not consider the additional constraints in the optical layer. The existing papers on VON mapping over fixed grid or flexible-grid optical networks either do not consider the survivability constraint or do not consider how to minimize the equipment cost. Thus, in this dissertation, we propose cost-optimized solution for survivable VON mapping, with the consideration of equipment selection and placement.

2.4 Research in Network Design and Resource Provisioning of Flexible-Grid Optical Networks

The current research topics on network design and resource provisioning of flexible-grid optical networks include RSA, survivable flexible-grid optical networks, and traffic grooming in flexible-grid optical networks.

A group of papers investigates the RSA problem under static traffic scenario. In the static RSA problem, a set of lightpaths need to be found for a given set of connection requests, and the objective is to minimize the spectrum usage. For each lightpath, a set of contiguous spectrum slots are reserved according to the capacity requirement, and these spectrum slots need to be continuous along the path. In [88, 89, 90, 91, 92, 93, 94, 95, 96], ILPs or heuristic algorithms are used to solve the static RSA problem without considering impairment constraints. [97, 12, 98] solve the static RSA problem with impairment constraints.

Another group of papers studies the RSA problem under dynamic traffic scenario. The dynamic RSA problem is to assign routing and spectrum for each arriving connection request, such that the spectrum usage for each connection request and the blocking rate are minimized. In [99], the dynamic RSA problem is addressed without impairment constraints. It shows that the blocking rate in flexible-grid optical networks is reduced by 66% compared to fixed-grid optical networks in a ring topology. [100, 101, 102] study the dynamic RSA problem without impairment constraints and the same modulation format is used for each lightpath. In [103], a distance adaptive algorithm is proposed for the dynamic RSA algorithm with impairment constraints. [104] investigates how the flexible channel spacing effects the quality of transmission (QoT) of channels with heterogeneous line rates.

Providing survivability is an essential requirement for flexible-grid optical networks. Survivability can be provided by protection or restoration. [105, 106, 107] study how to provide dedicated protection to each connection request with the minimum spectrum usage. In [108, 109, 110, 111], two connection requests are allowed to share spectrum or transponders on the backup paths if their working paths are disjoint. In [112], the authors improve the survivability of the network with higher spectral-efficiency with a bandwidth-squeezed restoration algorithm. In [113], Chen *et al.* propose restoration algorithms to recover from multi-link failures.

Traffic grooming in flexible-grid optical networks can be done in either the electrical layer or the optical layer. [114, 115, 116] study the electronic traffic grooming problem. In

[114], the spectrum efficiency of flexible-grid optical networks with grooming is compared with the non-grooming scenario via ILP. [115] proposes a heuristic algorithm to solve the static grooming problem. In [116], the traffic grooming problem is solved in flexible-grid optical networks while providing survivability through a shared path protection. [117, 118, 119, 120, 121] study the problem of optical layer traffic grooming. [117] and [118] show that optical layer traffic grooming can reduce the network cost and energy consumption compared to electronic traffic grooming. In [119], Zhang *et al.* propose an optical traffic grooming architecture that can offer finer switching granularity. In [120] and [121], Zhang *et al.* survey the evolution of traffic grooming from fixed-grid optical networks to flexible-grid optical networks, and then study the traffic grooming problem when optical layer is sliceable.

However, the papers discussed above either do not consider the impairment constraints or do not consider concentrating the RSs. Thus, in our work, we focus on the impact of RS concentration in the network cost, and design approaches to achieve the minimum cost.

CHAPTER 3

RS SELECTION FOR MLR OPTICAL NETWORKS WITH FIXED ROUTING

In this chapter, we study the problem of RS selection for MLR optical networks with fixed routing (MLR-RSS).[1] The objective is to minimize the number of RSs for a given set of requests. We first provide the problem definition of MLR-RSS and show that the MLR-RSS problem is NP-complete. An ILP model is formulated. We then present two heuristic algorithms, named Independent algorithm and Sequential algorithm, and two approximation algorithms, named MLR-combined algorithm and Weighted MLR-combined algorithm. The performance of the algorithms is compared via simulation and results show that the Weighted MLR-combined algorithm has the best performance. Results suggest that our proposed MLR algorithm outperforms existing SLR algorithms by more than 20%. Also, the RS distribution suggests that certain nodes in the network have a much higher probability of being chosen as RSs than the others.

3.1 Introduction

The advent of colorless and directionless ROADM enables the regenerators to be pre-deployed in optical networks, in order to achieve fast service setup and fast lightpath recovery. From the CAPEX and OPEX point of views, it is desirable to pre-deploy regenerators in a small number of RSs. In MLR optical networks, different line rates suffer from different levels of

[1] ©2014 IEEE. Reprinted, with permission, from Weisheng Xie, Jason P. Jue, Xi Wang, Qiong Zhang, Qingya She, Paparao Palacharla, Motoyoshi Sekiya, "Regenerator Site Selection for Mixed Line Rate Optical Networks," *IEEE/OSA Journal of Optical Communications and Networking (JOCN)*, March 2014.

impairments, resulting in different reachabilities. The different signal reachabilities add to the challenge of finding RSs in MLR optical networks.

In this chapter, we study the RS selection for MLR optical networks (MLR-RSS), when routing of each request is given. In practical scenarios, the routing may be pre-defined considering load-balancing, energy consumption, equipment cost, or other factors, and thus it is necessary to study the RS selection problem when routing is fixed. The impairment constraints are represented as the reachability for each line rate. The objective of our problem is to minimize the number of RSs. We make the following assumptions: 1) the links in the optical network are bidirectional; 2) routing is given for each request; and 3) the number of regenerators in a RS is not limited.

The rest of this chapter is organized as follows. In Section 3.2, we provide a detailed description of the MLR-RSS problem. In Section 3.3, an ILP model is formulated for the MLR-RSS problem. In Section 3.4, two heuristic algorithms and two approximation algorithms are presented. Numerical simulation results are shown in Section 3.5. Finally, we give a summary of our work in Section 3.6.

3.2 Problem Description

3.2.1 Network Model

The optical network can be represented as a graph $G(\mathbf{V}, \mathbf{E})$, where $\mathbf{V}$ is a set of nodes and $\mathbf{E}$ is a set of edges. For each request, a wavelength of the requested line rate is reserved along its given route, and regenerators are placed in the RSs along the route if needed.

In this chapter, reachability is used to measure the effect of impairments. The reachabilities of different line rates are different because of different physical impairments and component tolerance. Thus, we use a set of reachabilities $\mathbf{D}$ to denote different line rates' reachabilities. For example, in Figure 3.1, suppose we have two different line rates, lower rate

l_1 and higher rate l_2, and the reachabilities for l_1 and l_2 are 3 hops and 1 hop, respectively. Thus, for Path 1 (4 hops) from Node 1 to Node 5, we need 1 regenerator for l_1. For Path 2 (4 hops) from Node 1 to Node 5, we need 3 regenerators for l_2.

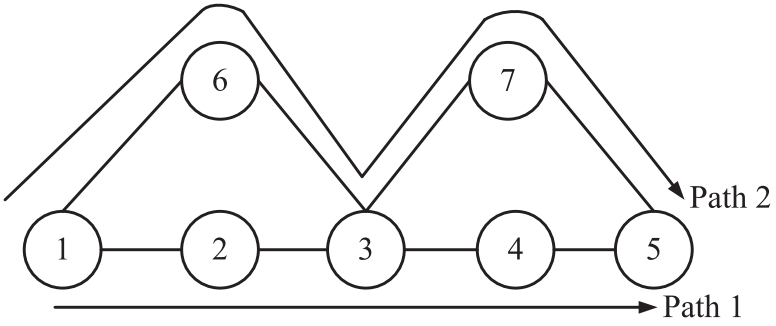

Figure 3.1. Example of network and regenerator placement

3.2.2 Problem Formulation

The MLR-RSS problem can be stated as follows:

Given physical topology $G(\mathbf{V}, \mathbf{E})$, where $\mathbf{V}$ is a set of nodes and $\mathbf{E}$ is a set of edges, a set of line rates $\mathbf{L}$, $l_k \in \mathbf{L}$, $1 \leq k \leq |\mathbf{L}|$, a reachability set $\mathbf{D}$, $\delta_k \in \mathbf{D}$, $1 \leq k \leq |\mathbf{L}|$, where δ_k is the reachability of line rate l_k, and a set of traffic demands $\mathbf{\Lambda}$ in which a request is defined as R [s, d, l_k, rt], where s is a source, d is a destination, l_k is the requested line rate, and rt is the actual route of the request.

Find the placement of RSs at nodes with the objective of minimizing the total number of RSs, such that

1. traffic constraint: all the requests are assigned the requested line rate;

2. impairment constraint: along any path, the length of each segment without regenerators does not exceed the corresponding line rate l_k's reachability limit δ_k.

An example is shown in Figure 3.1. Suppose we have two requests r_1[1, 5, l_1, (1-2-3-4-5)] and r_2[1, 5, l_2, (1-6-3-7-5)]. The reachabilities for l_1 and l_2 are 3 hops and 1 hop, respectively. For r_1, we can select Node 2, Node 3, or Node 4 as RS. For r_2, we have no choice but to select

Node 6, Node 3, and Node 7 as RSs. Thus, Node 6, Node 3 and Node 7 are the optimal RSs selection because only three sites are needed, which is the minimum possible number of RSs.

3.2.3 NP-Completeness

The decision version of the problem is: given $G(\mathbf{V}, \mathbf{E})$, $\mathbf{L}$, $\mathbf{D}$, the traffic demand set $\mathbf{\Lambda}$, and the total number of RSs *NR*, find the RSs selection to meet the constraints such that the total number of RSs is no larger than *NR*. Given an instance of the problem, we use as a certificate a subset $\mathbf{U} \subseteq \mathbf{V}$. The verification algorithm checks whether all the constraints are satisfied and whether the number of elements in $\mathbf{U}$ is at most *NR*. This process can certainly be done in polynomial time. Thus, the problem belongs to the NP class.

In [31], it is proved that the RS selection problem in SLR optical networks is NP-hard. Since this problem is a special case of our problem when only a single line rate is available, our problem is also NP-hard. Since this problem is shown to belong to the NP class above, the problem is NP-complete.

3.3 ILP Formulation

The ILP model has an input $\mathbf{R} = [r_{k,i,j}^{s,d}]_{|\mathbf{L}|\times|\mathbf{V}|\times|\mathbf{V}|}^{|\mathbf{V}|\times|\mathbf{V}|}$ to denote a modified version of the given path for a request from s to d using line rate l_k. The modified version of a given path is named the *reachability path*. $r_{k,i,j}^{s,d}$ equals 1 if edge (i, j) is on the *reachability path* from s to d using line rate l_k, otherwise it is 0. A *reachability path* is obtained by adding auxiliary links to the original given path. Given an original path as shown in Figure 3.2(a), for any two nodes v_i and v_j on the path, if their distance on the given path is not larger than the reachability, an auxiliary link is placed between v_i and v_j. Figure 3.2(b) shows an example of the reachability path when reachabilities are 2 hops and 3 hops, respectively. We can see that for any path from s to d on the reachability path corresponding to line rate l_k, by

placing line rate l_k's regenerators at all the intermediate nodes, the line rate l_k's signal is reachable from s to d on the given path.

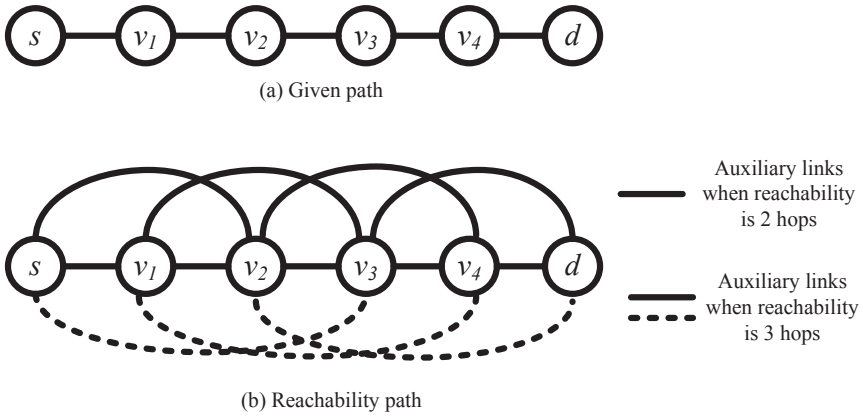

Figure 3.2. Example of reachability path

Next, we present the ILP formulation for MLR-RSS. First, we define some useful notations and variables.

3.3.1 Input Parameters

- $\mathbf{R} = [r^{s,d}_{k,i,j}]^{|\mathbf{V}|\times|\mathbf{V}|}_{|\mathbf{L}|\times|\mathbf{V}|\times|\mathbf{V}|}$: set of reachability paths;
- $\mathbf{REQ} = [req_{s,d,k}]_{|\mathbf{V}|\times|\mathbf{V}|\times|\mathbf{L}|}$: set of requests, $req_{s,d,k}$ is equal to 1 if there is a request from s to d using line rate l_k, otherwise 0;
- VL: a very large number.

3.3.2 Variables of ILP

- $\mathbf{X} = [x^{s,d}_{k,i,j}]^{|\mathbf{V}|\times|\mathbf{V}|}_{|\mathbf{L}|\times|\mathbf{V}|\times|\mathbf{V}|}$: $x^{s,d}_{k,i,j}$ is equal to 1 if edge (i, j) on the reachability path from s to d using line rate l_k is selected, otherwise 0;
- $\mathbf{Y} = [y^{s,d}_{k,i}]^{|\mathbf{V}|\times|\mathbf{V}|}_{|\mathbf{L}|\times|\mathbf{V}|}$: $y^{s,d}_{k,i}$ is equal to 1 if a line rate l_k's regenerator is placed at Node i on the path from s to d, otherwise 0;
- $\mathbf{Z} = [z_i]_{|\mathbf{V}|}$: z_i is equal to 1 if Node i is selected as a RS, otherwise 0.

3.3.3 Objective

The objective of MLR-RSS is:

$$min \sum_{i=1}^{|\mathbf{V}|} z_i \tag{3.1}$$

3.3.4 Constraints

$$\sum_{j=1}^{|\mathbf{V}|} x_{k,s,j}^{s,d} - \sum_{j=1}^{|\mathbf{V}|} x_{k,j,s}^{s,d} = req_{s,d,k}, \forall 1 \leq s \leq |\mathbf{V}|, 1 \leq d \leq |\mathbf{V}|, 1 \leq k \leq |\mathbf{L}| \tag{3.2}$$

$$\sum_{j=1}^{|\mathbf{V}|} x_{k,j,d}^{s,d} - \sum_{j=1}^{|\mathbf{V}|} x_{k,d,j}^{s,d} = req_{s,d,k}, \forall 1 \leq s \leq |\mathbf{V}|, 1 \leq d \leq |\mathbf{V}|, 1 \leq k \leq |\mathbf{L}| \tag{3.3}$$

$$\sum_{i=1}^{|\mathbf{V}|} x_{k,i,j}^{s,d} = \sum_{i=1}^{|\mathbf{V}|} x_{k,j,i}^{s,d}, \forall 1 \leq s \leq |\mathbf{V}|, 1 \leq d \leq |\mathbf{V}|, 1 \leq k \leq |\mathbf{L}|, 1 \leq j \leq |\mathbf{V}|, j \neq s, d \tag{3.4}$$

Constraints 3.2 to 3.4 guarantee the traffic constraint. In detail, Constraint 3.2 guarantees that when there is a request from s to d using line rate l_k, the source node s generates a traffic flow on the corresponding reachability path. Constraint 3.3 guarantees that the traffic flow terminates at destination d on the corresponding reachability path. Constraint 3.4 ensures that, for any intermediate node, the incoming flow and the outgoing flow should be the same.

$$x_{k,i,j}^{s,d} \leq r_{k,i,j}^{s,d}, \forall 1 \leq s \leq |\mathbf{V}|, 1 \leq d \leq |\mathbf{V}|, 1 \leq k \leq |\mathbf{L}|, 1 \leq i \leq |\mathbf{V}|, 1 \leq j \leq |\mathbf{V}| \tag{3.5}$$

Constraint 3.5 ensures that the routing of the request from s to d using line rate l_k is on the corresponding reachability path. By finding a path on the reachability path from s to d using line rate l_k and placing regenerators in the intermediate nodes, we can guarantee that the line rate l_k's signal is reachable between s and d.

$$y_{k,i}^{s,d} \geq x_{k,i,j}^{s,d}, \forall 1 \leq s \leq |\mathbf{V}|, 1 \leq d \leq |\mathbf{V}|, 1 \leq k \leq |\mathbf{L}|, 1 \leq j \leq |\mathbf{V}|, 1 \leq i \leq |\mathbf{V}|, i \neq s \tag{3.6}$$

Constraint 3.6 guarantees that for any edge on the reachability path from s to d using line rate l_k, a line rate l_k's regenerator is placed at the source end of the edge, excluding the source of the request s.

$$z_i \geq \frac{\sum_{s=1}^{|\mathbf{V}|}\sum_{d=1}^{|\mathbf{V}|}\sum_{k=1}^{|\mathbf{L}|} y_{k,i}^{s,d}}{VL}, \forall 1 \leq i \leq |\mathbf{V}| \tag{3.7}$$

Constraint 3.7 ensures that for any node where regenerator is placed, the node is selected as a RS.

3.4 Algorithms

3.4.1 Approximation Algorithm for SLR Optical Networks

In [31], an approximation algorithm is proposed for the RS selection problem in SLR optical networks (SLR-RSS). As this algorithm will be used as a sub-routine in our heuristic approaches, it is necessary to describe the algorithm. We call this algorithm the SLR combined (SLR-combined) algorithm in the following sections.

The SLR-combined algorithm reduces the SLR-RSS problem to the Set Cover Problem [122]. The input of the algorithm is a network $G(\mathbf{V}, \mathbf{E})$, a set of requests with given routes $\{[s_1, d_1], [s_2, d_2], \ldots, [s_m, d_m]\}$, $s_i \neq d_i$, $s_i, d_i \in \mathbf{V}$, where $[s_i, d_i]$ is a given route from source s_i to destination d_i. The input also includes a reachability $\delta > 0$. Since the SLR-combined algorithm is for SLR optical networks, only one reachability is needed as input. The output of the algorithm is a set of nodes $\mathbf{U} \subseteq \mathbf{V}$ that are selected as RSs. The algorithm process is divided into two cases depending on whether δ is odd or even.

If δ is odd, let $\mathbf{A} = \{a_{v,i} | v \in \mathbf{V}, v \in [s_i, d_i]\}$, and $\mathbf{B} = \cup\{b_v | v \in \mathbf{V}\}$. Let P_v be the set of paths that cross node v. For every path $p \in P_v$, the set b_v includes the following two types of elements: 1) all the elements in $\mathbf{A}$ corresponding to the nodes of p having a distance from v that is less than or equal to $\frac{\delta-1}{2}$; 2) if the distance between either two endpoints of path p

and node v is less than or equal to δ, then add to set b_v all the elements in $\mathbf{A}$ corresponding to all the nodes of p between v and such an endpoint.

If δ is even, let $\mathbf{A} = \{a_{j,i} | e_j \in \mathbf{E}, e_j \in [s_i, d_i]\}$, and $\mathbf{B} = \cup\{b_v | v \in \mathbf{V}\}$. Let P_v be the set of paths that cross node v. We define the distance between a node and the edges incident to it to be 1. For every path $p \in P_v$, the set b_v includes the following two types of elements: 1) all the elements in $\mathbf{A}$ corresponding to the edges of p having a distance from v that is less than or equal to $\frac{\delta}{2}$; 2) if the distance between either two endpoints of path p and node v is less than or equal to δ, then add to set b_v all the elements in $\mathbf{A}$ corresponding to all the edges of p between v and such an endpoint.

After $\mathbf{A}$ and $\mathbf{B}$ are found, the Set Cover algorithm in [122] is applied to find the minimum number of subsets $\mathbf{G} \subseteq \mathbf{B}$ that cover $\mathbf{A}$. If the solution obtained is $\mathbf{G} = \{b_{v_1}, b_{v_2}, ..., b_{v_t}\}$, then nodes $\mathbf{U} = \{v_1, v_2, ..., v_t\}$ are selected as RSs.

In [122], it is proved that the ratio between the results obtained by the Set Cover algorithm and the optimal value grows at most logarithmically in the largest cardinality of the subset, that is, the approximation ratio of the Set Cover algorithm proposed in [122] is $O(\log(\max_i |b_i|))$. In the SLR-combined algorithm, when node i is on the middle of all the paths of the requests, and both the distance between node i and the source and the distance between node i and the destination are δ, then b_i has the largest possible cardinality, which is $2m\delta$. Thus, the approximation ratio of SLR-combined algorithm is $O(\log m + \log \delta)$.

An example is shown below to illustrate this algorithm. Consider the topology in Figure 3.1. There is only one line rate l in the network. There are two requests r_1[1, 5, l, (1-2-3-4-5)] and r_2[1, 5, l, (1-6-3-7-5)]. The reachability of a line rate l's signal is 3 hops. Then, by running the SLR-combined algorithm, we have

$\mathbf{A} = \{a_{1,1}, a_{2,1}, a_{3,1}, a_{4,1}, a_{5,1}, a_{1,2}, a_{6,2}, a_{3,2}, a_{7,2}, a_{5,2}\}$

$b_1 = \{a_{1,1}, a_{2,1}, a_{1,2}, a_{6,2}\}$

$b_2 = \{a_{1,1}, a_{2,1}, a_{3,1}, a_{4,1}, a_{5,1}\}$

$b_3 = \{a_{1,1}, a_{2,1}, a_{3,1}, a_{4,1}, a_{5,1}, a_{1,2}, a_{6,2}, a_{3,2}, a_{7,2}, a_{5,2}\}$

$b_4 = \{a_{1,1}, a_{2,1}, a_{3,1}, a_{4,1}, a_{5,1}\}$

$b_5 = \{a_{4,1}, a_{5,1}, a_{7,2}, a_{5,2}\}$

$b_6 = \{a_{1,2}, a_{6,2}, a_{3,2}, a_{7,2}, a_{5,2}\}$

$b_7 = \{a_{1,2}, a_{6,2}, a_{3,2}, a_{7,2}, a_{5,2}\}$.

The Set Cover algorithm in [122] is then applied to **A** and **B**. Obviously, b_3 alone has all the elements in **A**, so b_3 is the solution, which means only Node 3 is selected as a RS.

3.4.2 Heuristic Approaches for MLR Optical Networks

To deal with MLR optical networks, the first approach is to run the above SLR-combined algorithm for each of the line rates $l_1, l_2, ..., l_n$ to obtain the results $\boldsymbol{U_1}, \boldsymbol{U_2}, ..., \boldsymbol{U_n}$. The final result **U** is the union of $\boldsymbol{U_1}, \boldsymbol{U_2}, ..., \boldsymbol{U_n}$. As this approach deals with each line rate independently, we call it the Independent algorithm. The full algorithm is described in Algorithm 1.

Algorithm 1 Independent algorithm

Input: graph $G(\mathbf{V}, \mathbf{E})$, the available line rate set **L**, the reachability set **D**, and the request set $\mathbf{\Lambda}$.
Output: a subset $\mathbf{U} \subseteq \mathbf{V}$ that denotes the nodes selected as RSs.
//Main procedure
Begin
for all line rate l_i, $l_i \in \mathbf{L}$ **do**
  Run the SLR-combined algorithm and obtain the result $\boldsymbol{U_i}$.
end for
$\mathbf{U} = \bigcup \boldsymbol{U_i}$.
End

The Independent algorithm places RSs for each line rate without considering the placement of RSs of other line rates. To improve this, we can place RSs for each line rate sequentially, that is, when placing RSs for one line rate, we consider reusing the already placed RSs first. If one request cannot be satisfied with the already placed RSs, we take

the *unsatisfied segment* of the request and put it in a remaining requests set $\boldsymbol{RR}$. The *unsatisfied segment* is defined as follows. Given a request of line rate l_k with the routing [s, v_1, v_2, ... , d], s, d, $v_i \in \mathbf{V}$, take any two of the neighboring RSs v_i and v_{i+x}, which are already placed, along this path. If $x > \delta_k$, then [v_i, v_{i+1}, ..., v_{i+x-1}, v_{i+x}] is an unsatisfied segment. Also, if the distance between s and its nearest RS v_i or the distance between d and its nearest RS v_j is greater than δ_k, then [s, v_1, v_2, ..., v_i] or [v_j, v_{j+1}, ..., d] is also an unsatisfied segment. After all the unsatisfied segments of all the requests of a corresponding line rate are found, we run the SLR-combined algorithm again on the remaining request set $\boldsymbol{RR}$ and add the results to the already placed RSs. We call this algorithm the Sequential algorithm. If the algorithm starts with the highest line rate, then it is a Sequential High Line Rate First (Sequential HLRF) algorithm. Otherwise, if the algorithm starts with the lowest line rate, then it is a Sequential Low Line Rate First (Sequential LLRF) algorithm. The full Sequential HLRF algorithm is described in Algorithm 2.

Algorithm 2 Sequential HLRF algorithm

Input: graph $G(\mathbf{V}, \mathbf{E})$, the available line rate set $\mathbf{L}$, the reachability set $\mathbf{D}$, and the request set $\mathbf{\Lambda}$.
Output: a subset $\mathbf{U} \subseteq \mathbf{V}$ that denotes the nodes selected as RSs.
//Main procedure
Begin
$\mathbf{U} = \emptyset$.
for line rate l_i from l_n (highest rate) to l_1 (lowest rate) **do**
  for all paths p of line rate l_i **do**
    if path p cannot be satisfied with the already placed RSs $\mathbf{U}$ **then**
      Take the unsatisfied segment of p and add it to set $\boldsymbol{RR_i}$.
    end if
  end for
  Run the SLR-combined algorithm on $\boldsymbol{RR_i}$ and obtain the result $\boldsymbol{U_i}$.
  $\mathbf{U} = \mathbf{U} \bigcup \boldsymbol{U_i}$.
end for
End

3.4.3 Approximation Algorithms for MLR Optical Networks

The third approach places RSs neither from the highest line rate nor from the lowest line rate, but combines these two. This approach is called the MLR Combined (MLR-combined) algorithm. The MLR-combined algorithm differs from the SLR-combined algorithm in that for each element in sets $\mathbf{A}$ and b_v, $v \in \mathbf{V}$, we add one more index to denote the line rate. For line rate l_k, $\mathbf{A} = \{a_{v,i,k} | v \in \mathbf{V}, v \in [s_i, d_i]\}$ (when δ_k is odd), or $\mathbf{A} = \{a_{j,i,k} | e_j \in \mathbf{E}, e_j \in [s_i, d_i]\}$ (when δ_k is even), where k is the index of line rate l_k. Then for each line rate, we add to set b_v the above mentioned two types of elements of corresponding line rate. At the end, the Set Cover algorithm in [122] is applied to obtain the solution.

The full algorithm is described in Algorithm 3. Let $m_1, m_2, ..., m_n$ denote the number of paths of line rates $l_1, l_2, ...l_n$. Since the largest possible cardinality of each set of $\mathbf{B}$ is $\sum_{i=1}^{n} 2m_i\delta_i$, the approximation ratio of the MLR-combined algorithm is $O(\log(\sum_{i=1}^{n} 2m_i\delta_i))$.

In the Set Cover algorithm part of the MLR-combined algorithm, we select the set b_v with the maximum cardinality without considering what line rates' elements are included in this set. Suppose a high line rate request and a low line rate request pass the same node v. There may be more elements of the low line rate request in the set b_v than the high line rate request, since the low line rate usually has longer reachability than the high line rate. If cardinality is the only metric when selecting the next set, then we indeed give low line rate a higher priority, especially when the reachability of low line rate is much longer than the high line rate. An example is shown in Figure 3.3. In this example, we have two requests r_1[1, 7, l_1, (1-2-3-4-5-6-7)], r_2[1, 7, l_2, (1-8-3-9-5-6-7)]. Assume the reachabilities of l_1 and l_2 are 3 hops and 1 hop, respectively. Then we have

$\mathbf{A} = \{a_{1,1,1}, a_{2,1,1}, a_{3,1,1}, a_{4,1,1}, a_{5,1,1}, a_{6,1,1}, a_{7,1,1}, a_{1,2,2}, a_{8,2,2}, a_{3,2,2}, a_{9,2,2}, a_{5,2,2}, a_{6,2,2}, a_{7,2,2}\}$

$b_1 = \{a_{1,1,1}, a_{2,1,1}, a_{1,2,2}\}$

$b_2 = \{a_{1,1,1}, a_{2,1,1}, a_{3,1,1}\}$

$b_3 = \{a_{1,1,1}, a_{2,1,1}, a_{3,1,1}, a_{4,1,1}, a_{3,2,2}\}$

Algorithm 3 MLR-combined algorithm

Input: graph $G(\mathbf{V}, \mathbf{E})$, the available line rate set $\mathbf{L}$, the reachability set $\mathbf{D}$, and the request set $\mathbf{\Lambda}$.
Output: a subset $\mathbf{U} \subseteq \mathbf{V}$ that denotes the nodes selected as RSs.
Begin
//Initial phase
if δ_k is odd **then**
  Let $\mathbf{A} = \{a_{v,i,k} | v \in \mathbf{V}, v \in [s_i, d_i], l_k \in \mathbf{L}\}$ for all *v, i, k*.
else
  Let $\mathbf{A} = \{a_{j,i,k} | e_j \in \mathbf{E}, e_j \in [s_i, d_i], l_k \in \mathbf{L}\}$ for all *j, i, k*.
end if
//Main procedure
for line rate l_k from l_1 to l_n **do**
  if δ_k is odd **then**
    for all $v \in \mathbf{V}$ **do**
      Let P_v be the set of paths that cross node v.
      for all $p \in P_v$ **do**
        add to set b_v two types of elements
        1) all the elements in $\mathbf{A}$ corresponding to the nodes of p having the distance from v that is less than or equal to $\frac{\delta_k - 1}{2}$;
        2) if the distance between either two endpoints of path p and node v is less than or equal to δ_k, then add to set b_v all the elements in $\mathbf{A}$ corresponding to all the nodes of p between v and such an endpoint.
      end for
    end for
  else if δ_k is even **then**
    for all $v \in \mathbf{V}$ **do**
      Let P_v be the set of paths that cross node v.
      for all $p \in P_v$ **do**
        add to set b_v two types of elements
        1) all the elements in $\mathbf{A}$ corresponding to the edges of p having the distance from v that is less than or equal to $\frac{\delta_k}{2}$;
        2) if the distance between either two endpoints of path p and node v is less than or equal to δ_k, then add to set b_v all the elements in $\mathbf{A}$ corresponding to all the edges of p between v and such an endpoint.
      end for
    end for
  end if
end for
//Apply Set Cover algorithm
while $b_v \neq \emptyset$ for any $v \in \mathbf{V}$ **do**
  Find a set b_v with the maximum cardinality $|b_v|$;
  Add v to set $\mathbf{U}$, replace each b_i, $i \in \mathbf{V}$, by $b_i - b_v$.
end while
End

$b_4 = \{a_{1,1,1}, a_{2,1,1}, a_{3,1,1}, a_{4,1,1}, a_{5,1,1}, a_{6,1,1}, a_{7,1,1}\}$

$b_5 = \{a_{4,1,1}, a_{5,1,1}, a_{6,1,1}, a_{7,1,1}, a_{5,2,2}\}$

$b_6 = \{a_{5,1,1}, a_{6,1,1}, a_{7,1,1}, a_{6,2,2}, a_{7,2,2}\}$

$b_7 = \{a_{6,1,1}, a_{7,1,1}, a_{7,2,2}\}$

$b_8 = \{a_{1,2,2}, a_{8,2,2}\}$

$b_9 = \{a_{9,2,2}\}$

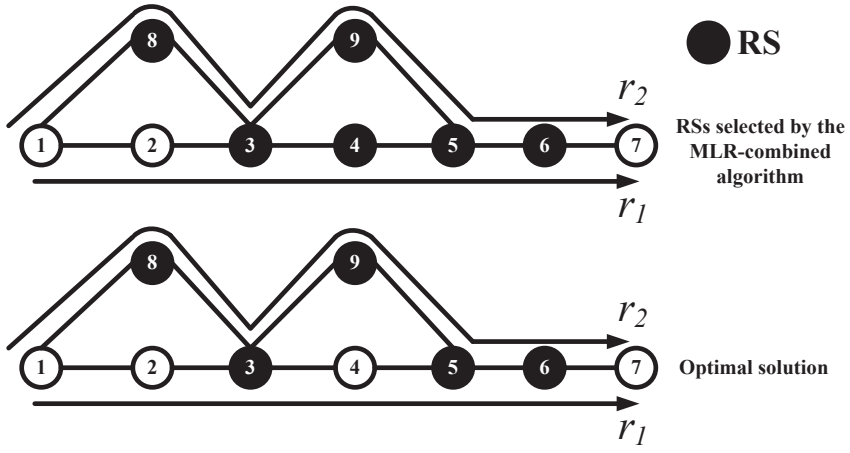

Figure 3.3. Example of a suboptimal solution obtained by the MLR-combined algorithm

The MLR-combined algorithm selects b_4 first, but as shown in Figure 3.3, this is not the optimal solution. Although b_4 has the largest cardinality, its elements are all low line rate's elements. Since low line rate has more elements than high line rate, we should not simply choose the set with the largest cardinality. A solution to solve the problem is assigning different weights to different line rates to compensate for the difference in reachabilities.

We associate a weight α_i with each line rate l_i. The total weight of set b_v is $W_v = \alpha_1 N_1 + \alpha_2 N_2 + ... + \alpha_n N_n + \epsilon|b_v|$, where N_i is the number of elements corresponding to line rate l_i in b_v, $\sum_i \alpha_i = 1$, and ϵ is a very small constant value. The optimal values of $\alpha_1, \alpha_2, ..., \alpha_n$ can be found through experiments. By adding a weight to each line rate, we have the Weighted MLR-combined algorithm. This algorithm differs from the MLR-combined algorithm only in the final Set Cover algorithm. In the MLR-combined algorithm, a set b_v with the maximum

cardinality $|b_v|$ is selected while in the Weighted MLR-combined algorithm, a set b_v with the maximum weight $W_v = \alpha_1 N_1 + \alpha_2 N_2 + ... + \alpha_n N_n + \epsilon |b_v|$ is selected. Since the MLR-combined algorithm is a special case of the Weighted MLR-combined algorithm when the weights of all line rates are equal, the performance of the Weighted MLR-combined algorithm won't be worse than that of the MLR-combined algorithm. Thus, the approximation ratio of the Weighted MLR-combined algorithm is also $O(\log(\sum_{i=1}^{n} 2m_i\delta_i))$.

3.5 Numerical Results

In this section, we present some numerical results in order to compare the performance of the Independent, Sequential HLRF, Sequential LLRF, MLR-combined, Weighted MLR-combined algorithms, and the ILP model.

The heuristic and approximation algorithms are implemented in Java, and the ILP model is solved by IBM ILOG CPLEX Optimization Studio $v12.2$. All the simulation experiments are performed on a server with 16×2.4 GHz processors and 12 GB memory. In the simulation, we choose two line rates: 100 Gbps and 400 Gbps. Experiments 1 to 4 test the average number of RSs and regenerators under different network load, different ratios of 100 Gbps requests, different reachability of 100 Gbps signal, and different reachability of 400 Gbps signal, respectively. Experiment 5 and Experiment 6 investigate the RS distribution under uniform traffic and non-uniform traffic, respectively .

For Experiments 1 and 2, the ILP is tested on the 24-node network shown in Figure 3.4 while the algorithms are tested on both the 24-node network and the 75-node CORONET [1] shown in Figure 3.5. Experiments 3 to 6 are conducted on the 75-node CORONET only. Experiments 1 to 5 are under uniform traffic. When generating uniform traffic, every node in the network has equal probability to be selected as source or destination. Experiment 6 is conducted on CORONET with non-uniform traffic. When generating non-uniform traffic, we select 25 most populated cities and these cities' probabilities of being chosen as sources

or destinations are 10 times higher than the other 50 cities. For the 24-node network, we pre-calculate a set of paths for each s-d pair. When generating a request for the 24-node network, we first determine the source node and the destination node, and then a path is randomly chosen from the set of paths, which have hop counts more than the corresponding line rate's reachability, between this s-d pair. When generating a request for the 75-node CORONET, different from the 24-node network, we always use the shortest hop distance path for every s-d pair. If the shortest hop distance is not greater than the corresponding line rate's reachability, we discard this s-d pair and randomly select another s-d pair until its shortest hop distance is greater than the corresponding line rate's reachability. There are no two requests with the same end nodes, unless they require different line rates. The experiment results are average values of more than 50 simulation runs on the 24-node network or more than 1000 simulation runs on the 75-node CORONET. We have fewer simulation runs on the 24-node network due to the long running time of ILP.

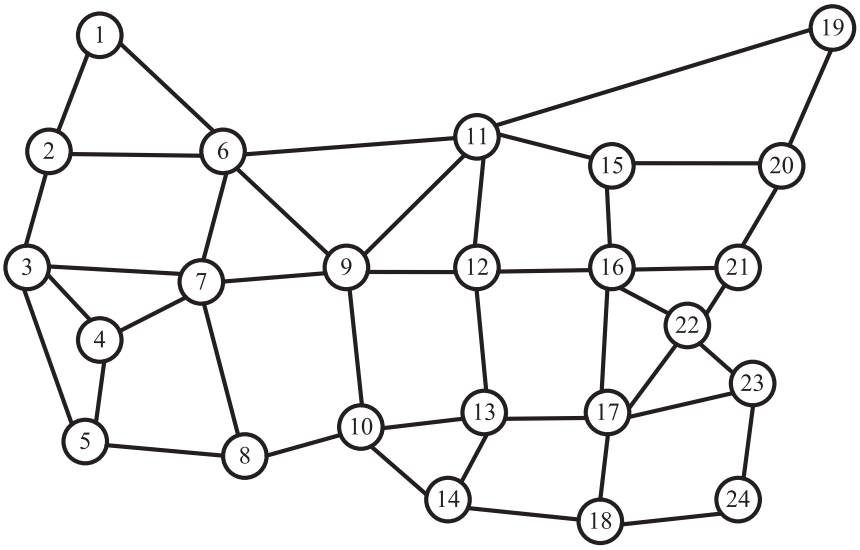

Figure 3.4. 24-node network topology

The reachabilities of 100 Gbps and 400 Gbps are assumed to be 5 hops and 3 hops, respectively, except Experiment 3 and Experiment 4, in which different reachabilities are

Figure 3.5. 75-node CORONET [1]

tested. In the simulation, given a total number of requests, half of them are 100 Gbps requests and the other half are 400 Gbps requests, except Experiment 2, in which this ratio is changed. For the Weighted MLR-combined algorithm, we have a weight α associated with 100 Gbps and a weight $\beta = 1 - \alpha$ associated with 400 Gbps. The value of α is determined as follows: we compare all the results obtained by the Weighted MLR-combined algorithm when $\alpha = 0$, 0.1, 0.2, ... , or 1, and choose the α value that leads to the best results. The ϵ value is set to 10^{-4}.

Experiment 1. In the first experiment, we study the average number of RSs and regenerators under different network load.

We first test the algorithms and the ILP on the 24-node network. As Figure 3.6 depicts, the Weighted MLR-combined algorithm has the best performance among all the algorithms, and its performance is only slightly worse than that of the ILP. The difference of the Weighted MLR-combined algorithm and the ILP is 7.7% on average, which is not more than one RS in the 24-node network. The performance of the Independent algorithm is the worst, as it simply combines the results of two line rates' RS selection without considering sharing RSs among different line rates. The Independent algorithm increases the number of RSs by

22.7% on average, compared to the Weighted MLR-combined algorithm. This result shows that selecting RSs for all the line rates together is better than selecting RSs for each line rate independently and combining them. Thus, the existing SLR algorithm is not effective for MLR networks, and we need MLR algorithms, such as the Weighted MLR-combined algorithm, for MLR networks. The Sequential HLRF algorithm outperforms the Sequential LLRF algorithm, because under this specific setting, the placement of RSs for the lower line rate has more flexibility due to the longer reachability; thus, starting from the high line rate enables the lower line rate to better reuse those RSs that are placed for the higher line rate.

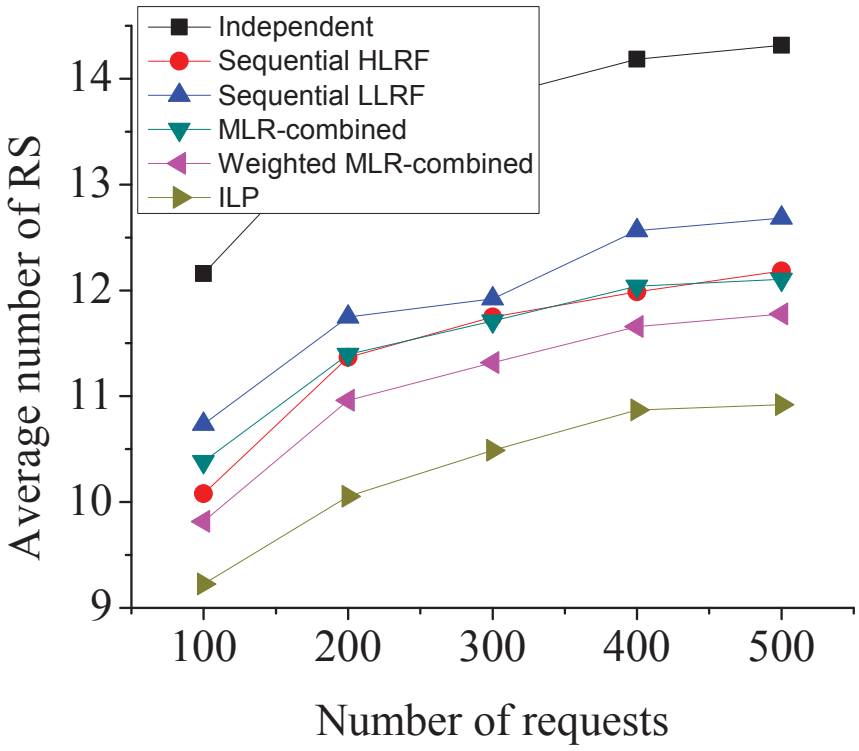

Figure 3.6. Number of RSs vs. total number of requests for 24-node network

Figure 3.7 shows the average number of regenerators when the total number of requests are 100, 300, and 500, respectively, under the 24-node network. In Figure 3.7, "Ind.", "HLRF", "LLRF", "MLR-C", "W-MLR-C", and the "ILP" refer to the Independent, Sequential HLRF, Sequential LLRF, MLR-combined, Weighted MLR-combined algorithms,

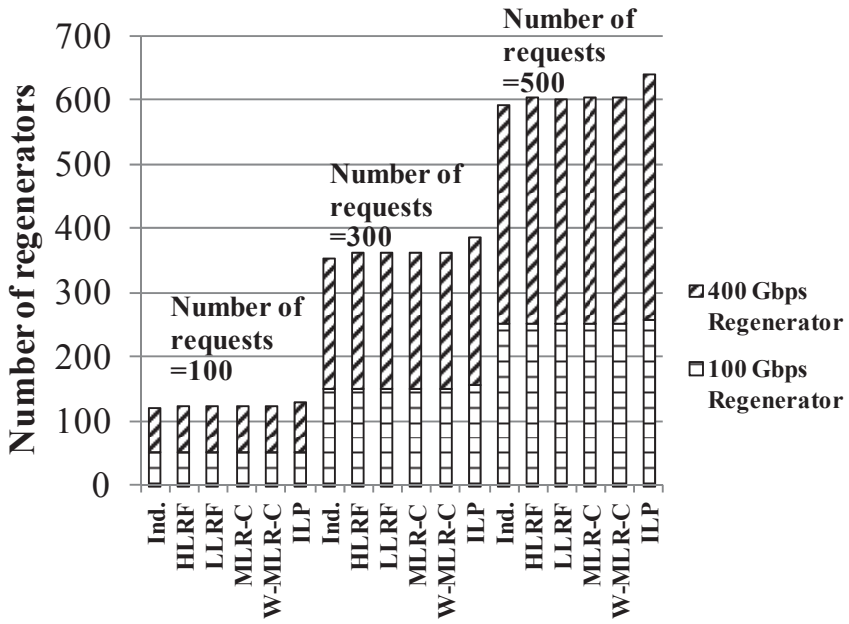

Figure 3.7. Number of regenerators vs. total number of requests for 24-node network

and the ILP model, respectively. These abbreviations apply to the following figures as well. From Figure 3.7, we can see that the Independent algorithm results in the fewest number of regenerators; however, the number of regenerators used by other algorithms is very close to that of the Independent algorithm. The ILP model uses the most regenerators. Since the objective of the ILP is just to minimize the number of RSs, it may result in a considerably larger number of regenerators.

We then test the algorithms on the 75-node CORONET. The ILP was not able to obtain a solution for this network. Figure 3.8 shows the average number of RSs. It shows that the Weighted MLR-combined algorithm has the best performance. The Independent algorithm requires an additional 26.0% more RSs than the Weighted MLR-combined algorithm. Figure 3.9 shows the average number of regenerators. From Figure 3.9, we can see that the Weighted MLR-combined algorithm doesn't use more regenerators than the Independent algorithm. Sometimes the number of regenerators used by the Weighted MLR-combined algorithm is even lower than that of the Independent algorithm. This result shows that the Weighted

MLR-combined algorithm can select RSs wisely. The number of RSs can be reduced while the number of regenerators is not increased.

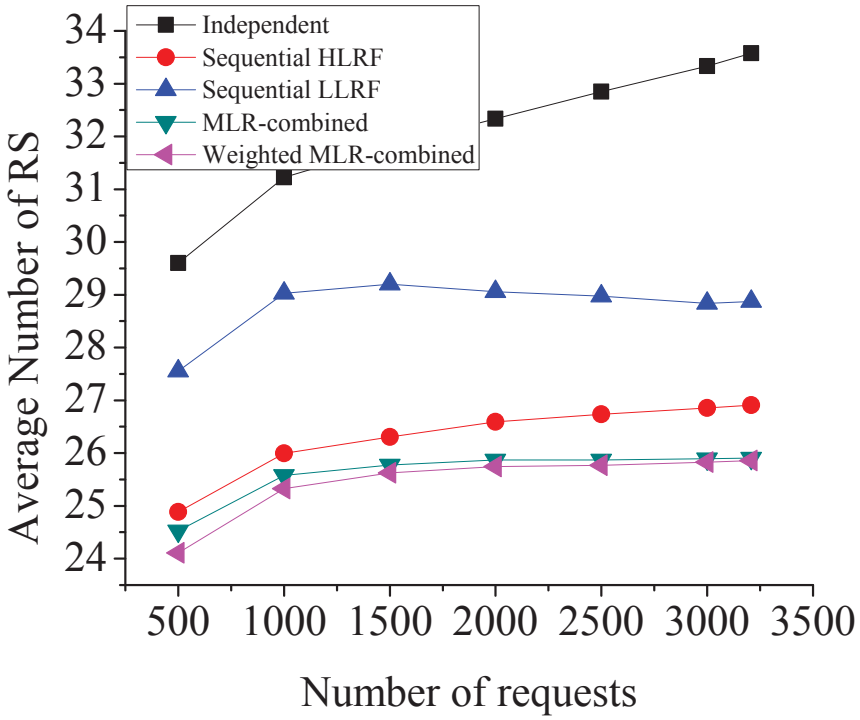

Figure 3.8. Number of RSs vs. total number of requests for 75-node network

Experiment 2. In the second experiment, we study the average number of RSs and regenerators under different ratios of 100 Gbps requests to the total number of requests.

For the experiment on the 24-node network, the total number of requests in the network is 250. The number of 100 Gbps requests changes from 0 to 100% of the total number of requests. Figure 3.10 shows that, although the ILP has the best performance, the Weighted MLR-combined algorithm only increases the number of RSs by 7.6% on average, compared to the ILP, that is, not more than one additional RS is required. Meanwhile, the Independent algorithm uses 20.7% more RSs than the Weighted MLR-combined algorithm. When the ratio is 0 or 1, all the algorithms, except the ILP, will have the same results. This is because when the ratio is 0 or 1, the requests will be all 400 Gbps requests or all 100 Gbps requests. In this case, the Independent, Sequential HLRF, Sequential LLRF, MLR-combined, and

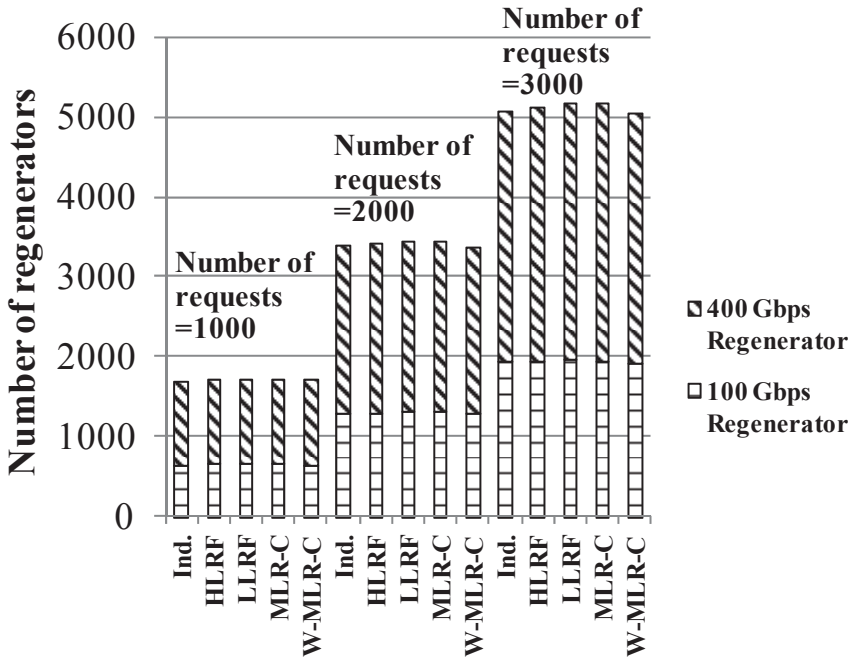

Figure 3.9. Number of regenerators vs. total number of requests for 75-node network

Weighted MLR-combined algorithms will operate as the SLR-combined algorithm since there are only one line rate's requests. Figure 3.11 shows the average number of regenerators. We can see that the ILP uses more regenerators than the other algorithms, and by around 5.7% on average more than that of the Weighted MLR-combined algorithm.

The algorithms are then tested on the 75-node network. The total number of requests in the network is 1500. As Figure 3.12 depicts, the Weighted MLR-combined algorithm still outperforms the other algorithms. Specifically, the Weighted MLR-combined algorithm reduces the number of RSs by averagely 20.2% compared to the Independent algorithm. When the ratio of 100 Gbps requests is low, the average number of RSs obtained by all the algorithms doesn't change much, because when the ratio of 100 Gbps requests is low, the placement of RSs are mainly for 400 Gbps requests, and these sites are sufficient to satisfy 100 Gbps requests. From Figure 3.13, we can see that although the Weighted MLR-combined algorithm shows a little increase in the the number of regenerators compared to that of the Independent algorithm, the difference is negligible.

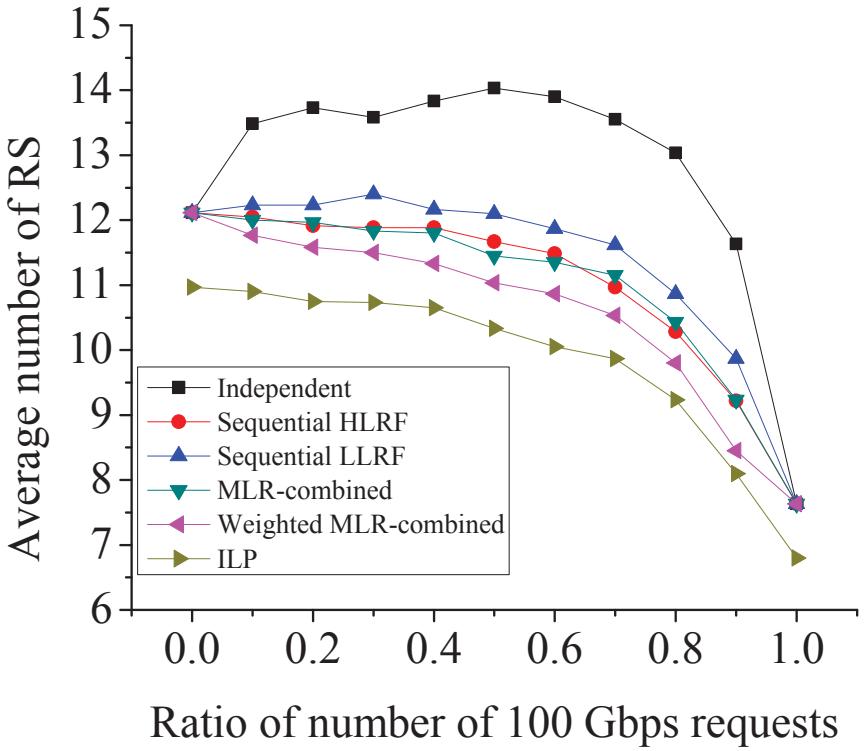

Figure 3.10. Number of RSs vs. different ratios of 100 Gbps requests in total number of requests for 24-node network

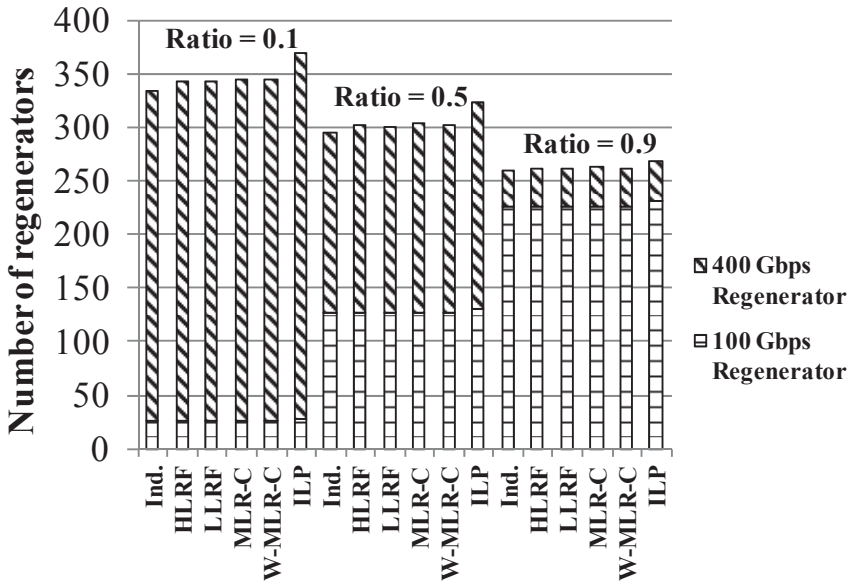

Figure 3.11. Number of regenerators vs. different ratios of 100 Gbps requests in total number of requests for 24-node network

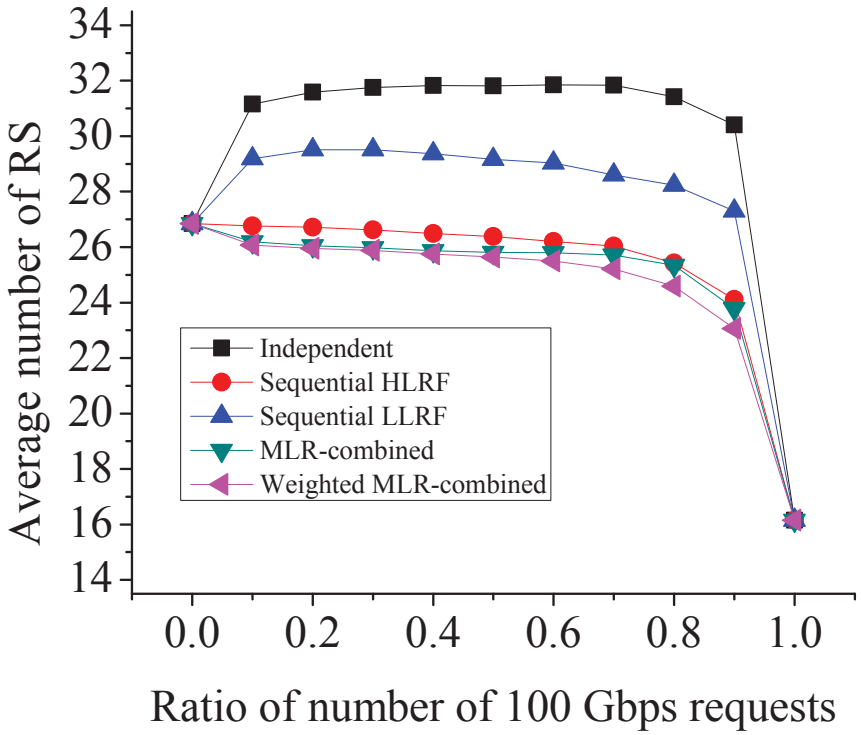

Figure 3.12. Number of RSs vs. different ratios of 100 Gbps requests in total number of requests for 75-node network

Experiment 3. In the third experiment, we study the average number of RSs and regenerators while varying the reachability of 100 Gbps signal. The reachability of 400 Gbps signal is 3 hops and the reachability of 100 Gbps signals ranges from 4 to 9 hops.

The algorithms are tested on the 75-node network. The total number of requests in the network is 200. As Figure 3.14 shows, the Weighted MLR-combined algorithm has the best performance, and it outperforms the Independent algorithm by 18.8% on average. The number of RSs obtained by the Sequential HLRF, the MLR-combined, and the Weighted MLR-combined algorithms almost doesn't change. The reason is that, under this network load and the reachabilities, the RSs are mainly determined by the 400 Gbps requests. The RSs determined by the 400 Gbps requests are sufficient for 100 Gbps requests, even when the 100 Gbps reachability is 4 hops. Thus, no matter how the reachability of 100 Gbps signal increases, the RSs are always determined by the 400 Gbps requests, and thus the

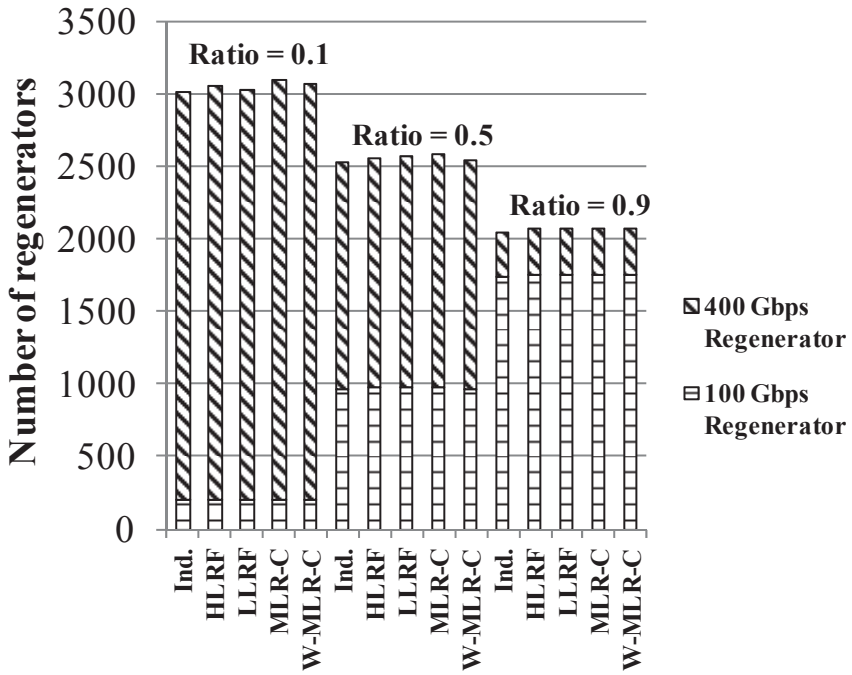

Figure 3.13. Number of regenerators vs. different ratios of 100 Gbps requests in total number of requests for 75-node network

number of RSs doesn't change. However, if we start from the lower rate, the RSs selected by the lower rate may not be reused by the higher rate, and thus results in more RSs than starting from the higher rate. This is why the Sequential LLRF algorithm requires more RSs than the Sequential HLRF algorithm when the 100 Gbps reachability is short. When the reachability of 100 Gbps signal grows, the performance of the Sequential LLRF algorithm will become better than that of the Sequential HLRF algorithm. Although starting from 400 Gbps requests means that 100 Gbps requests have higher possibility to reuse those RSs that are placed for 400 Gbps requests, when the need for RSs for 100 Gbps becomes less, the advantage of Sequential HLRF over Sequential LLRF becomes weaker. On the other hand, when the need for RSs for 100 Gbps requests becomes less, starting from 100 Gbps requests means that we start from a smaller number of RSs, and these RSs are more likely to be reused by 400 Gbps requests; thus, Sequential LLRF will outperform Sequential HLRF when the reachability of 100 Gbps signal grows. Figure 3.15 shows that the number of

regenerators used by the Weighted MLR-combined algorithm is almost the same as that of the Independent algorithm.

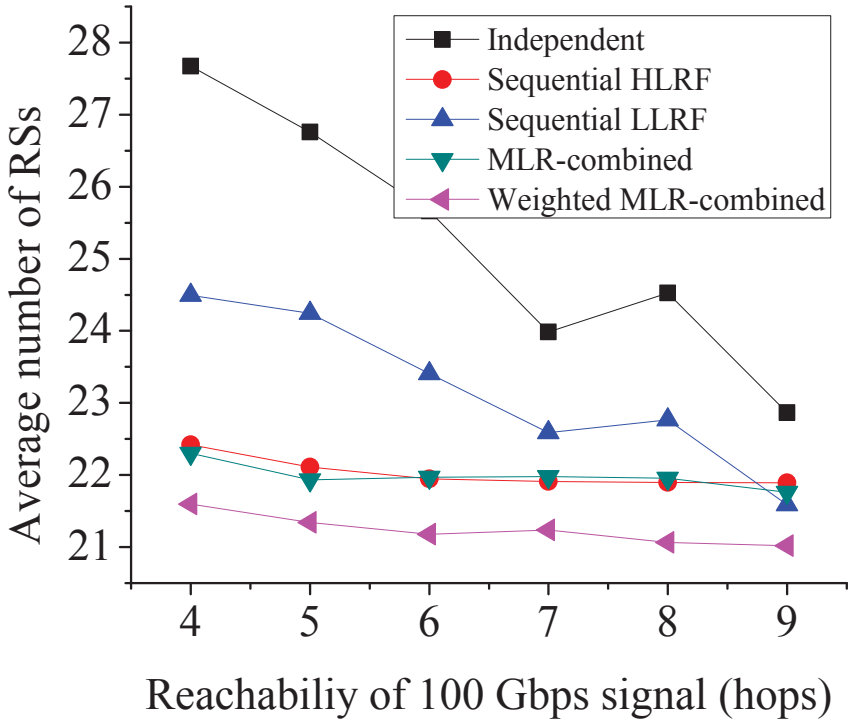

Figure 3.14. Number of RSs vs. different reachabilities of 100 Gbps signal for 75-node network

Experiment 4. In the fourth experiment, we study the average number of RSs and regenerators while varying the reachability of 400 Gbps signal. The reachability of 100 Gbps signal is 9 hops and the reachability of 400 Gbps signals ranges from 3 to 8 hops.

The algorithms are tested on the 75-node network. The total number of requests in the network is 200. Again, as Figure 3.16 shows, the Weighted MLR-combined algorithm has the best performance, and it outperforms the Independent algorithm by 23.3%, on average. For all algorithms, the number of RSs decreases as the reachability of 400 Gbps signal increases. Comparing Figure 3.14 and Figure 3.16, the number of RSs may not decrease when the reachability of 100 Gbps signal increases; however, the number of RSs will decrease when the reachability of 400 Gbps signal increases. Thus, when the number of 100 Gbps requests

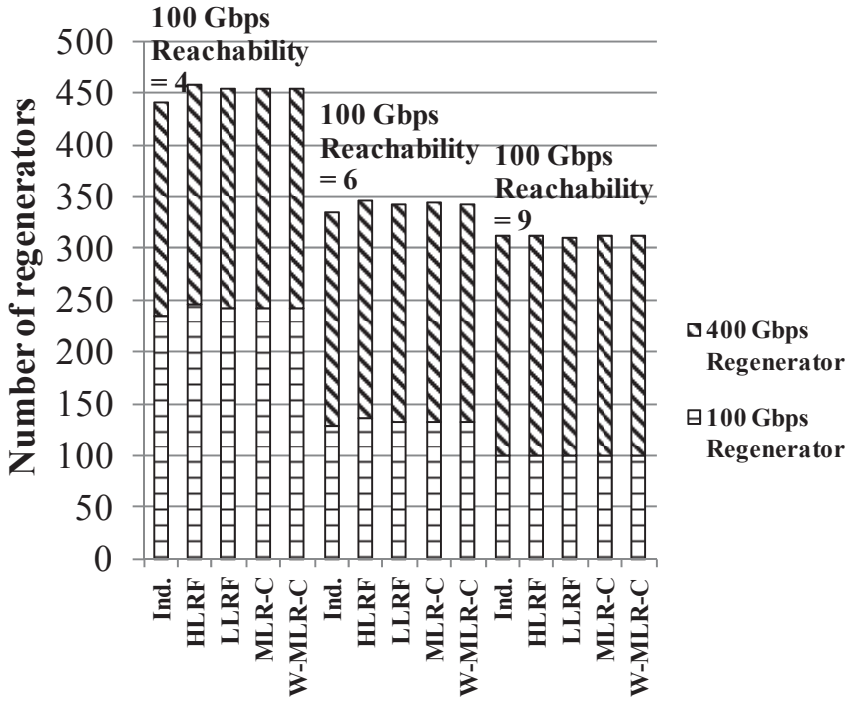

Figure 3.15. Number of regenerators vs. different reachabilities of 100 Gbps signal for 75-node network

and 400 Gbps requests are the same, the number of RSs mainly depends on the reachability of 400 Gbps signal, since the RSs placed by 400 Gbps requests may be reused by the 100 Gbps requests. This result suggests that when the number of different line rates' requests are not much different, the RSs are mostly determined by the higher rates. Figure 3.17 shows that the number of regenerators used by the Weighted MLR-combined algorithm is almost the same as that of the Independent algorithm, showing that the Weighted MLR-combined algorithm can concentrate RSs without using many more regenerators.

Experiment 5. In the fifth experiment, we study how the RSs are distributed in the network under uniform traffic. Specifically, we study if there are certain nodes in the network that are more likely to be chosen as RSs. We use the results obtained by the Weighted MLR-combined algorithm in Experiment 1. The traffic is uniform, i.e., each node has equal probability to be chosen as source or destination. Let $C_{i,j}$ denote the number of times node i is chosen as a RS under network load j, and let H_j denote the number of simulation runs

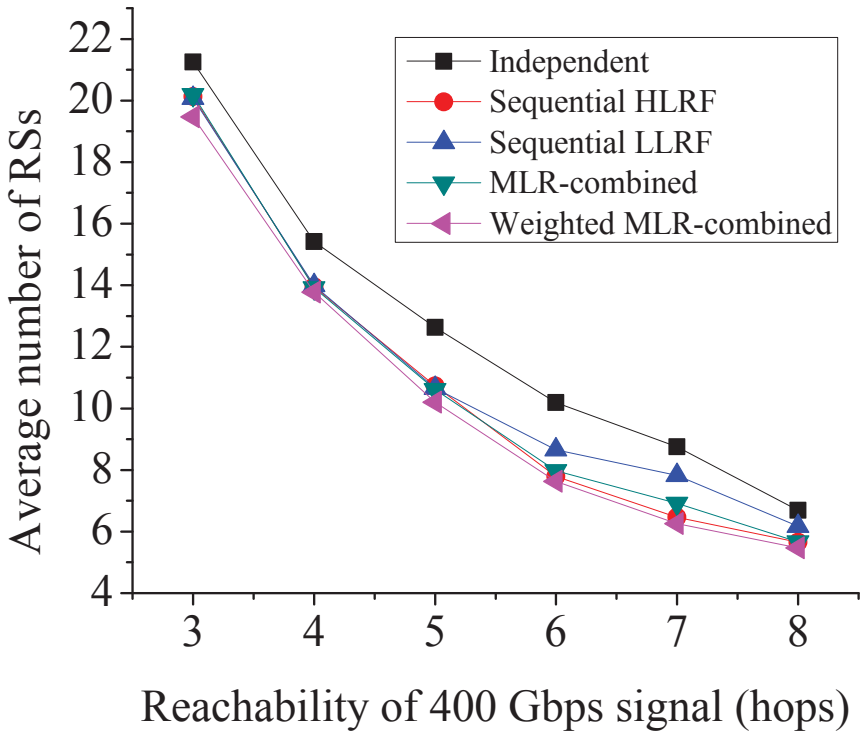

Figure 3.16. Number of RSs vs. different reachabilities of 400 Gbps signal for 75-node network

under network load j. Then, the probability of node i being chosen as a RS under network load j is defined as $prob_{i,j} = \frac{C_{i,j}}{H_j}$. We then visualize the network based on $prob_{i,j}$, in which each network node's size, color, and shape are determined by its $prob_{i,j}$. Figure 3.18a to 3.18c show the networks under network load of 1000, 2000, and 3000 total requests, respectively. In the figures, a node is originally a circle. The circle is bigger and redder with higher $prob_{i,j}$, and finally, those nodes with $prob_{i,j}$ larger than 90% are transformed into stars.

From Figure 3.18a to 3.18c, we can see that some nodes have extremely high probabilities (more than 90%), while some nodes have very low probabilities (less than 1%). This polarization is even more obvious when the network load increases, that is, the high probability node has even higher probability and the low probability node has even lower probability. The reason is that given a fixed set of s-d pairs to choose, when the network load is high, the traffic pattern is more certain. That is, under high traffic load, the set of requests change less

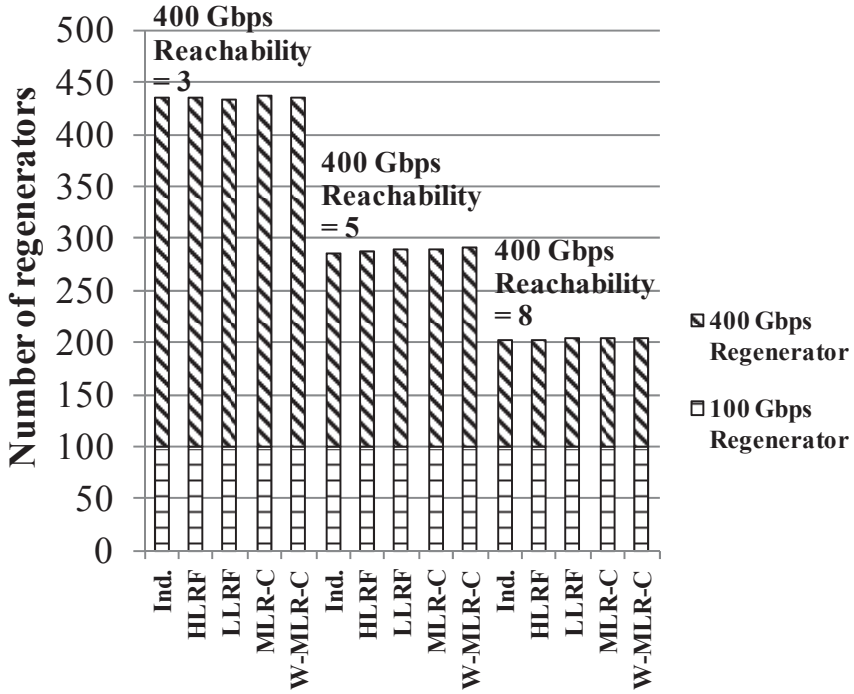

Figure 3.17. Number of regenerators vs. different reachabilities of 400 Gbps signal for 75-node network

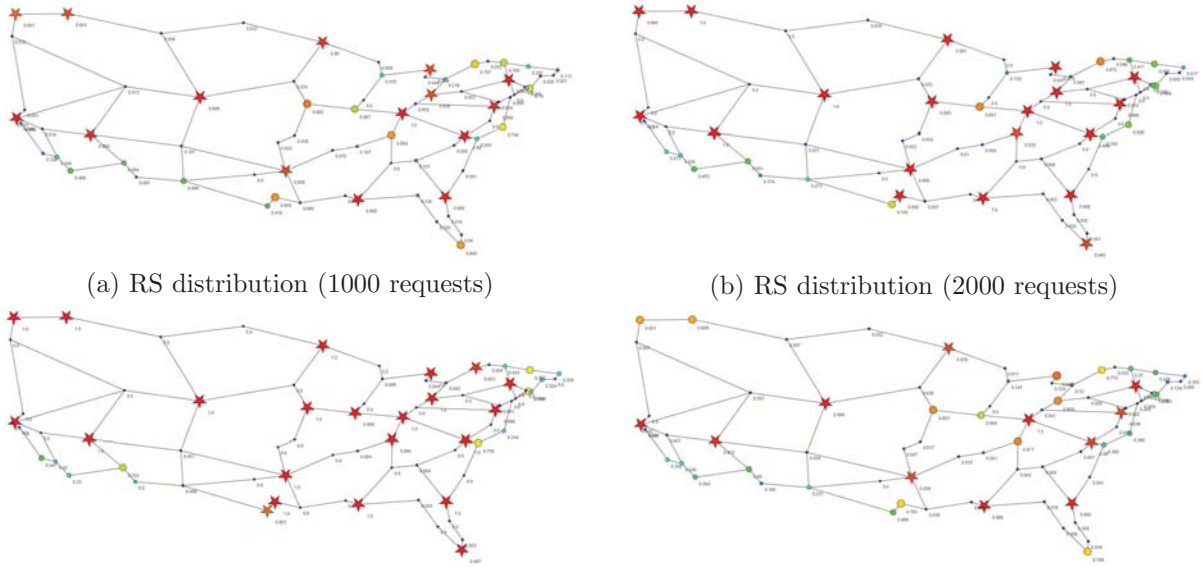

(a) RS distribution (1000 requests)

(b) RS distribution (2000 requests)

(c) RS distribution (3000 requests)

(d) RS distribution (SDPE)

Figure 3.18. RS distribution under uniform traffic

in different simulation runs than the low traffic load. The RS distribution is more certain when the traffic pattern is more certain.

To further evaluate the probabilities under different network load, we have the following statistical calculation. First, we have the average probability of $prob_{i,j}$ under J different network loads, which is $prob_i = \frac{\sum_{j=1}^{J} prob_{i,j}}{J}$. Then, we calculate the standard deviation of $prob_{i,j}$ under J different network loads, which is $\sigma_i = \sqrt{\frac{\sum_{j=1}^{J}(prob_{i,j}-prob_i)^2}{J}}$. Finally, we define the Standard Deviation-weighted Probability Expectation (SDPE) of node i as (1-σ_i) $\times$ $prob_i$. SDPE combines the average probability and standard deviation of node i under different network load. If a node has high SDPE, it means this node has constantly high probability of being chosen as a RS under different network load. Figure 3.18d shows the network based on SDPE. We can see that the polarization is still obvious in SDPE values. This polarization suggests a way to select RSs when traffic demands are uncertain. We can first choose the nodes with extremely high SDPE as a base, and then add additional RSs according to the real traffic demands.

Experiment 6. In the sixth experiment, we study how the RSs are distributed in the network under non-uniform traffic. The simulation parameters are the same as those of Experiment 5, except that we choose 25 most populated nodes out of the 75 nodes, and these nodes' probabilities of being chosen as sources or destinations are 10 times higher than the other 50 nodes. Figure 3.19a to 3.19c show the RS distribution under network load of 1000, 2000, and 3000 total requests, respectively, with non-uniform traffic. Figure 3.19d shows the RS distribution based on SDPE.

From Figure 3.19a to 3.19d, we can see that the observations obtained under uniform traffic are also true under non-uniform traffic. Some nodes have extremely high probabilities of being selected as RSs, while some nodes have very low probabilities. This polarization becomes more obvious when the network load increases. Compare Figure 3.18d and Figure 3.19d, we find that the sets of high probability nodes are very similar under uniform traffic

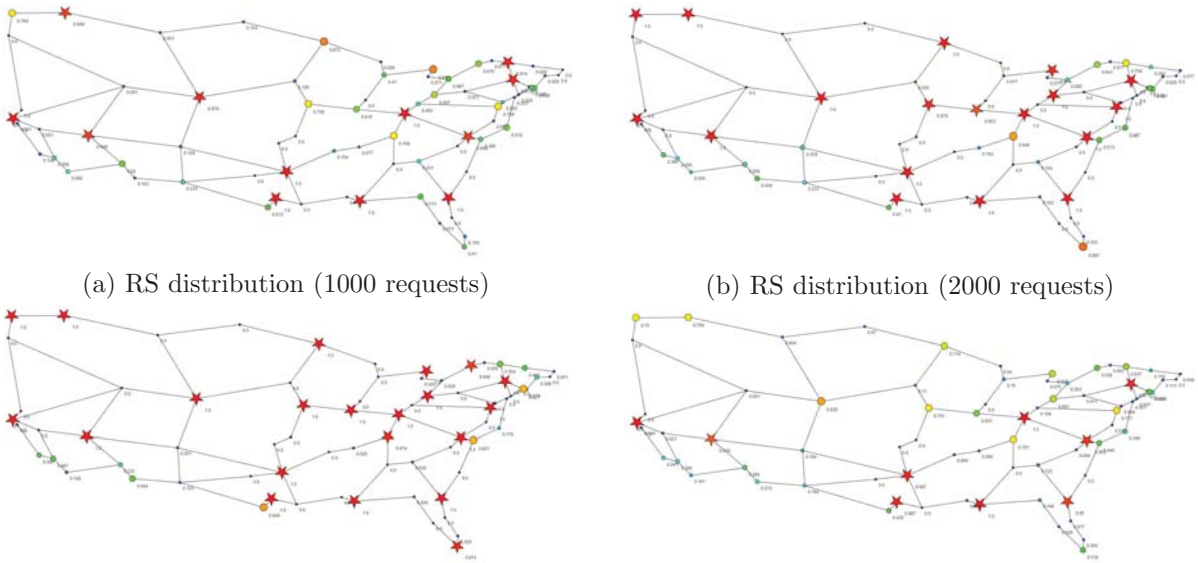

(a) RS distribution (1000 requests)

(b) RS distribution (2000 requests)

(c) RS distribution (3000 requests)

(d) RS distribution (SDPE)

Figure 3.19. RS distribution under non-uniform traffic

and non-uniform traffic. In Figure 3.19d, there are 9 stars and 8 out of them are also stars in Figure 3.18d. It further justifies our proposed method of selecting RSs. Since there are certain nodes having high probabilities of being chosen as RSs, under different traffic patterns and different network load, we can select them as a base and add additional RSs when necessary.

3.6 Conclusion

In this chapter, we focus on the problem of RS selection for MLR optical networks (MLR-RSS), which aims to minimize the number of RSs when routing is given with a request. We show that MLR-RSS is NP-complete, and then formulate an ILP model to solve the problem. Two heuristic algorithms and two approximation algorithms are proposed, named Independent algorithm, Sequential algorithm, MLR-combined algorithm, and Weighted MLR-combined algorithm. The numerical results show the performance comparison of these algorithms and show that the Weighted MLR-combined algorithm outperforms other algorithms.

The Weighted MLR-combined algorithm requires not more than one RS than the ILP, showing near optimal performance. It is shown that the MLR approach can save more than 20% compared to using SLR approach for each line rate independently and then combining them. The RS distribution shows that certain nodes in the network are more likely to be selected as RSs than the other nodes, under both uniform traffic and non-uniform traffic. It suggests a way for selecting RSs, that is, selecting the nodes with high SDPE first, and then adding extra RSs when necessary.

CHAPTER 4

RS SELECTION FOR MLR OPTICAL NETWORKS WITH FLEXIBLE ROUTING

In this chapter, we study two RS selection problems in MLR optical networks, when the routing is not given with a request and can be flexible.[1] One research problem's objective is to minimize the number of RSs, while the other problem's objective is to minimize the combined cost of RSs and regenerators. ILP models are formulated for both problems. We then present our heuristic approaches based on three steps, namely ordering of the requests, routing of the requests, and post processing. The performance of the algorithms and the ILP is compared via simulation and results show that our proposed heuristic approaches have near-optimal performance. Results suggest that we can save around 20% in the combined cost of RSs and regenerators, if we select RSs wisely.

4.1 Introduction

In optical networks, physical degradation effects, such as linear and non linear physical layer impairments cause the signal quality to degrade as the signal propagates through the network [17]. In MLR optical networks, different line rates may suffer from different levels of impairments. Regenerators are used to restore the signal quality. It is desirable to concentrate regenerators in a few properly selected RSs in order to reduce both CAPEX and

[1] ©2012 IEEE. Reprinted, with permission, from Weisheng Xie, Jason P. Jue, Xi Wang, Qiong Zhang, Qingya She, Paparao Palacharla, Motoyoshi Sekiya, "Regenerator Site Selection for Mixed Line Rate Optical Networks with Flexible Routing," *Int. Conference on Optical Networking Design and Modeling (ONDM)*, April 2012, and ©2013 IEEE. Reprinted, with permission, from Weisheng Xie, Jason P. Jue, Xi Wang, Qiong Zhang, Qingya She, Paparao Palacharla, Motoyoshi Sekiya, "Regenerator Site Selection and Regenerator Placement for Mixed Line Rate Optical Networks," *Int. Conference on Computing, Networking, and Communications (ICNC)*, January 2013

OPEX. The research challenge is how to properly select a set of RSs in an arbitrary MLR optical network. The research problem in this chapter is different from that in Chapter 3, in that routing is not given with each connection request.

In this chapter, we consider two research problems related to RS selection in MLR optical networks, when routing is not given with each connection request. The first problem is called RS selection in MLR optical networks with flexible routing (MLR-RSSFR), whose objective is to minimize the number of RSs while satisfying all the connection requests. However, selecting as few RSs as possible may lead to longer paths for some connection requests, and thus increase the regenerator cost. To address this problem, we propose the second research problem named RS selection and regenerator placement in MLR optical networks with flexible routing (MLR-RSSRP), whose objective is to minimize the combined cost of RSs and regenerators. We formulate the ILP models and propose heuristic approaches for both problems. The heuristic approaches are based on three steps: ordering of the requests, routing of the requests, and post processing. Simulation on both small-scale and large-scale networks is conducted to compare the performance of our algorithms and the ILP models. We make the following assumptions: 1) the links in the optical network are bidirectional; 2) routing is not given for each connection request; and 3) the number of regenerators in a RS is not limited.

The rest of this chapter is organized as follows. In Section 4.2, we show the network model used and show that both problems are NP-hard. In Section 4.3, we give a formal problem statement of the MLR-RSSFR problem, then formulate an ILP model and propose heuristic approaches for MLR-RSSFR. In Section 4.4, we discuss the problem statement, ILP formulation, and heuristic approaches for MLR-RSSRP. Simulation results are shown in Section 4.5. Finally, we give a summary of our work in Section 4.6.

4.2 Network Model and NP-Hardness

The optical network can be represented as a graph $G(\mathbf{V}, \mathbf{E})$, where $\mathbf{V}$ is a set of nodes and $\mathbf{E}$ is a set of edges. For each request, wavelengths of the requested line rate are reserved along a path, and regenerators are placed in the RSs along the path if needed.

In this chapter, reachability is used to measure the effect of impairments. The reachabilities of different line rates are different because of different physical impairments. Thus, we use a set of reachabilities $\mathbf{A}$ to denote different line rates' reachabilities. For example, in Figure 4.1, suppose we have two different line rates, lower rate l_1 and higher rate l_2, and the reachabilities for l_1 and l_2 are 2000 km and 1200 km, respectively. Thus, in Solution I, for r_1 from Node 1 to Node 4, we need 1 regenerator for l_1. For r_2 from Node 2 to Node 4, we need 1 regenerator for l_2. If any regenerators are placed at a node, the node is considered to be a RS.

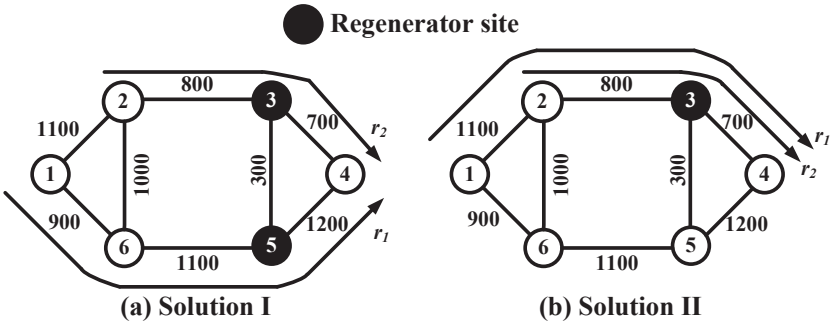

Figure 4.1. Example of network and regenerator placement (link lengths in km)

In [31], it is proved that the RS selection problem in SLR optical networks with flexible routing is NP-hard. Since that problem is a special case of our MLR-RSSFR problem when only a single line rate is available, our problem is also NP-hard. Furthermore, the MLR-RSSFR problem is a special case of the MLR-RSSRP problem, when the cost of a RS is 1 and the cost of a regenerator is 0, thus the MLR-RSSRP problem is NP-hard as well. Since both MLR-RSSFR and MLR-RSSRP are NP-hard, we will concentrate on formulating the

ILP models and developing heuristic approaches for both problems, instead of trying to find the polynomial-time optimal algorithms.

4.3 Problem MLR-RSSFR

4.3.1 Problem Formulation

The RS selection problem in MLR optical networks with flexible routing (MLR-RSSFR) can be stated as follows:

Given physical topology $G(\mathbf{V}, \mathbf{E})$, where $\mathbf{V}$ is a set of nodes and $\mathbf{E}$ is a set of edges, a set of line rates $\mathbf{L}$, $l_k \in \mathbf{L}$, $1 \leq k \leq |\mathbf{L}|$, a reachability set $\mathbf{A}$, $a_k \in \mathbf{A}$, $1 \leq k \leq |\mathbf{L}|$, where a_k is the reachability of line rate l_k, and a set of traffic demands $\mathbf{R}$ in which a request is defined as $r_{s,d,k}$, where s is a source, d is a destination, k is the requested line rate, $r_{s,d,k}$ is the requested number of line rate l_k's wavelengths from s to d. Note that for the MLR-RSSFR problem, the number of wavelengths of each request does not matter because the objective of MLR-RSSFR is to minimize the number of RSs, and RSs have to be placed even if only one wavelength is required, as long as the signal is not reachable. However, in the MLR-RSSRP problem, we need to count the number of regenerators and the regenerators are counted per wavelength, thus the number of wavelengths of each request will matter.

Find the routing for each request and the placement of RSs at nodes with the objective of minimizing the total number of RSs, such that

1. traffic constraint: all the requests are assigned the requested line rate, which means that no blocking occurs;

2. impairment constraint: along any path, the length of each segment without regenerators does not exceed the corresponding line rate l_k's reachability limit a_k.

An example is shown in Figure 4.1. Suppose we have two requests: r_1 from Node 1 to Node 4, whose requested line rate is l_1, and r_2 from Node 2 to Node 4, whose requested line

rate is l_2. The reachabilities for l_1 and l_2 are 2000 km and 1200 km, respectively. In Solution I, r_1 has the routing (1-6-5-4), while r_2 has the routing (2-3-4). This solution results in two RSs. If we change the routing of r_1 to (1-2-3-4), only one RS is required, which is Node 3. Thus, Node 3 is the optimal RS selection because only one site is needed, which is the minimum possible number of RSs for this set of requests.

4.3.2 ILP Formulation

The ILP model is based on a directed reachability graph in which auxiliary links are constructed between node pairs whose shortest path distance is shorter than or equal to the reachability. For a given physical topology $G(\mathbf{V}, \mathbf{E})$, its reachability graph corresponding to the reachability a_k (line rate l_k's reachability) is defined as $G'_k(\mathbf{V'}, \mathbf{E'})$. $G'_k(\mathbf{V'}, \mathbf{E'})$ is constructed as follows. The set of nodes $\mathbf{V'}$ is the same set of nodes $\mathbf{V}$ in the given physical topology, $\mathbf{V'} = \mathbf{V}$. For any pair of nodes in $\mathbf{V'}$, v_1 and v_2, if their shortest path is shorter than or equal to the reachability a_k, that is, they are reachable from each other without any regeneration, then two directed links (one is from v_1 to v_2 while the other is from v_2 to v_1) are added between this node pair. Thus, if a pair of nodes are not directly connected with any auxiliary links, but are connected through some intermediate nodes, then regeneration is needed at these intermediate nodes. These nodes are where RSs and regenerators are placed. Finally, the costs of the directed links are set to 1. Under different reachability a_k, a given physical topology $G(\mathbf{V}, \mathbf{E})$ can have different reachability graphs. Figure 4.2 shows an example of the reachability graphs of the physical topology shown in Figure 4.1, when the reachabilities are 1200 km and 2000 km, respectively.

We present the ILP formulation for MLR-RSSFR in the following. First, we define some useful notations and variables.

Input parameters

- $\mathbf{R} = [r_{s,d,k}]_{|\mathbf{V}|\times|\mathbf{V}|\times|\mathbf{L}|}$: set of requests;

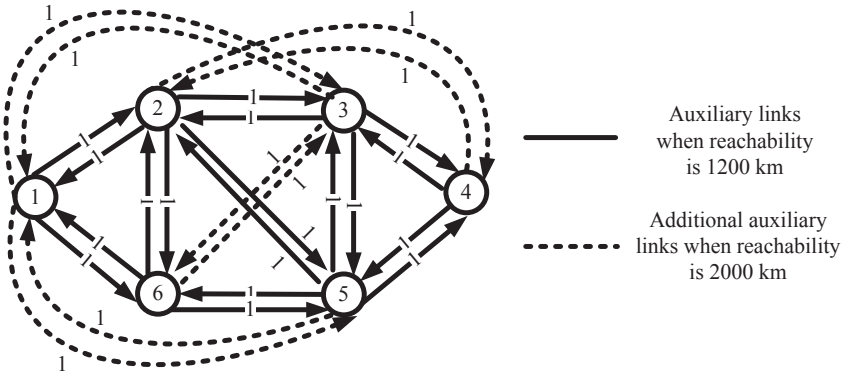

Figure 4.2. Example of reachability graphs

• **E'** $= [e'_{i,j,k}]_{|\mathbf{V}|\times|\mathbf{V}|\times|\mathbf{L}|}$: $e'_{i,j,k}$ equals to 1 if there is an edge from Node i to Node j in G'_k, otherwise 0;

• VL: a pre-defined very large number.

Variables of ILP

• $\mathbf{X} = [x^{s,d}_{i,j,k}]^{|\mathbf{V}|\times|\mathbf{V}|}_{|\mathbf{V}|\times|\mathbf{V}|\times|\mathbf{L}|}$: $x^{s,d}_{i,j,k}$ equals to the value of $r_{s,d,k}$ if edge $e'_{i,j,k}$ is on the path of request $r_{s,d,k}$;

• $\mathbf{Y} = [y^{s,d_1}_{i,k}]^{|\mathbf{V}|\times|\mathbf{V}|}_{|\mathbf{V}|\times|\mathbf{L}|}$: $y^{s,d}_{i,k}$ is the number of line rate l_k's regenerators placed at Node i on the path from s to d;

• $\mathbf{S} = [s_i]_{|\mathbf{V}|}$: s_i equals to 1 if Node i is selected as a RS, otherwise 0.

Objective

The objective of MLR-RSSFR is to minimize the following function:

$$min\ \ obj = \sum_i s_i \tag{4.1}$$

Constraints

$$\sum_j x^{s,d}_{s,j,k} - \sum_j x^{s,d}_{j,s,k} = r_{s,d,k}, \forall 1 \le s \le |\mathbf{V}|, 1 \le d \le |\mathbf{V}|, 1 \le k \le |\mathbf{L}| \tag{4.2}$$

$$\sum_{j} x_{j,d,k}^{s,d} - \sum_{j} x_{d,j,k}^{s,d} = r_{s,d,k}, \forall 1 \leq s \leq |\mathbf{V}|, 1 \leq d \leq |\mathbf{V}|, 1 \leq k \leq |\mathbf{L}| \tag{4.3}$$

$$\sum_{j} x_{i,j,k}^{s,d} = \sum_{j} x_{j,i,k}^{s,d}, \forall 1 \leq s \leq |\mathbf{V}|, 1 \leq d \leq |\mathbf{V}|, 1 \leq k \leq |\mathbf{L}|, 1 \leq i \leq |\mathbf{V}|, i \neq s, d \tag{4.4}$$

Constraints 4.2 - 4.4 guarantee the traffic constraint. In detail, Constraint 4.2 guarantees that the source node generates the lightpath corresponding to the required line rate. Constraint 4.3 ensures that the destination can receive the same line rate's lightpath generated at the source node. Constraint 4.4 ensures that the incoming and outgoing flows are the same for any intermediate nodes.

$$x_{i,j,k}^{s,d} \leq e'_{i,j,k}, \forall 1 \leq s \leq |\mathbf{V}|, 1 \leq d \leq |\mathbf{V}|, 1 \leq i \leq |\mathbf{V}|, 1 \leq j \leq |\mathbf{V}|, 1 \leq k \leq |\mathbf{L}| \tag{4.5}$$

Constraint 4.5 guarantees that every link of the path for each request is on the corresponding reachability graph G'_k.

$$y_{i,k}^{s,d} = \sum_{j} x_{i,j,k}^{s,d}, \forall 1 \leq s \leq |\mathbf{V}|, 1 \leq d \leq |\mathbf{V}|, 1 \leq k \leq |\mathbf{L}|, 1 \leq i \leq |\mathbf{V}|, i \neq s \tag{4.6}$$

Constraint 4.6 guarantees the impairment constraint, by placing regenerators on each intermediate node of the path for a request on the corresponding reachability graph G'_k.

$$s_i \geq \frac{\sum\limits_{s,d,k} y_{i,k}^{s,d}}{VL}, \forall 1 \leq i \leq |\mathbf{V}| \tag{4.7}$$

Constraint 4.7 ensures that a RS is placed at a node when there are any regenerators placed in this node.

4.3.3 Heuristic Approaches

We develop heuristic approaches for the MLR-RSSFR problem based on three steps. The first step is the ordering of the requests, that is, deciding which request will be routed first. A desired ordering strategy is to let the later routed requests have a better chance to reuse the RSs placed for the earlier routed requests. The second step is the routing for each request. A desired routing strategy should route the request to the existing RSs and result in as few additional RSs as possible. In the third step, we do some post processing to further improve the results. Our heuristic approaches follow this ordering, routing, and post processing process. In this section, we discuss the strategies for the above three steps and propose our heuristic approaches based on these strategies.

Ordering of the requests

Ordering based on flexibility *Flexibility* is defined as the number of choices a request has to place minimum number of RSs. Figure 4.3 shows the flexibility of a request, whose line rate's reachability is 500 km. In this example, we suppose every link has the same distance 100 km, thus only one regenerator is needed for each path shown in Figure 4.3. The nodes that can be selected as RSs are shown in black. For example, the length of Path 1 is 600 km and the reachability of the request's line rate is 500 km. One regenerator is sufficient to satisfy this request. This regenerator can be placed at one of the following five nodes: Node 2, Node 3, Node 4, Node 5, or Node 6. Thus, this request has 5 choices to place one regenerator and the flexibility of this request is 5.

Since the requests with greater flexibilities have more choices to place minimum number of RSs, they have a better chance to reuse the RSs that are placed for the requests with lower flexibilities. Thus, we can order the requests by their flexibilities and process the requests with lowest flexibilities first. We call this ordering least flexible first (LFF).

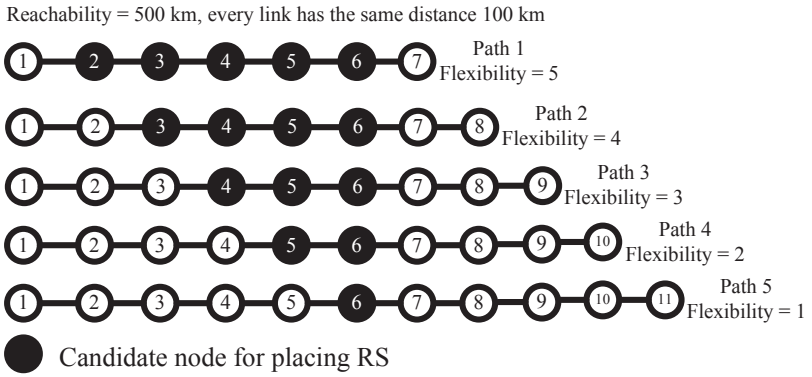

Figure 4.3. Example of flexibilities under different path lengths

Let $f_{s,d,k}$ denote the flexibility from Node s to Node d using line rate l_k. $f_{s,d,k}$ is equal to the number of shortest paths from Node s to Node d on line rate l_k's reachability graph G'_k. For example, in Figure 4.4, there are three shortest paths from Node 1 to Node 4 when the reachability is 2000 km: (1-2-4), (1-3-4), and (1-5-4), and thus the flexibility is 3. $f_{s,d,k}$ can be obtained by running the Breath-First-Search (BFS) algorithm to find all the shortest paths between Node s and Node d on G'_k. More specifically, the BFS algorithm starts from Node s and stops at the depth where destination d is reached. We then calculate the number of paths that have Node d as the destination and record the number as $f_{s,d,k}$. Note that the flexibilities of all the node pairs in all the reachability graphs can be pre-calculated as an input to our heuristic algorithm.

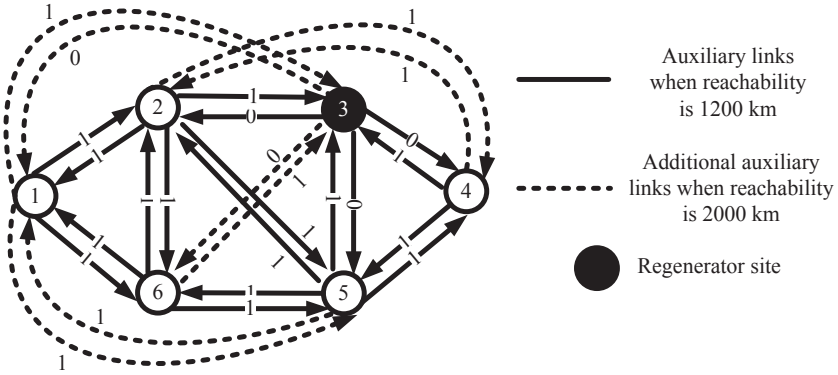

Figure 4.4. Example of MARS algorithm

Ordering based on required number of RSs For a connection request $r_{s,d,k}$, suppose its shortest path distance on G'_k is $SP(s,d,k)$, then the required number of RSs is $SP(s,d,k)$ - 1. If requests that require the most RSs are routed first, we call it most RSs first (MRF). If requests that require the fewest RSs are routed first, we call it fewest RSs first (FRF).

Ordering based on line rates In this ordering strategy, we order the requests according to their corresponding line rates. If requests with highest line rate are routed first, we call this ordering high line rate first (HLRF). If requests with lowest line rate are routed first, we call it low line rate first (LLRF).

Routing of the requests

Given an ordered set of requests, we find the routing for each request one by one starting from the first request. Initially, all the costs of the directed links are set as 1. For a request, the shortest path algorithm is applied to find the path with minimum total cost between source and destination. When a node has been selected as RS, all the costs of the egress links of this node are set to 0. This process is repeated for all the requests. In this way, a request can find the minimum number of additional RSs for itself. Thus, we name this routing algorithm the minimum additional RSs (MARS) algorithm. The full MARS algorithm is described in Algorithm 4. An example of the MARS algorithm is shown in Figure 4.4. Suppose Node 3 has been selected as a RS and all the costs of Node 3's egress links are set as 0. If the signal reachability is 1200 km, then for a request from Node 1 to Node 4, it will choose the path (1-2-3-4) and Node 2 will be a new RS. If the signal reachability is 2000 km, for a request from Node 1 to Node 4, it will choose the path (1-3-4) and no new RS will be selected.

Post Processing

The above routing step only adds RSs without deleting any of them. However, it is possible that some earlier selected RS v may become unnecessary when one or several later selected

Algorithm 4 Minimum Additional Regenerator Sites (MARS)

Input: a set of reachability graphs under different reachabilities G'_k(**V'**, **E'**) and the ordered request set **R'**.
Output: a subset **U** $\subseteq$ **V** that denotes the nodes selected as RSs.
//Main procedure
Begin
U $= \emptyset$.
for all requests r_i, $r_i \in$ **R' do**
  //Find the RSs for r_i
  I $= \emptyset$.
  Run Dijkstra's algorithm on the corresponding reachability graph according to r_i's required line rate to find the shortest path between source and destination of r_i.
  Take the intermediate nodes of the shortest path into the set **I**.
  //Update reachability graphs
  for all node $v \in$ **I** and $v \notin$ **U do**
    for all reachability graphs G'_k(**V'**, **E'**) **do**
      Set the weights of all the egress links of v as 0.
    end for
  end for
  U $=$ **U** $\bigcup$ **I**.
end for
End

RSs can cover the source-destination pairs that v originally covered. An example is shown in Figure 4.5. Suppose we have two connection requests: r_1 from Node 1 to Node 4 requires line rate l_1, and r_2 from Node 2 to Node 4 requires line rate l_2. Suppose the reachabilities of line rate l_1 and line rate l_2 are 1200 km and 2000 km, respectively. Using the MARS algorithm, the results will be choosing Path 1 for r_1 and choosing Path 2 for r_2. Node 5 and Node 3 are selected as RSs, as shown in Figure 4.5(a). However, as Figure 4.5(b) shows, if we change r_1 from Path 1 to Path 3, we only need one RS, so choosing Node 5 as a RS becomes unnecessary.

Thus we propose a post processing approach to improve our solutions. For every RS v in the output of the routing step, we delete v and check the connection requests passing through v. These requests have to be switched to other paths. If the requests can be routed with the remaining RSs, then v is deleted, otherwise v remains in the set of RSs. This

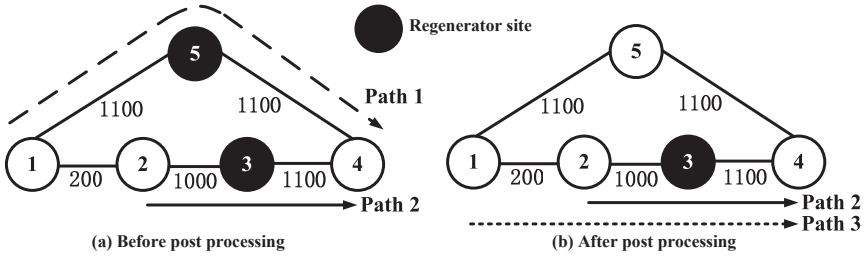

Figure 4.5. Example of post processing

process is repeated for every RS. We check if a request r_i can be routed with the remaining RSs in the following steps: take r_i's corresponding reachability graph; if a node is not a RS and this node is not the source of r_i, remove all of its egress links; check if a path can be found on this modified reachability graph.

Complete heuristic approaches

Our heuristic approaches follow the three-step process: ordering of the requests, routing of the requests, and post processing. Initially, for each line rate l_k, whose signal reachability is a_k, we remove from set $\mathbf{R}$ all the pairs of nodes $(a,\ b)$, whose requested line rate is l_k and the shortest path between a and b has length at most a_k. This is because paths with length at most a_k do not need any regenerator. Depending on different ordering strategies, we have different heuristic approaches. In the first heuristic approach, we order the requests according to least flexible first (LFF). Then, if any requests have the same flexibility, requests of highest line rate will be routed first. We name this algorithm the Least Flexible First-High Line Rate First (LFF-HLRF) algorithm. The full LFF-HLRF algorithm is described in Algorithm 5.

For comparison, we also propose other heuristics by varying the requests ordering strategies. If we order the requests by HLRF, and then requests having the same line rate are sorted by MRF, we then have the HLRF-MRF algorithm. Similarly, we have the LLRF-MRF algorithm. We have implemented and tested all possible combinations of two ordering

Algorithm 5 Least Flexible First-High Line rate first (LFF-HLRF)

Input: physical topology $G(\mathbf{V}, \mathbf{E})$, the reachability set **A**, and the request set **R**.
Output: a subset $\mathbf{U} \subseteq \mathbf{V}$ that are the nodes selected as RSs.
//Main procedure
Begin
//Remove requests that do not need regeneration
For each line rate l_k, whose signal reachability is a_k, we remove from **R** the request whose line rate is l_k and the shortest path between source and destination has length at most a_k.

//Ordering of the requests
Order the requests based on LFF. For requests having the same flexibility, order them based on HLRF. Denote the ordered set of requests as **R'**.
//Reachability graphs construction
for all reachabilities a_k, $a_k \in$ **A do**
  Construct the reachability graph G'_k(**V'**, **E'**) based on corresponding reachability a_k.
end for
//Routing of the requests
Run the MARS algorithm on set **R'** to obtain **U**, the set of RSs
//Post processing
for all v *in* **U do**
  U = **U** - v
  if not all the requests in **R'** can be routed with the RSs in **U then**
    U = **U** $\bigcup v$
  end if
end for
End

schemes out of LFF, MRF, FRF, HLRF, and LLRF, but due to limited space, we have only included the simulation results for those combinations that yielded the best performance.

4.4 Problem MLR-RSSRP

Different from Problem MLR-RSSFR, the objective of Problem MLR-RSSRP is to minimize the combined cost of RSs and regenerators. Concentrating RSs may lead to longer paths for some connection requests, resulting in more regenerators placed. If the cost (both CAPEX and OPEX) of a RS is much higher than that of a regenerator, then concentrating the RSs is cost-efficient; however, if the cost of a regenerator is close to the cost of a RS, then the

cost of a regenerator is not negligible. Thus, besides Problem MLR-RSSFR, we also need to consider Problem MLR-RSSRP.

In the following problem formulation, ILP, and heuristic algorithms sub-sections, we only emphasize the differences of MLR-RSSRP from MLR-RSSFR, because of the similarities between these two problems.

4.4.1 Problem Formulation

Besides all the given parameters in MLR-RSSFR, in MLR-RSSRP we are also given a set of regenerator costs $\mathbf{C}$, $c_k \in \mathbf{C}$, $1 \leq k \leq |\mathbf{L}|$, where c_k is the cost of a line rate l_k's regenerator and the cost of a RS C_{RS}. The objective of the MLR-RSSRP problem is to minimize the total cost of RSs and regenerators.

For the example shown in Figure 4.1, suppose the normalized costs of line rate l_1 and l_2's regenerators are 1 and 3, respectively. The normalized cost of a RS is 5. r_1 requests two line rate l_1's wavelengths, while r_2 requests three line rate l_2's wavelengths. Then, in Solution I, a total of 2 l_1's regenerators, 3 l_2's regenerators, and 2 RSs are needed, with a total cost of 21. Similarly, in Solution II, the total cost is 16, which is the minimum possible total cost for this example.

4.4.2 ILP Formulation

We can reuse most of the ILP model for MLR-RSSFR except for the following two modifications:

Adding two input parameters

- $\mathbf{C} = [c_k]_{|\mathbf{L}|}$: set of regenerator cost;
- C_{RS}: cost of a RS.

Changing the objective to the following

$$min\ obj = C_{RS} \cdot \sum_{i} s_i + \sum_{s,d,i,k} c_k \cdot y_{i,k}^{s,d} \tag{4.8}$$

4.4.3 Heuristic Approaches

The MLR-RSSRP problem can be solved with a modified three-step heuristic approach that solves the MLR-RSSFR problem. We describe the modifications below.

Ordering of the requests

The LFF, HLRF, and LLRF ordering strategies are reused without any modifications. The ordering strategies based on required number of RSs are changed to ordering strategies based on cost of connection request. Given a connection request $r_{s,d,k}$, its cost is $r_{s,d,k} \cdot c_k \cdot NR + C_{RS} \cdot NR$, where NR is the minimum number of RSs required to satisfy this request. NR can be obtained by running the shortest path algorithm on the reachability graph G'_k(**V'**, **E'**) to find out a path with the fewest hop counts. The intermediate nodes of this path are where regeneration is needed. If requests that require the highest cost are routed first, we call it highest cost first (HCF). If requests that require the lowest cost are routed first, we call it lowest cost first (LCF).

Routing of the requests

The routing strategy for MLR-RSSRP is similar to the MARS algorithm except for one modification in the reachability graph update. Given a request $r_{s,d,k}$, the costs of the egress links of a node in the reachability graph G'_k(**V'**, **E'**) are set as $r_{s,d,k} \cdot c_k + C_{RS}$, if this node is not a RS; or $r_{s,d,k} \cdot c_k$, if this node has been selected as a RS. The other steps are the same as the MARS algorithm.

Post processing

The post processing step is also needed in solving the MLR-RSSRP problem. The post processing in MLR-RSSRP is different from that in MLR-RSSFR when checking if a selected RS should be deleted or not. In MLR-RSSRP, a RS can be deleted only when all the requests can be routed with the remaining RSs and with lower total cost.

4.4.4 Baseline Algorithm

We use a baseline algorithm to compare with our heuristic approaches. The baseline algorithm uses the shortest path routing for each connection request without considering the RS selection. However, the baseline algorithm always results in the fewest regenerators. Specifically, the baseline algorithm follows the following steps. For each connection request, a shortest path is found. We check from the source to the destination, and place RSs (if there is not any) and regenerators only when the signal needs regeneration.

4.5 Simulation Results

In this section, we present some simulation results to show the performance of our proposed heuristic algorithms and the ILP model, for both the MLR-RSSFR problem and the MLR-RSSRP problem.

The heuristic algorithms are implemented in Java, and the ILP model is solved by IBM ILOG CPLEX Optimization Studio $v12.2$. All the simulation experiments are performed on a server with 16×2.4 GHz processors and 12 GB memory. The ILP is only tested on the 24-node network shown in Figure 4.6, due to the exponential computation time of ILP. The heuristic algorithms are tested on both the 24-node network and the 75-node CORONET [1] shown in Figure 3.5.

In the simulation, we choose two line rates: 100 Gbps and 400 Gbps. The reachabilities of 100 Gbps and 400 Gbps are assumed to be 2000 km and 1200 km, respectively. In the

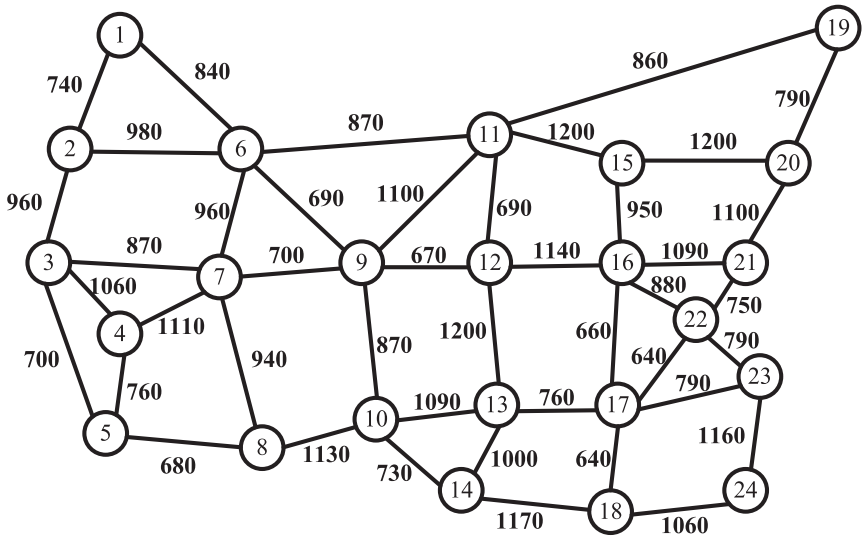

Figure 4.6. 24-node network topology (link lengths in km)

simulation, given a total number of requests, half of them are 100 Gbps requests and the other half are 400 Gbps requests, except Experiment 2 and Experiment 5, in which this ratio is changed. For each connection request, the number of requested wavelengths for each line rate is uniformly distributed in [1, 5]. The normalized costs of a 100 Gbps regenerator and a 400 Gbps regenerator are assumed to be 100 and 300, respectively. The normalized cost of a RS is assumed to be 1000, which is 10 times the cost of a 100 Gbps regenerator, except in Experiment 4, in which we test different RS cost. The experiment results are average values of 50 simulation runs on the 24-node network or 10,000 simulation runs on the 75-node CORONET. We have fewer simulation runs on the 24-node network due to the long running time of the ILP.

When generating connection requests, every node in the network has equal probability to be selected as source or destination. For each request, we randomly select a source and a destination. If the shortest path distance of this s-d pair is not greater than the corresponding line rate's reachability, we discard this s-d pair and randomly select another s-d pair until its shortest path distance is greater than the corresponding line rate's reachability. There are no two requests with the same end nodes, unless they require different line rates.

In the following experiments, Experiments 1 and 2 show the performance of the heuristics and ILP for the MLR-RSSFR problem with the objective of minimizing the RSs. Experiments 3 to 5 are for the MLR-RSSRP problem with the objective of minimizing the combined cost of RSs and regenerators. We have different heuristic approaches based on different request ordering strategies. Due to space limit, we only show the algorithms with the best results. For the MLR-RSSFR problem, we show the LFF-HLRF, HLRF-MRF, and LLRF-MRF algorithms. For the MLR-RSSRP problem, we show the LFF-HCF, HLRF-HCF, and LLRF-HCF algorithms.

Experiment 1. In the first experiment, we study the average number of RSs under different network load for the MLR-RSSFR problem.

We first test the heuristics and the ILP on the 24-node network. As Figure 4.7 depicts, the LFF-HLRF algorithm has slightly better performance than the HLRF-MRF or LLRF-MRF algorithm. The difference of the LFF-HLRF algorithm and the ILP is 14.2% on average, which is not more than 2 RSs in the 24-node network.

We then test the algorithms on the 75-node CORONET. From Figure 4.8, we can see that the LFF-HLRF algorithm has the best results among all the algorithms, showing the good performance of the LFF ordering strategy. The performance of the HLRF-MRF algorithm is better than the LLRF-MRF algorithm. The reason why the HLRF sorting is better than the LLRF sorting is that higher line rates have shorter reachabilities than lower line rates, and thus have less flexibility in most cases. By placing RSs for high line rates first, the requests of lower line rates have a better chance to reuse the RSs placed for higher line rates.

Experiment 2. In the second experiment, we study the average number of RSs under different ratios of 100 Gbps requests to the total number of requests, for the MLR-RSSFR problem.

For the experiment on the 24-node network, the total number of requests in the network is 40. The number of 100 Gbps requests changes from 0 to 100% of the total number of

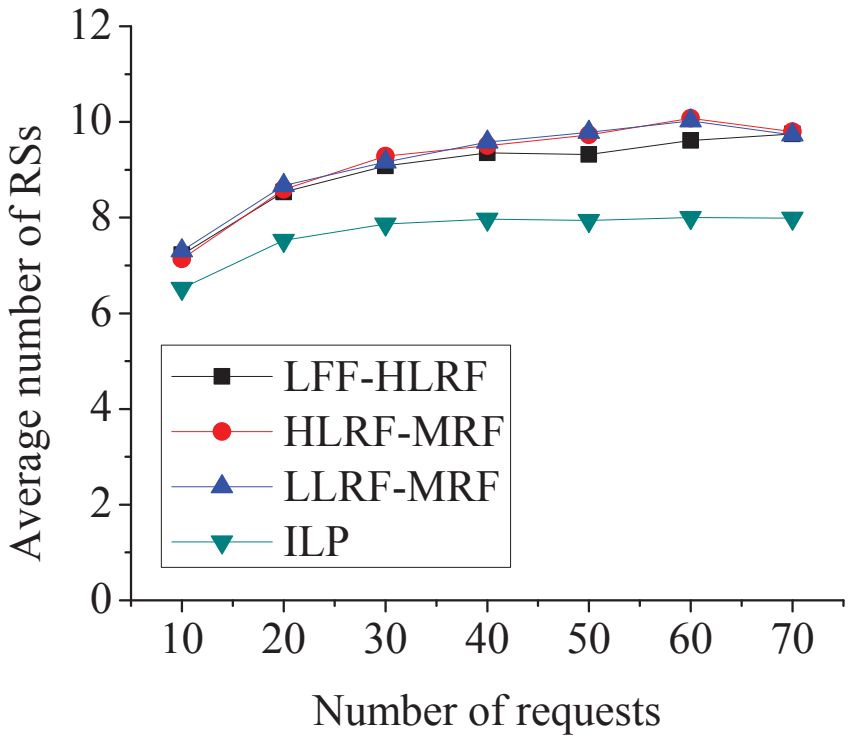

Figure 4.7. Average number of RSs vs number of requests for 24-node network

requests. From Figure 4.9, we can see that although the ILP has the best performance, the LFF-HLRF algorithm only increases the number of RSs by 14.4% on average, that is, not more than 2 additional RSs are required.

The algorithms are then tested on the 75-node network. The total number of requests in the network is 80. As Figure 4.10 depicts, the LFF-HLRF algorithm still outperforms the other algorithms. Figure 4.10 also shows that the HLRF-MRF algorithm and the LLRF-MRF algorithm have the same performance when ratio of 100 Gbps requests is 0 or 100%. The reason is that when the ratio of 100 Gbps requests is 0 or 100%, all the requests are either 400 Gbps requests or 100 Gbps requests. Then, the HLRF algorithm and the LLRF algorithm are the same since there is only one line rate's requests. Since 100 Gbps requests have longer reachabilities and requires fewer RSs compared to the 400 Gbps requests of the same path length, the total number of RSs decreases as the ratio of 100 Gbps requests increases.

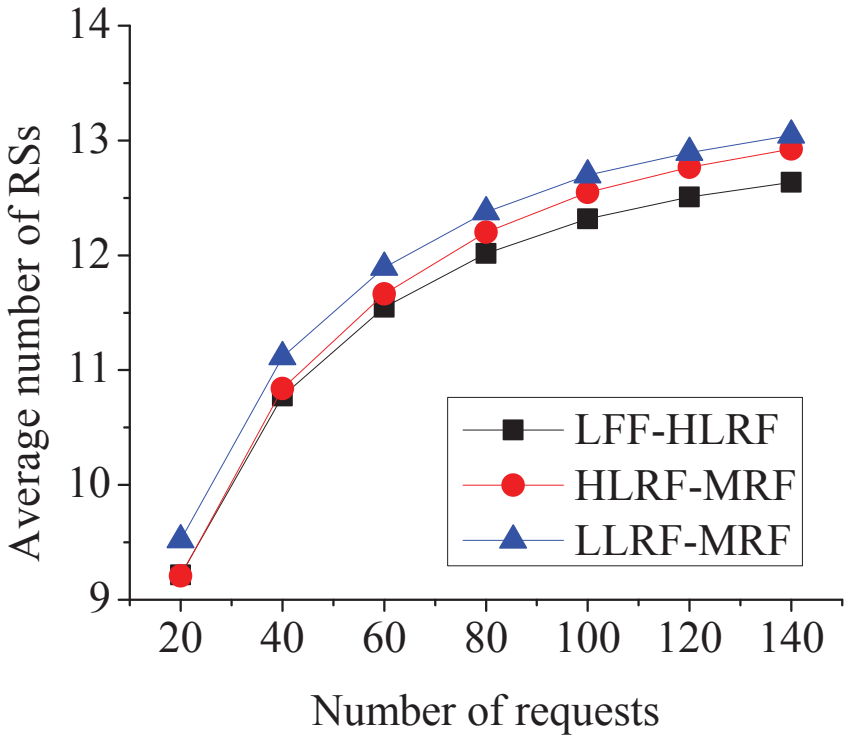

Figure 4.8. Average number of RSs vs number of requests for 75-node network

Experiment 3. In the third experiment, we study the total cost of RSs and regenerators under different network load, for the MLR-RSSRP problem.

Figure 4.11 shows the total RS and regenerator cost under different network load in the 24-node network. It is shown that the LFF-HCF algorithm increases the total cost by 4.3% on average, compared to the ILP. The baseline algorithm results in the highest cost under any network load.

From Figure 4.12, we can see that under the 75-node network, the LFF-HCF algorithm still has the best performance. The baseline algorithm increases the total cost by 20.0% on average, compared to the LFF-HCF algorithm.

Experiment 4. In the fourth experiment, we investigate the total RS and regenerator cost under different cost of a RS, for the MLR-RSSRP problem. The number of requests in the network is 80.

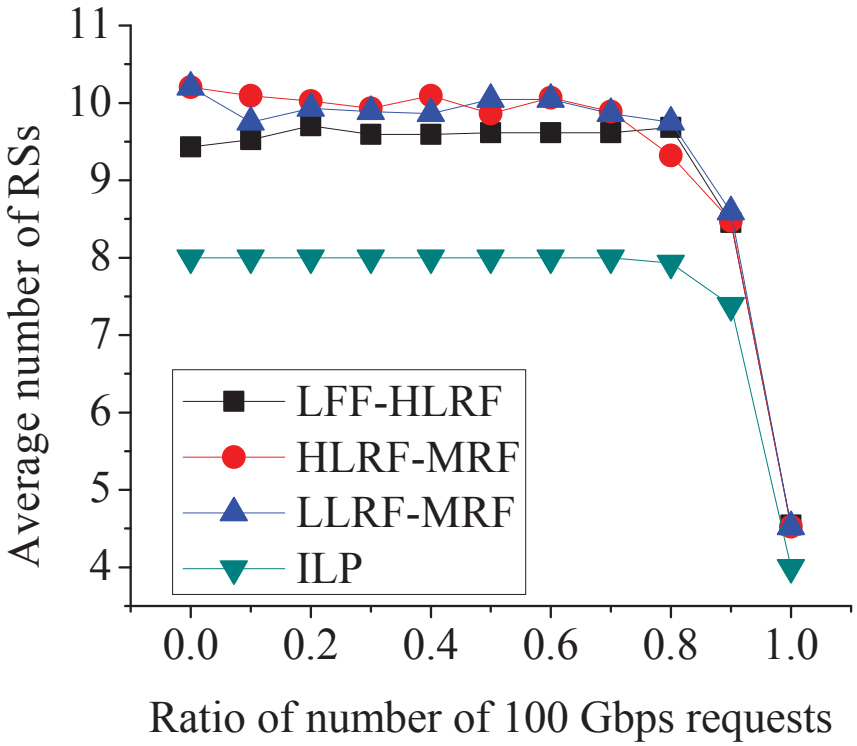

Figure 4.9. Average number of RSs vs. ratio of 100 Gbps requests in total number of requests for 24-node network

Figure 4.13 shows the experiment results on the 75-node CORONET. It is shown that when the cost of a RS is below 100 (same cost as a 100 Gbps regenerator), the LFF-HCF only has a slight decrease in total cost, compared to the baseline algorithm. When the cost of a RS is low, since the cost of a regenerator is higher than that of a RS, LFF-HCF uses shortest path routing, and thus the performance of LFF-HCF and the baseline algorithm are very close. However, along with the increase of the RS cost, the total cost obtained by LFF-HCF increases much slower than the baseline algorithm, because the LFF-HCF algorithm can concentrate regenerators to form fewer RSs when the RS cost is high. When the cost of a RS is 10 times the cost of a 100 Gbps regenerator, the cost saving of the LFF-HCF algorithm is 17.5%, compared to the baseline algorithm. When the cost of a RS is 100 times the cost of a 100 Gbps regenerator, the total cost obtained by the baseline algorithm is almost twice

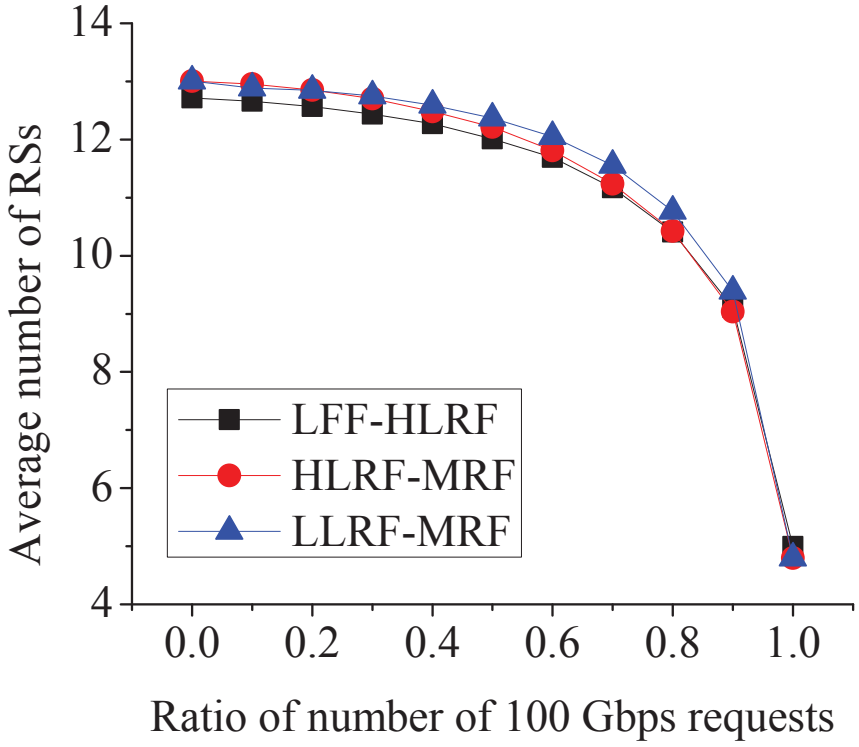

Figure 4.10. Average number of RSs vs. ratio of 100 Gbps requests in total number of requests for 75-node network

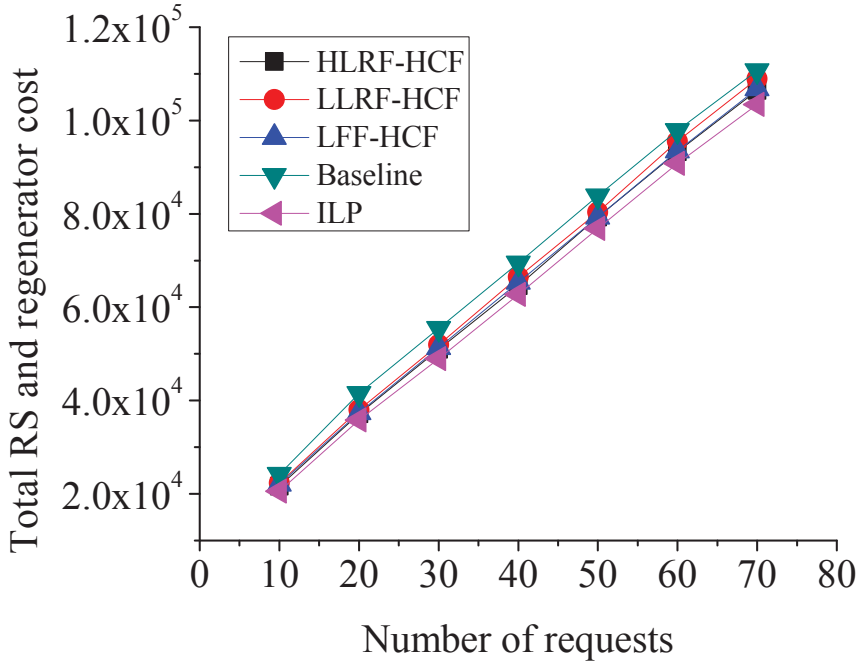

Figure 4.11. Total cost vs. number of requests for 24-node network

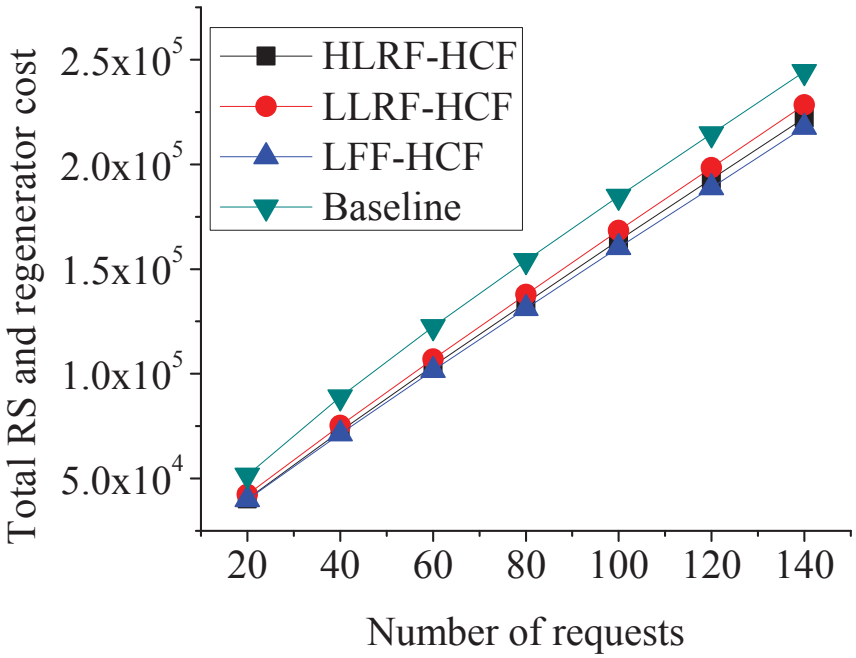

Figure 4.12. Total cost vs. number of requests for 75-node network

as much as that obtained by LFF-HCF. Thus, when the cost of a RS is higher than that of a regenerator, the RS concentration needs to be considered in order to save cost.

Figure 4.14 shows the separate equipment cost for Figure 4.13. We can see that when the cost of a RS is 1 or 10, the RS cost is negligible. When the cost of a RS is 100 or 1000, the LFF-HCF algorithm has significant lower RS cost than the baseline algorithm and almost the same cost of regenerators as the baseline algorithm. It shows that if we choose RSs wisely, it is possible to greatly reduce the number of RSs with only a little increase in the number of regenerators.

Experiment 5. In the fifth experiment, we study the total RS and regenerator cost under different ratios of 100 Gbps requests to the total number of requests, for the MLR-RSSRP problem. The number of requests in the network is 80, and the cost of a RS is 1000.

Figure 4.15 shows the experiment results on the 75-node CORONET. From Figure 4.15, we can see that the LFF-HCF algorithm outperforms the other three algorithms. The cost

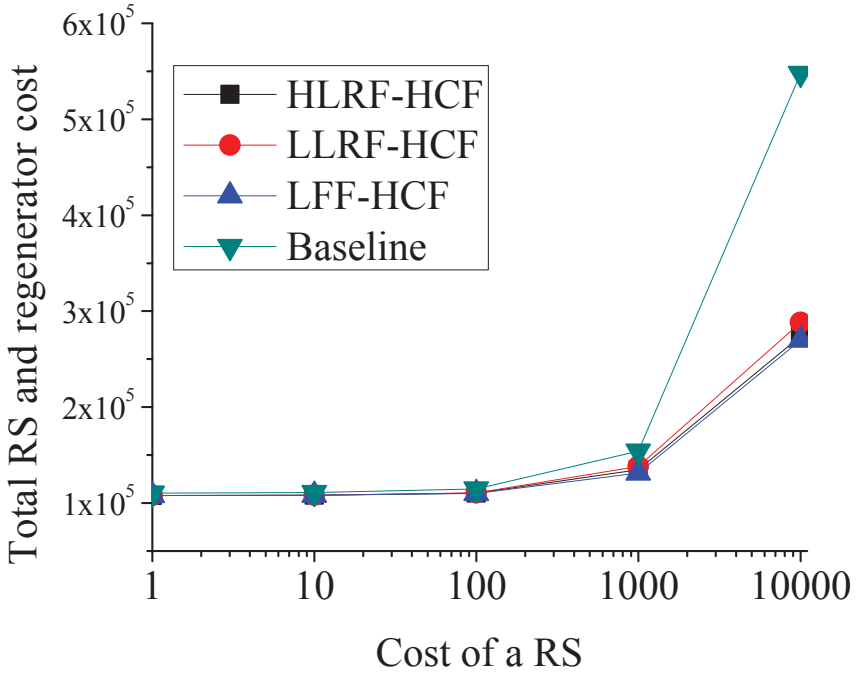

Figure 4.13. Total cost vs. cost of a RS

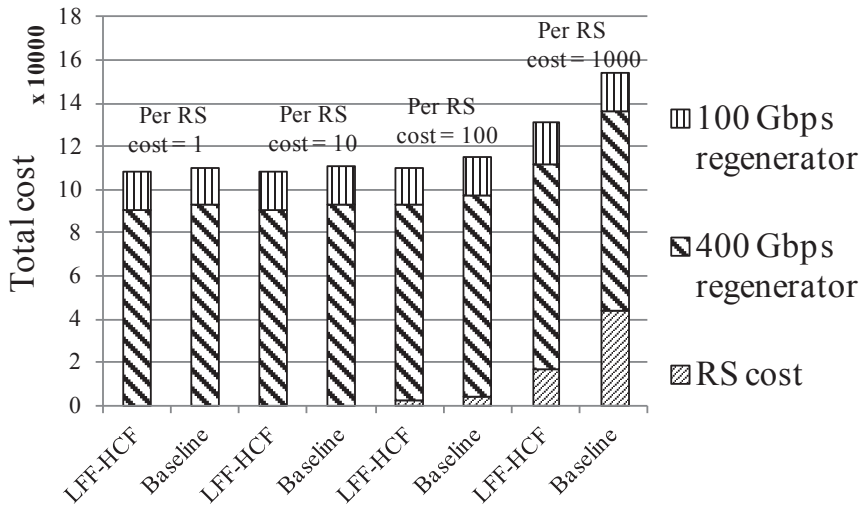

Figure 4.14. RS and regenerator cost vs. cost of a RS

saving of the LFF-HCF algorithm is around 22.5% on average, compared to the baseline algorithm. Figure 4.16 shows the separate equipment cost. We can see that when the ratio of 100 Gbps requests increases, the LFF-HCF algorithm has lower RS cost and almost the same regenerator cost, compared to the baseline algorithm. Again, it shows that the LFF-HCF algorithm can concentrate RSs with only a few additional regenerators.

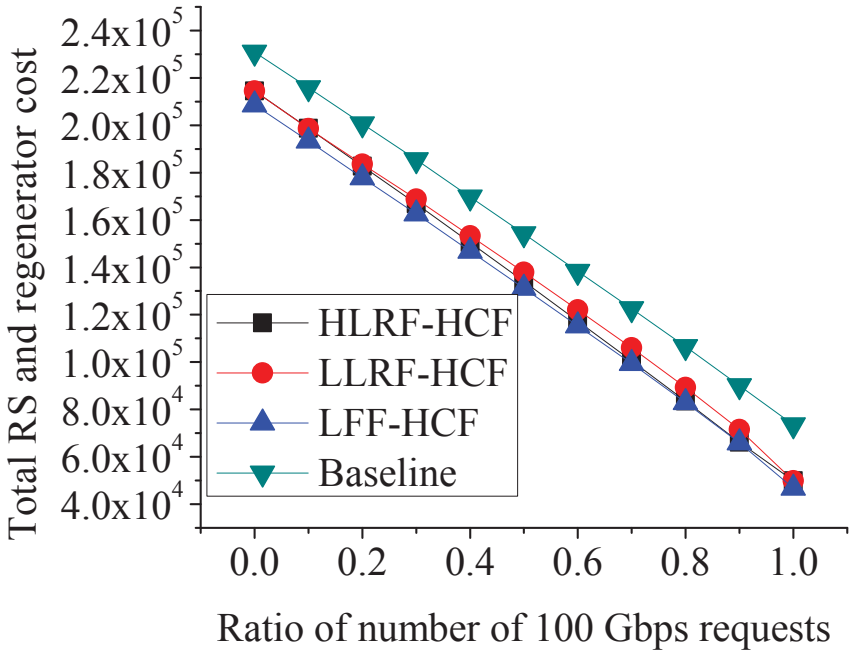

Figure 4.15. Total cost vs. ratio of 100 Gbps requests in total number of requests

4.6 Conclusion

In this chapter, we focus on the problems of RS selection for MLR optical networks, when routing is flexible and not given with each connection request. We study two related problems: MLR-RSSFR and MLR-RSSRP. The objective of MLR-RSSFR is to minimize the number of RSs, while the objective of MLR-RSSRP is to minimize the combined cost of RSs and regenerators. The MLR-RSSFR and the MLR-RSSRP problems are shown to be NP-hard, so we formulate the ILP models and develop heuristic approaches to solve the

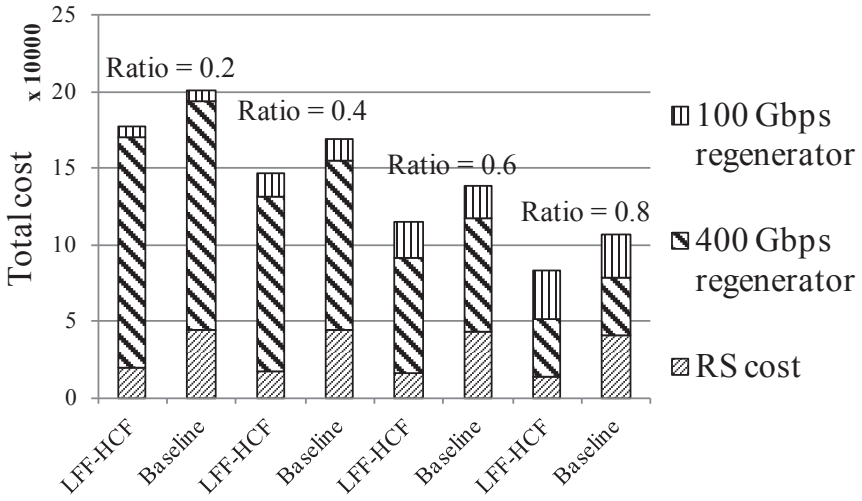

Figure 4.16. RS and regenerator cost vs. ratio of 100 Gbps requests in total number of requests

problems. The heuristic approaches follow three steps: ordering of the requests, routing of the requests, and post processing. For the ordering strategies, we invent a novel metric called flexibility to decide which request to be routed first. The numerical results show the performance comparison of these algorithms and show that the heuristic algorithms utilizing the flexibility-based ordering strategy outperform the other heuristic algorithms in both MLR-RSSFR and MLR-RSSRP. The performance of our heuristic approaches are close to that of ILP, showing near-optimal performance. The results also shows that, by selecting a set of RSs wisely, we can save around 20% cost in RSs and regenerators.

CHAPTER 5

ENERGY-EFFICIENT IMPAIRMENT-CONSTRAINED REGENERATOR PLACEMENT IN MLR OPTICAL NETWORKS

In this chapter, we study the energy-efficient impairment-constrained regenerator placement (EIRP) problem with the objective of minimizing the total energy consumption in MLR optical networks.[1] The destination of each path is guaranteed to receive the data correctly from the source based on the regenerator placement. We first provide the problem definition of EIRP and prove that the EIRP problem is NP-complete. We then formulate the problem as an integer linear program (ILP) and give results for small scale problems. Two heuristic approaches, named high line rate first (HLRF) and reroute only (RO), are presented. Numerical results show that HLRF achieves good results in both large and small scale problems, and that HLRF achieves higher energy efficiency than RO.

5.1 Introduction

Recent studies have shown that communication networks account for up to 10% of the world-wide power consumption [32], and that the power usage of the US network infrastructure (mostly optical networks) is between 5 to 24 TWh/year or \$0.5-2.4B/year [33]. Therefore, energy efficient (green) networking has attracted extensive research attention. When we place regenerators in the MLR optical network, full placement of regenerators may cause high energy consumption in the optical network. Furthermore, regenerators placed along a path with a higher line rate will consume higher energy [62]. Therefore, we wish to place

[1] ©2012 IEEE. Reprinted, with permission, from Weisheng Xie, Yi Zhu, Jason P. Jue, "Energy-Efficient Impairment-Constrained 3R Regenerator Placement in Optical Networks," *IEEE International Conference on Communications (ICC)*, June 2012.

as few regenerators as possible and choose proper line rates for lightpaths in order to guarantee that the destination can receive data correctly from the source while minimizing the total energy consumption in the optical network. We name this problem the energy-efficient impairment-constrained regenerator placement (EIRP) problem.

Our work considers regenerator placement for multiple rates under impairment constraints that are represented as the reachability for each line rate. For a given set of requests, we find a path (or multiple paths) for each request. We then jointly decide the line rate for each path and place regenerators along each path if the distance is longer than the reachability for the chosen line rate. The objective of our problem is to minimize the total energy consumption, which includes the energy consumed by transponders and regenerators. In this chapter, we make the following assumptions: 1) the links in the optical network are bidirectional; 2) all requests are bidirectional; 3) no traffic grooming capability is considered at intermediate nodes, which means that two requests can be groomed into a single wavelength if and only if they share the same source-destination pair; 4) no wavelength convertor is placed at any node; 5) optical amplifiers (a.k.a. 1R regenerators) have already been deployed; and 6) sufficient link resources (e.g. wavelengths) are available in the optical network, which means that if all wavelengths use the highest line rate, no request will be blocked.

The rest of this chapter is organized as follows. In Section 5.2, we provide a detailed problem description of energy-efficient impairment-constrained regenerator placement. In Section 5.3, we propose a brief ILP formulation of the problem. Two heuristic algorithms are presented in Section 5.4. In Section 5.5, we report some numerical results. Finally, we give a summary of our work in Section 5.6.

5.2 Energy-Efficient Impairment-Constrained Regenerator Placement

5.2.1 Network Model and Energy Consumption Model

The optical network can be represented as a graph $G(\mathbf{V}, \mathbf{E})$, where $\mathbf{V}$ is the set of nodes, and $\mathbf{E}$ is the set of edges. Figure 5.1 gives an example of the optical network. Every link in $\mathbf{E}$ has the same number (W) of wavelengths. When a lightpath from a source to a destination is established in the optical network, it reserves a wavelength along the path, determines a proper line rate from a set $\mathbf{L}$ of available line rates, and places regenerators along the path if needed.

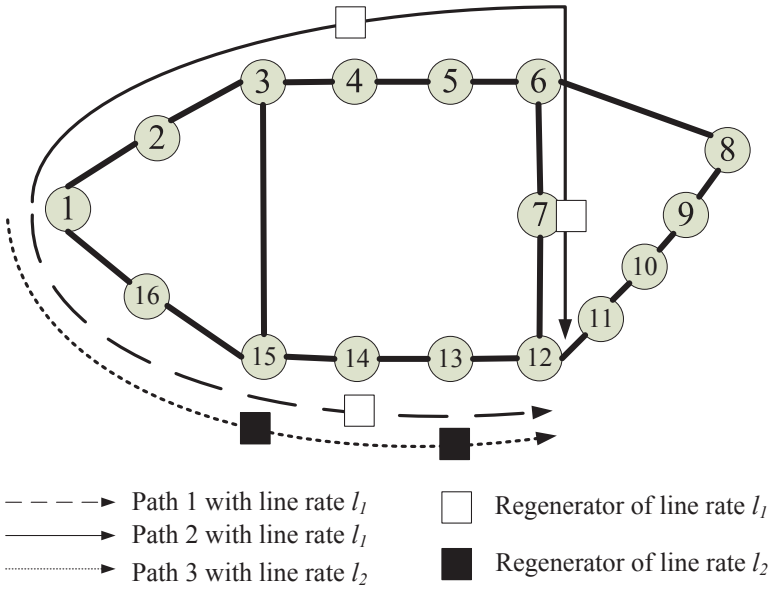

Figure 5.1. Network model and regenerator placement

In this chapter, we use reachability in terms of hop counts to measure the effect of impairments. Since different line rates may suffer different physical impairments, the reachabilities for different line rates are also different. Therefore, we have a set of reachabilities $\mathbf{A}$ corresponding to the line rate set $\mathbf{L}$. For example, suppose we have two different line rates, lower rate l_1 and higher rate l_2, and the reachabilities for l_1 and l_2 are 3 hops and 2 hops,

respectively. Thus, when we set up a lightpath from Node 1 to Node 12, for Path 1 we need 1 regenerator for l_1 at Node 14. For Path 2, we need 2 regenerators for l_1 at Nodes 4 and 7. For Path 3, we need 2 regenerators for l_2 at Nodes 15 and 13. The different paths and different line rate selections will lead to different energy consumption.

The total energy consumption in the optical network can be divided into the following categories [53]:

1. transmission equipment (e.g., WDM transponders);
2. electronic traffic processing;
3. electronic or optical switching devices;
4. optical amplifiers (typically EDFAs);
5. 3R regenerators;
6. network control (e.g., signaling or clock recovery).

Some of these factors are constant for all line rates. For example, similar to [63], the network control is considered to be constant, which means that the energy consumption is independent of the line rates in the optical network. Furthermore, the energy consumed by optical amplifiers is constant since we suppose that all optical amplifiers have already been deployed in the network. Since the energy needed for each optical switch is much less than the transponders [123], we neglect the energy consumed by optical switching devices. Finally, the energy needed for electronic processing only takes place at the source and the destination for each request, and the energy consumed by the electronic processing is a constant value which only depends on the request traffic. Therefore, in our work, we focus on the energy consumption of WDM transponders and 3R regenerators, which depends on the line rates of the lightpaths. For example, according to [62], the energy consumptions for transponders of 10 Gbps and 40 Gbps are 35 W and 73 W, respectively. 3R regenerators consume 85 W and 161 W for 10 Gbps and 40 Gbps, respectively.

5.2.2 Problem Formulation

The energy-efficient impairment-constrained regenerator placement (EIRP) problem can be stated as follows:

Given graph $G(\mathbf{V}, \mathbf{E})$, the total number of wavelengths on each edge W, an available line rate set $\mathbf{L}$, $l_k \in \mathbf{L}$, $1 \leq k \leq |\mathbf{L}|$, a reachability set $\mathbf{A}$, $a_k \in \mathbf{A}$, $1 \leq k \leq |\mathbf{L}|$, where a_k is the reachability of line rate l_k , energy consumption sets, $\mathbf{B}$, $b_k \in \mathbf{B}$, $1 \leq k \leq |\mathbf{L}|$, where b_k is the energy consumed by transponder of line rate l_k, and $\mathbf{C}$, $c_k \in \mathbf{C}$, $1 \leq k \leq |\mathbf{L}|$, where c_k is the energy consumed by 3R regenerator of line rate l_k, and a request set $\mathbf{R} = [r_{i,j}]_{|\mathbf{V}|\times|\mathbf{V}|}$, where each $r_{i,j}$ is the total traffic from node i to node j. Find the routing and wavelength assignment and the proper line rate and regenerator placement for each request with the objective of minimizing the total energy consumed by the transponders and 3R regenerators such that

1. traffic constraint: all requested traffic is assigned to one or more wavelengths, which means that no blocking occurs;

2. wavelength constraint: on each edge in $\mathbf{E}$, the total number of wavelengths assigned cannot exceed W;

3. rate constraint: the total traffic which goes through one wavelength cannot exceed the line rate for this wavelength;

4. impairment constraint: along any path, the length of each segment without regenerators should not exceed the reachability limit.

An example is shown in Figure 5.1. Suppose we have two different line rates, $l_1 = 10$ Gbps and $l_2 = 40$ Gbps, $W = 2$, and the traffic request between Node 1 and Node 12 is 30 Gbps. We set $\mathbf{B} = \{35, 73\}$, $\mathbf{C} = \{85, 161\}$, and $\mathbf{A} = \{3, 2\}$. We can use the route Path 3 and assign one 40 Gbps wavelength as shown with the dotted line (which requires 468 W), or we can use two 10 Gbps wavelengths along Path 1 and one 10 Gbps wavelength along Path 2 to achieve an energy consumption of 550 W.

5.2.3 NP-Completeness

The decision version of EIRP is: given graph $G(\mathbf{V}, \mathbf{E})$, W, $\mathbf{L}$, $\mathbf{A}$, $\mathbf{B}$, $\mathbf{C}$, the request set $\mathbf{R}$, and the total energy value TE, find the routing and wavelength assignment, the proper line rate, and the regenerator placement for each request to meet the constraints such that the total energy is no larger than TE. The placement of regenerators and the routing of traffic with proper wavelengths and line rates can be determined in polynomial time. Therefore, we can determine whether or not the total energy is greater than TE in polynomial time. Furthermore, all the constraints can be checked within polynomial time. Therefore, the EIRP problem belongs to the NP Class. We know that the traditional RWA problem is NP-complete, and RWA is a special case of EIRP when only a single line rate available. Therefore, the EIRP problem is also NP-complete.

5.3 ILP Formulation

In this section, we present the ILP formulation for EIRP. First, we define some useful notation and variables.

5.3.1 Input Parameters

- $M = |\mathbf{L}|$: total number of available line rates;
- W: total number of wavelengths on each link;
- $\mathbf{R} = [r_{i,j}]_{|\mathbf{V}|\times|\mathbf{V}|}$: set of requests;
- $\mathbf{L} = [l_m]_M$: set of available line rates (decreasing order);
- $\mathbf{A} = [a_m]_M$: set of reachability for each line rate;
- $\mathbf{B} = [b_m]_M$: set of energy consumed by transponders for each line rate;
- $\mathbf{C} = [c_m]_M$: set of energy consumed by regenerators for each line rate;
- $\mathbf{E} = [e_{i,j}]_{|\mathbf{V}|\times|\mathbf{V}|}$: adjunct matrix representing edges of G;

- P: maximum possible paths between the source and the destination;
- VL: very large number.

5.3.2 Variables of ILP

- $\mathbf{X} = [x_{i,j,m}^{s,d,p,w}]_{|\mathbf{V}|\times|\mathbf{V}|\times M}^{|\mathbf{V}|\times|\mathbf{V}|\times P\times W}$: relationship among path, line rate, and wavelength, whose element $x_{i,j,m}^{s,d,p,w}$ is 1 if edge (i,j) is along the path p from s to d with wavelength w and line rate l_m, otherwise 0;
- $\mathbf{Y} = [y_m^{s,d,p,w}]_M^{|\mathbf{V}|\times|\mathbf{V}|\times P\times W}$: relationship among path, line rate, wavelength, and regenerator placement, whose element $y_m^{s,d,p,w} \geq 0$ is the number of regenerators which are placed along the path p from s to d with wavelength w and line rate l_m;
- $\mathbf{Z} = [z_m^{s,d,p,w}]_M^{|\mathbf{V}|\times|\mathbf{V}|\times P\times W}$: relationship among path, line rate, wavelength, and transponders, whose element $z_m^{s,d,p,w}$ is 1 if we set up a path p from s to d with wavelength w and line rate l_m, otherwise 0;

5.3.3 Objective

The objective of EIRP is to minimize the following function:

$$min\ obj = \sum_{s,d,p,w} c_m \cdot y_m^{s,d,p,w} + \sum_{s,d,p,w} 2 \cdot b_m \cdot z_m^{s,d,p,w} \tag{5.1}$$

Note that the first part of the objective is the energy consumed by the 3R regenerators and the second part is the energy consumed by the transponders. Since we need a pair of transponders for each lightpath, we multiply the second term by 2.

5.3.4 Constraints

$$\sum_{m,j,p,w} l_m \cdot (x_{s,j,m}^{s,d,p,w} - x_{j,s,m}^{s,d,p,w}) \geq r_{s,d}, \forall 1 \leq s \leq |\mathbf{V}|, 1 \leq d \leq |\mathbf{V}| \tag{5.2}$$

$$\sum_{m,j,p,w} l_m \cdot (x_{j,d,m}^{s,d,p,w} - x_{d,j,m}^{s,d,p,w}) \geq r_{s,d}, \forall 1 \leq s \leq |\mathbf{V}|, 1 \leq d \leq |\mathbf{V}| \tag{5.3}$$

$$\begin{aligned} \sum_i x_{i,j,m}^{s,d,p,w} = \sum_i x_{j,i,m}^{s,d,p,w}, \forall 1 \leq s \leq |\mathbf{V}|, 1 \leq d \leq |\mathbf{V}|, \\ 1 \leq p \leq P, 1 \leq w \leq W, 1 \leq j \leq |\mathbf{V}|, j \neq s, d \end{aligned} \tag{5.4}$$

Constraints 5.2-5.4 guarantee traffic constraint and rate constraint. In detail, Constraint 5.2 guarantees that the source node generates a traffic flow greater than or equal to the requested traffic. Constraint 5.3 guarantees that the destination receives the same amount of data generated at the source node. Constraint 5.4 ensures that for any intermediate node, the incoming and outgoing flows should be the same.

$$\sum_{s,d,p,w,m} x_{i,j,m}^{s,d,p,w} \leq W, \forall 1 \leq i \leq |\mathbf{V}|, 1 \leq j \leq |\mathbf{V}| \tag{5.5}$$

Constraint 5.5 guarantees the wavelength constraint. More specifically, it guarantees that the number of occupied wavelengths on any link cannot exceed the link's wavelength capacity.

$$\begin{aligned} a_m \cdot (y_m^{s,d,p,w} + 1) \geq \sum_{i,j} (x_{i,j,m}^{s,d,p,w} \cdot e_{i,j}), \forall 1 \leq s \leq |\mathbf{V}|, 1 \leq d \leq |\mathbf{V}|, \\ 1 \leq p \leq P, 1 \leq w \leq W, 1 \leq m \leq M \end{aligned} \tag{5.6}$$

$$\begin{aligned} a_m \cdot y_m^{s,d,p,w} \leq \sum_{i,j} (x_{i,j,m}^{s,d,p,w} \cdot e_{i,j}), \forall 1 \leq s \leq |\mathbf{V}|, 1 \leq d \leq |\mathbf{V}|, \\ 1 \leq p \leq P, 1 \leq w \leq W, 1 \leq m \leq M \end{aligned} \tag{5.7}$$

Constraints 5.6-5.7 ensure that all paths meet the impairment constraint and that we place as few regenerators as possible to save the energy.

$$z_m^{s,d,p,w} \leq \sum_{i,j} x_{i,j,m}^{s,d,p,w}, \forall 1 \leq s \leq |\mathbf{V}|, 1 \leq d \leq |\mathbf{V}|, \\ 1 \leq p \leq P, 1 \leq w \leq W, 1 \leq m \leq M \tag{5.8}$$

$$z_m^{s,d,p,w} \geq \frac{\sum_{i,j} x_{i,j,m}^{s,d,p,w}}{VL}, \forall 1 \leq s \leq |\mathbf{V}|, 1 \leq d \leq |\mathbf{V}|, \\ 1 \leq p \leq P, 1 \leq w \leq W, 1 \leq m \leq M \tag{5.9}$$

Constraints 5.8-5.9 guarantee that when we set up a lightpath with the line rate l_m, we should place transponders for that line rate l_m.

5.4 Heuristic Approaches

Although the ILP formulation can provide insight regarding the EIRP problem, it can only be used to solve small scale problems because EIRP is NP-complete. In this section, we propose an algorithm to solve large scale problems.

Our algorithm starts by finding all-pair shortest paths in the graph G. Initially, for any request from s to d, we have a shortest path from s to d, which is recorded as $SP(s, d)$. Based on $SP(s, d)$ and reachability information in $\mathbf{A}$, we can determine the regenerator placement along the path $SP(s, d)$. Therefore, we have the energy consumption set $ec_m^{s,d} \in \mathbf{EC}_{s,d}$ for each line rate l_m. Based on the request $r_{s,d}$, we can determine the number of paths together with the proper line rate for each path so that the energy consumption for the request $r_{s,d}$ is minimized. Note that all these paths are along the same route $SP(s, d)$. If the number of line rates is given, this process can be done and achieve the optimal solution in polynomial time through dynamic programming. After processing all requests in $\mathbf{R}$, we have the total energy consumption, which is the lower bound for our EIRP problem. Note that we may not achieve this lower bound since we do not consider the wavelength constraint on each edge in the initial phase.

In the main procedure of the algorithm, we create M matrices $[\mathbf{T}_m]_M$. Each matrix $[\mathbf{T}_m] = [t^{s,d}]_m^{|\mathbf{V}|\times|\mathbf{V}|}$ contains the number of wavelengths needed to set up lightpaths from s to d using line rate l_m. We start from the highest line rate l_1 and move to the lowest rate l_M. For the current line rate l_m and wavelength request $t^{s,d}$, if the path $SP(s,d)$ has enough wavelengths to allocate $t^{s,d}$, then we allocate $t^{s,d}$ wavelengths along $SP(s,d)$. Otherwise, we have two choices: 1) increase the line rate l_m to l_1 to reduce $t^{s,d}$ and reserve the wavelengths along path $SP(s,d)$; and 2) reroute the traffic to another path(s) with the maximum number of available wavelengths. Of these two options, we select the one that results in less increase in energy consumption. Note that for 2), we may need to increase the line rate if we cannot find enough wavelengths to allocate $t^{s,d}$ wavelengths. After wavelength reservation, we update the graph to reserve the wavelengths with lower line rates. Since we start from the highest line rate, we name the algorithm the high line rate first (HLRF) algorithm. The full HLRF algorithm is described in Algorithm 6.

The complexity for the initial phase is $O(|\mathbf{V}|^2 \cdot k^{M+1})$ where $k = \lceil \frac{r}{l_M} \rceil$ and r = max $\{r_{s,d}\}$. Since the total number of line rates is given and small in practice, the initial phase can run in a polynomial time. In the main procedure, for a single request $t^{s,d}$, we need $O(|\mathbf{V}|^2)$ time if we need to reroute the traffic and $O(|\mathbf{V}|)$ time if we can allocate the wavelength. Thus, we need $O(|\mathbf{V}|^4 \cdot M)$ to allocate all requests in the worst case. Therefore, the algorithm can be run within $O(|\mathbf{V}|^4 \cdot M + |\mathbf{V}|^2 \cdot k^{M+1})$ time.

We provide another simple heuristic for comparison. The heuristic is shown as follows:

Step 1: same as the initial phase of HLRF;

Step 2: select the request with the highest $\frac{r_{s,d}}{SP(s,d)}$;

Step 3: calculate the optimal solution $t^{s,d}$ (shown in HLRF) for the chosen request $r_{s,d}$;

Step 4: route the traffic along the path $SP(s,d)$. If there is no wavelength available along the path $SP(s,d)$, find an alternative path and allocate the traffic.

Step 5: continue Steps 2-4 until all requests are allocated.

Algorithm 6 High Line Rate First (HLRF)

Input: graph $G(\mathbf{V}, \mathbf{E})$, W, $\mathbf{L}$, $\mathbf{A}$, $\mathbf{B}$, $\mathbf{C}$, the request set $\mathbf{R}$
Output: routing and wavelength assignment associating with the proper line rate and regenerator placement for each request
Begin
//Initial phase
Find shortest paths between any pair of nodes and record them as $SP(s,d)$ for each node pair s and d
Find the regenerator placement along $SP(s,d)$ for line rate l_m and calculate the energy consumption $ec_m^{s,d}$
//Calculate the optimal solution for request $r_{s,d}$
for each request $r_{s,d}$ **do**
for $w_1 = 0$ to $\left\lceil \frac{r_{s,d}}{l_1} \right\rceil$ **do**
for $w_2 = 0$ to $\left\lceil \frac{r_{s,d} - w_1 \cdot l_1}{l_2} \right\rceil$ **do**
...
for $w_m = 0$ to $\left\lceil \frac{r_{s,d} - \sum_{i=1}^{m-1} w_i \cdot l_i}{l_m} \right\rceil$ **do**
...
for $w_{M-1} = 0$ to $\left\lceil \frac{r_{s,d} - \sum_{i=1}^{M-2} w_i \cdot l_i}{l_{M-1}} \right\rceil$ **do**
$w_M = \left\lceil \frac{r_{s,d} - \sum_{i=1}^{M-1} w_i \cdot l_i}{l_M} \right\rceil$
Find $E_{s,d} = \min \{ \sum_{m=1}^{M} w_m \cdot ec_{s,d}^m \}$ and record $t^{s,d}$ for each line rate l_m
end for
...
end for
...
end for
end for
end for
Calculate total energy $TE = \sum_{s,d} E_{s,d}$

Algorithm 6 continued

//Main procedure
for line rate l_m from l_1 (highest rate) to l_M (lowest rate) **do**
Form $\mathbf{T}_m = [t^{s,d}]_m^{|\mathbf{V}|\times|\mathbf{V}|}$
Pick $t^{s,d}$ with maximum $\frac{t^{s,d}}{|SP(s,d)|}$ where $|SP(s,d)|$ is the distance of $SP(s,d)$
$TE0 = 0$
if $w(SP(s,d)) \geq t^{s,d}$, where $w(SP(s,d))$ is the number of available wavelengths which can be reserved along $SP(s,d)$ **then**
Allocate $t^{s,d}$ wavelengths along the path $SP(s,d)$
else
$TE1 = TE2 = TE3 = VL$ //VL is the very large number
Let $q^{s,d} = \left\lceil \frac{t^{s,d}}{l_1} \right\rceil$
if $w(SP(s,d)) \geq q^{s,d}$ **then**
calculate the increasing energy consumption $TE1$ using $q^{s,d}$ paths with line rate l_1 instead of $t^{s,d}$ paths with line rate l_m
end if
Find another path $AP(s,d)$ with maximum available wavelengths
if $w(AP(s,d)) \geq t^{s,d}$ **then**
Calculate the increasing energy consumption $TE2$ using $t^{s,d}$ $AP(s,d)$ paths instead of $t^{s,d}$ $SP(s,d)$ paths
else
Calculate the increasing energy consumption $TE3$ using $q^{s,d}$ $AP(s,d)$ paths with line rate l_1 instead of $t^{s,d}$ $AP(s,d)$ paths with line rate l_m
end if
Allocate the wavelength based on the minimum increasing energy $TE0 = \min\{TE1, TE2, TE3\}$
end if
//Update the information
$TE = TE + TE0$
$t^{s,d} = 0$
Continue the process until all $t^{s,d}$ in $\mathbf{T}_m$ are considered
end for

Since we only reroute the traffic when there are insufficient wavelengths along the shortest path, we name this algorithm reroute only (RO) algorithm.

5.5 Numerical Results

In this section, we present some numerical examples to show that the ILP can solve small-scale problems very well, while our heuristic algorithms can achieve good performance for large-scale networks. The ILP model was solved using IBM ILOG CPLEX Optimization Studio $v12.2$.

The energy costs used for the following experiments are given in Table. 5.1. For Experiment 1, the proposed algorithms and the ILP are applied to the topology shown in Figure 5.1. The reachabilities of 10 Gbps, 40 Gbps signals are 3 and 2 hops, respectively. We reduce the actual reachabilities of 10 Gbps and 40 Gbps signals for simplicity of simulation because of the small network size. For Experiments 2-4, the proposed algorithms are applied to the 75-node CORONET CONUS topology [1]. The reachabilities of 10 Gbps, 40 Gbps and 100 Gbps signals are 5, 3, and 2 hops, respectively.

Table 5.1. Energy consumption of network devices

Device	**Energy consumption (W)**
10 Gbps Transponder	35
10 Gbps Regenerator	85
40 Gbps Transponder	73
40 Gbps Regenerator	161
100 Gbps Transponder	140
100 Gbps Regenerator	295

Experiment 1 In the first experiment, we check the performance of the ILP model and show that our proposed RO and HLRF algorithms can obtain results close to the ILP model. The average traffic demands are 10 Gbps, 20 Gbps, 30 Gbps, and 40 Gbps. We run the experiment for both 10 wavelengths per link and 12 wavelengths per link. We

compare the total energy consumption and the number of regenerators for the ILP model, the RO algorithm, and the HLRF algorithm. Table 5.2 gives the results of Experiment 1. We observe that the ILP always achieves the minimum energy consumption and optimal regenerator placement, while RO and HLRF achieve results close to the ILP. As the average traffic demand increases, ILP, RO, and HLRF use more wavelengths, resulting in more regenerator placement and higher energy consumption.

Experiment 2 We study energy consumption for a network with different average traffic demands between node pairs. The number of wavelength for each link is set as 64, 80 or 96. Traffic demands between node pairs have an average value ranging from 40 to 320 Gbps.

As Figure 5.2 depicts, when the average traffic demand is low, the energy consumption of 64-wavelength, 80-wavelength and 96-wavelength calculated by both RO and HLRF are the same as the lower bound, which is the minimum energy consumption without a constraint on the number of wavelengths. For HLRF, when the average traffic demand grows to 120 Gbps, the energy consumption of the 64-wavelength network starts to diverge from those of the 80-wavelength network, the 96-wavelength network and the lower bound. Because of the constraint on the number of wavelengths, the 64-wavelength network starts to increase the wavelength capacity or reroute traffic, which increases the energy consumption. The energy consumption obtained by HLRF is only slightly higher than the lower bound, showing that our proposed algorithm can achieve high energy efficiency.

In Figure 5.3, the difference in total energy consumption is defined as the total energy consumption of HLRF or RO minus that of lower bound. Figure 5.3 shows that the total energy consumption of RO is higher than that of HLRF. Since RO only considers rerouting traffic while HLRF considers both rerouting traffic and increasing the wavelength capacity, the HLRF algorithm will achieve higher energy efficiency than RO.

Experiment 3 For the HLRF algorithm, we study how the average traffic demand and number of wavelengths per link affect the energy consumption of each line rates wavelength,

Table 5.2. Total energy consumption and number of regenerators vs. average traffic demand and number of wavelengths per link

Traffic Demands (Gbps)	ILP Model						RO						HLRF					
	Wavelengths: 10			Wavelengths: 12			Wavelengths: 10			Wavelengths: 12			Wavelengths: 10			Wavelengths: 12		
	TE[a]	R1[b]	R2	TE	R1	R2	TE	R1	R2	TE	R1	R2	TE	R1	R2	TE	R1	R2
10	2621	3	6	2621	3	6	2621	3	6	2621	3	6	2621	3	6	2621	3	6
20	3612	3	11	3612	3	11	3612	3	11	3612	3	11	3612	3	11	3612	3	11
30	4405	9	6	4402	7	9	4742	7	13	4402	7	9	4405	9	6	4402	7	9
40	5865	12	10	5691	12	8	6344	16	8	6183	15	8	6031	13	10	5861	13	8

[a]TE is total energy consumption in watt.

[b]R1 and R2 are the number of 40 Gbps regenerators and 10 Gbps regenerators, respectively.

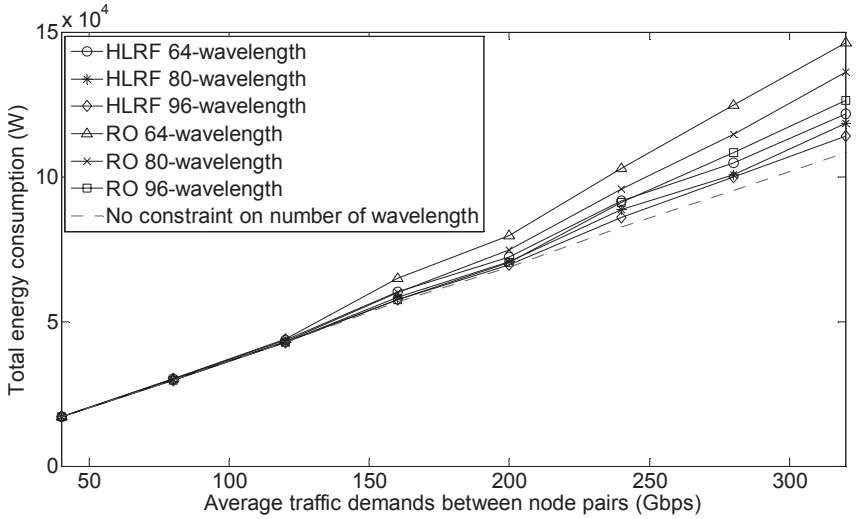

Figure 5.2. Total energy consumption vs. average traffic demand

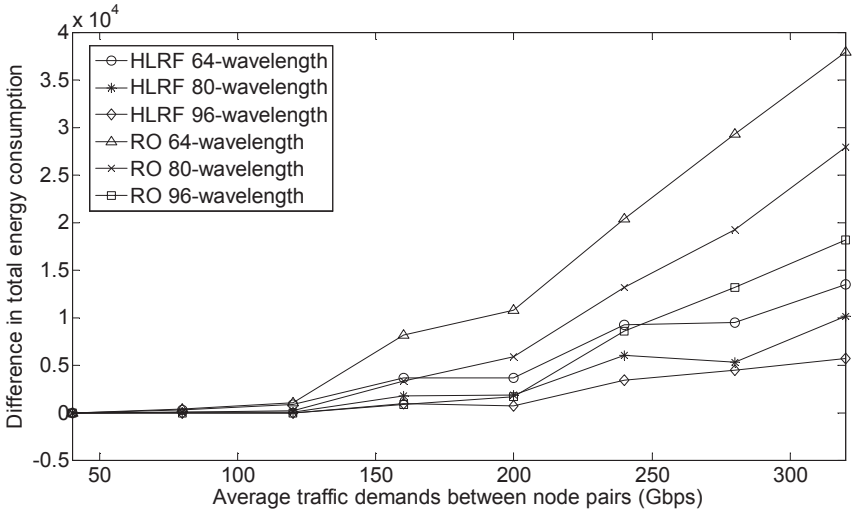

Figure 5.3. Difference in total energy consumption vs. average traffic demand

the number of each line rates wavelengths, and the number of each line rates regenerators, respectively. The number of wavelengths per link is set to 64, 80 or 96.

From Figures 5.4 - 5.6, we can see that, when average traffic demand grows from 160 Gbps to 240 Gbps, for 80-wavelength and 96-wavelength, the number of 10 Gbps wavelength increases slightly; however, the number of 10 Gbps regenerators increase considerably, which means that some 10 Gbps wavelengths are rerouted. When average traffic demand grows from 240 Gbps to 320 Gbps, for 64-wavelength, the number of 10 Gbps wavelengths decreases considerably while the number of 100 Gbps wavelength increases faster than the average traffic demand, which means that some 10 Gbps wavelengths are increased to 100 Gbps wavelengths. Thus, both rerouting and increasing line rates contribute to keeping the energy consumption minimal.

Figures 5.4 - 5.6 also show that, when average traffic demand is 240 Gbps or 320 Gbps, the numbers of 10 Gbps wavelengths in the 64-wavelength networks are far fewer than that of 80-wavelength and 96-wavelength networks; however, the 64-wavelength network requires almost the same number of 10 Gbps regenerators as that of 80 or 96-wavelength network, since more 10 Gbps wavelengths are rerouted in the 64-wavelength network.

5.6 Conclusion

In this chapter, we focus on the energy-efficient impairment-constrained regenerator placement (EIRP) problem, which aims to minimize the total energy consumption in the optical network with mixed line rates. We show that EIRP is NP-complete, and then formulate an ILP model for it. We also propose two heuristic approaches, named HLRF and RO, to solve large scale cases. The numerical results show that the ILP can solve small scale problems properly and that the energy consumption obtained by HLRF is only slightly higher than the lower bound and the ILP model. The numerical results also demonstrate that HLRF

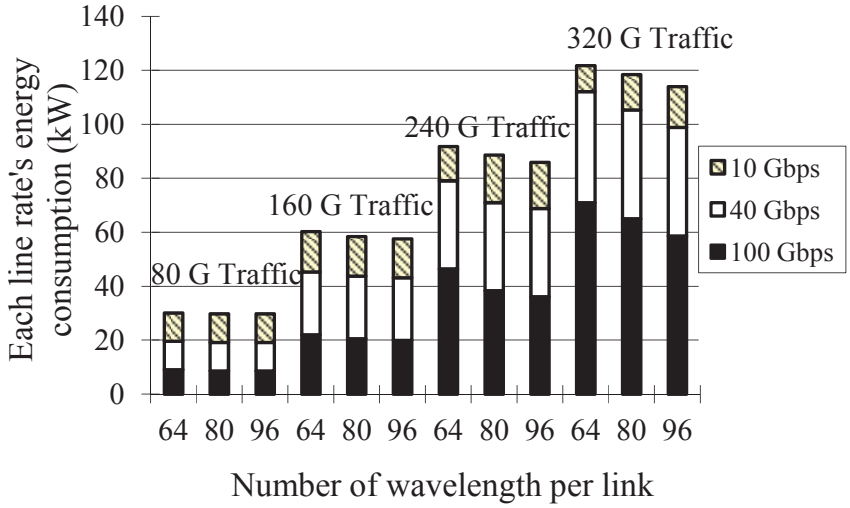

Figure 5.4. Energy consumption of each line rate vs. average traffic demand and different number of wavelengths per link

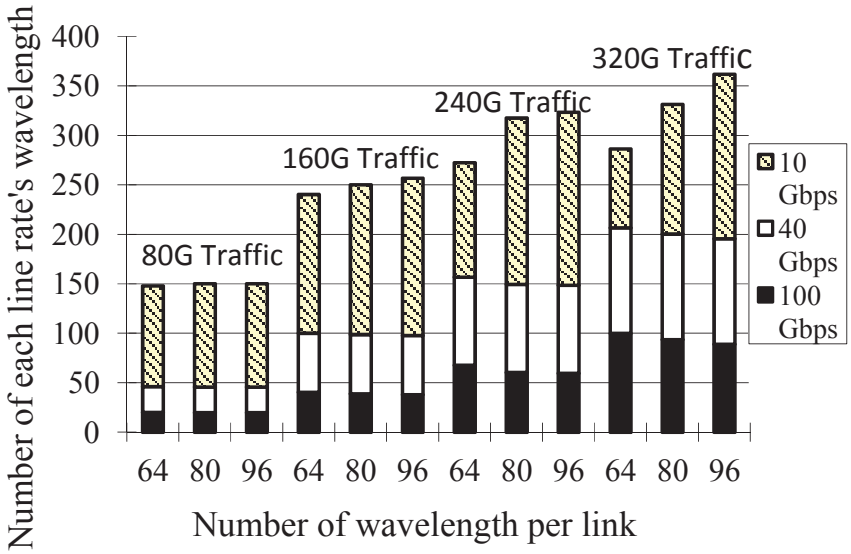

Figure 5.5. Number of each line rates wavelengths vs. average traffic demand and different number of wavelengths per link

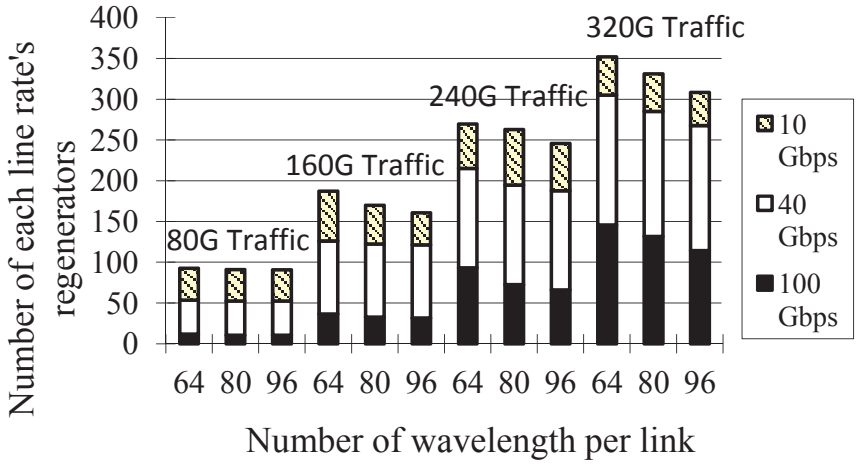

Figure 5.6. Number of each line rates regenerators vs. average traffic demand and different number of wavelengths per link

outperforms RO, in terms of energy efficiency. One possible area of future work is to consider the EIRP problem with traffic grooming at intermediate nodes.

CHAPTER 6

SURVIVABLE IMPAIRMENT-CONSTRAINED VON MAPPING IN FLEXIBLE-GRID OPTICAL NETWORKS

In this chapter, we study the problem of survivable impairment-constrained virtual optical network mapping in flexible-grid optical networks (SIC-VONM).[1] The objective is to minimize the total cost of working and backup resources, including transponders, regenerators, and shared infrastructure, for a given set of virtual optical networks, which can survive single link failures. We first provide the problem definition of SIC-VONM, and then formulate the problem as an ILP. We also develop a novel heuristic algorithm, together with a baseline algorithm and a lower bound for comparison. Numerical results show that our proposed heuristic achieves results that are very close to those of the ILP for small scale problems, and that our proposed heuristic can solve large scale problems very well.

6.1 Introduction

The network virtualization is being extended to the optical domain, in order to provide services which require high throughput and low latency. Meanwhile, the physical optical networks are evolving from fixed-grid networks, where an optical channel follows the rigid ITU-T standard, towards flexible-grid optical networks, where the spectrum is allocated according to the capacity and reachability requirements. In flexible-grid optical networks, different optical channels may have different line rates and modulation formats, which require

[1] ©2014 IEEE. Reprinted, with permission, from Weisheng Xie, Jason P. Jue, Qiong Zhang, Xi Wang, Qingya She, Paparao Palacharla, Motoyoshi Sekiya, "Survivable Virtual Optical Network Mapping in Flexible-Grid Optical Networks," *Int. Conference on Computing, Networking, and Communications (ICNC)*, February 2014

different spectrum amount. VON mapping plays a vital role in the resource allocation of optical network virtualization. In the VON mapping problem, a virtual node is mapped to a physical node, while a virtual link is mapped to one or multiple optical paths. VON mapping needs to consider the optical layer constraints, such as the impairment constraint, and spectrum consecutiveness and continuity constraint.

In this chapter, VON mappings that can survive single link failures are studied in flexible-grid optical networks under impairment constraints. These impairment constraints are represented as the reachability for each line rate and modulation format. Every virtual node is mapped to a physical node selected from its set of candidate nodes, and each virtual link is mapped to two link-disjoint paths. We also need to determine the number and configuration of the optical channels for each virtual link. The objective is to minimize the total network cost consisting of transponder cost, regenerator cost, and shared infrastructure cost. An ILP model is formulated and a heuristic algorithm is proposed. We make the following assumptions: 1) the links in the optical network are bidirectional; 2) every virtual node is mapped to one node in its set of candidate physical nodes; 3) two virtual nodes cannot be mapped to the same physical node; and 4) there are sufficient resources on physical nodes and links.

The rest of this chapter is organized as follows. In Section 6.2, we provide a detailed description of the problem. In Section 6.3, we propose an ILP formulation of the problem. A heuristic algorithm, together with a baseline algorithm and a lower bound are presented in Section 6.4. In Section 6.5, numerical simulation results are shown. Finally, we give a summary of our work in Section 6.6.

6.2 Problem Description

6.2.1 Network Model and Cost Model

The physical optical network can be represented as a graph $G_P(\mathbf{V}, \mathbf{E})$, where $\mathbf{V}$ is a set of physical nodes, $\mathbf{E} = [e_{i,j}]$ is an adjacency matrix representing edges of G_P, where $e_{i,j}$ is the

link length of edge (i, j). The VON can also be represented as a graph $G_V(\mathbf{N}, \mathbf{T}, \mathbf{C})$, where $\mathbf{N}$ is a set of virtual nodes, $\mathbf{T} = [t_{i,j}]$ represents a set of virtual links, where each virtual link is a connection request and $t_{i,j}$ is the amount of traffic on virtual link (i, j). $\mathbf{C} = [c_n]_{|\mathbf{N}|}$ specifies the sets of candidate physical nodes, where c_n is a set of physical nodes to which virtual node n can be mapped.

In this chapter, we use reachability in physical distance (km) to measure the effect of impairments. The reachability of an optical channel is determined by its line rate and modulation format. We use the term *configuration* to denote a combination of line rate and modulation format. Different configurations have different reachabilities, channel width, transponder cost, and regenerator cost. An example is shown in Table 6.1, [110].

Table 6.1. Configurations

Line Rate (Gbps)	**Channel width (GHz)**	**Modulation format**	**Reach (km)**	**Transponder Cost**	**Regenerator Cost**
40	25.0	DP-QPSK	1800	1.2	2.4
40	50.0	DP-BPSK	2500	1.0	2.0
100	37.5	DP-QPSK	1700	2.4	4.8
100	50.0	DP-BPSK	2000	2.0	4.0

We refer to the cost model used in [124]. The total network cost consists of the following three elements:

1. The transponders of different configurations;

2. The 3R regenerators of different configurations;

3. The shared infrastructure (SI) such as the fiber, inline optical amplifiers, and ROADMs.

The unit SI cost is the average cost of all shared infrastructure for 1 km of transmission distance and for consuming 1 GHz of optical bandwidth, i.e., \$/(km·GHz).

Given an optical channel of certain configuration $conf_k$ and its path P, the cost of this optical channel is $2{*}ct_k + NR(P){*}cr_k + C_U{*}Dist(P){*}f_k$, where ct_k is the cost of configuration $conf_k$'s transponder, $NR(P)$ is the number of required $conf_k$'s regenerators along the path

P, cr_k is the cost of $conf_k$'s regenerator, C_U is the unit SI cost, $Dist(P)$ is the distance of P, and f_k is the channel width of $conf_k$. The total network cost is the summation of all the optical channels' costs.

6.2.2 Problem Formulation

The survivable impairment-constrained virtual optical network mapping problem in flexible-grid optical networks (SIC-VONM) can be stated as follows:

Given a physical optical network $G_P(\mathbf{V}, \mathbf{E})$, a VON $G_V(\mathbf{N}, \mathbf{T}, \mathbf{C})$, a set of configurations **CONF**, $conf_k \in \mathbf{CONF}$, $conf_k = \{l_k, s_k\}$, $1 \leq k \leq K$, where l_k is the line rate of $conf_k$, s_k is the channel width of $conf_k$, and K is the number of available configurations. We are also given a reachability set $\mathbf{A}$, $a_k \in \mathbf{A}$, $1 \leq k \leq K$, where a_k is the reachability of $conf_k$, a set of regenerator costs $\mathbf{CR}$, $cr_k \in \mathbf{CR}$, $1 \leq k \leq K$, where cr_k is the cost of a $conf_k$'s regenerator, a set of transponder costs $\mathbf{CT}$, $ct_k \in \mathbf{CT}$, $1 \leq k \leq K$, where ct_k is the cost of a $conf_k$'s transponder, and the unit SI cost C_U.

Find the node mapping, the routing, and the configuration selection for each virtual link with the objective of minimizing the total network cost, subject to the following constraints:

1. node mapping constraint: each virtual node can only be mapped to a physical node specified in its set of candidate nodes; no two virtual nodes can be mapped to the same physical node;

2. survivability constraint: each virtual link is mapped to two link-disjoint paths; each path has enough equipment and bandwidth to support the required capacity of the virtual link;

3. impairment constraint: along any path, the length of each segment without regenerators does not exceed the corresponding configuration $conf_k$'s reachability limit a_k.

Note that the working path and the backup path of a virtual link may use the same set of transponders; however, the optical channels of the working path and the backup path

must have the same configurations. Another choice is that the working path and the backup path of a virtual link use separate sets of transponders, and they are allowed to use optical channels of different configurations. In this chapter, we assume the working path and the backup path share transponders, since it may reduce the total cost.

We show an example of the problem in Figure 6.1. Suppose we have two different configurations $conf_1$ = {40 Gbps, 50 GHz} and $conf_2$ = {100 Gbps, 50 GHz}. The reachabilities of $conf_1$ and $conf_2$ are 2500 km and 2000 km, respectively. The costs of transponders **CT** = {1, 2}, and the costs of regenerators **CR** = {2, 4}. Virtual node A can be mapped to physical node 1 or 6. Virtual nodes B and C have only one candidate node each, nodes 4 and 2, respectively, and thus are mapped accordingly. Solution I maps virtual node A to physical node 1. Two 40 Gbps channels are selected for virtual link (A, C); one 100 Gbps channel is selected for virtual link (B, C); three 40 Gbps channels are chosen for virtual link (A, B). As shown in Figure 6.1(c), Solution I needs ten 40 Gbps transponders, two 100 Gbps transponders, twelve 40 Gbps regenerators, three 100 Gbps regenerators, and 19.1×10^5 km·GHz. The total cost is 69.1. Solution II selects one 40 Gbps and one 100 Gbps channels for virtual link (A, B), the total cost is then reduced to 65. The total cost can be further reduced by mapping virtual node A to physical node 6. As shown in Figure 6.1(e), Solution III results in an optimal solution of 59.4. From this example, we can see that different node mapping, routing, and configuration selection will lead to different total cost.

6.3 ILP Formulation

We present the ILP formulation for SIC-VONM in this section. First, we define some useful notations and variables.

6.3.1 Input Parameters

- **CONF** = $[conf_k] = [\{l_k, s_k\}]_K$: set of configurations;

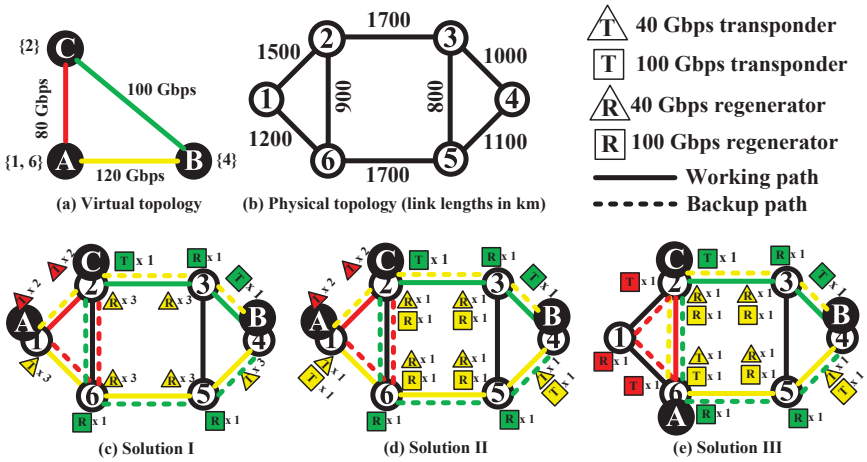

Figure 6.1. Example of virtual optical network mapping

- $\mathbf{T} = [t_{m,n}]_{|\mathbf{N}|\times|\mathbf{N}|}$: set of virtual links;
- $\mathbf{R} = [r_{m,n}]_{|\mathbf{N}|\times|\mathbf{N}|}$: equals 1 if there is a virtual link between node m and node n, otherwise 0;
- $\mathbf{CA} = [ca_{m,v}]_{|\mathbf{N}|\times|\mathbf{V}|}$: candidate nodes sets, where $ca_{m,v} = 1$ if virtual node m can be mapped to physical node v, otherwise 0;
- $\mathbf{CR} = [cr_k]_K$: set of costs of regenerators;
- $\mathbf{CT} = [ct_k]_K$: set of costs of transponders;
- C_U: unit SI cost;
- $\mathbf{P} = [p_{i,j}^{u,v}]_{L\times|\mathbf{E}|}^{|\mathbf{V}|\times|\mathbf{V}|}$: equals 1 if edge j is on path i from node u to node v, where L is the maximum number of paths between every s-d pair;
- $\mathbf{NR} = [nr_{k,i}^{u,v}]_{K\times L}^{|\mathbf{V}|\times|\mathbf{V}|}$: number of required $conf_k$'s regenerators on path i from node u to node v;
- $\mathbf{D} = [d_i^{u,v}]_K^{|\mathbf{V}|\times|\mathbf{V}|}$: physical distance of path i from node u to node v.

6.3.2 Variables of ILP

- $\mathbf{X} = [x_{u,v,i}]_{|\mathbf{V}|\times|\mathbf{V}|\times L}$: equals to 1 if path i from node u to node v is mapped by some virtual link, otherwise 0;

• $\mathbf{Y} = [y_{m,u}]_{|\mathbf{N}|\times|\mathbf{V}|}$: equals to 1 if virtual node m is mapped to physical node u, otherwise 0;

• $\mathbf{Z} = [z_{m,n,u,v}]_{|\mathbf{N}|\times|\mathbf{N}|\times|\mathbf{V}|\times|\mathbf{V}|}$: equals to 1 if virtual node m is mapped to physical node u, virtual node n is mapped to physical node v, and there is a virtual link between virtual node m and virtual node n;

• $\mathbf{N} = [n_{k,i}^{u,v}]_{K\times L}^{|\mathbf{V}|\times|\mathbf{V}|}$: number of $conf_k$'s optical channels needed on path i from node u to node v;

• $\mathbf{F} = [f_k^{u,v}]_K^{|\mathbf{V}|\times|\mathbf{V}|}$: number of $conf_k$'s transponder pairs needed from node u to node v.

6.3.3 Objective

The objective of SIC-VONM is to minimize the following function:

$$min\ obj = \sum_{u,v,k} 2 \cdot ct_k \cdot f_k^{u,v} + \sum_{u,v,k,i} cr_k \cdot n_{k,i}^{u,v} \cdot nr_{k,i}^{u,v} + \sum_{u,v,k,i} d_i^{u,v} \cdot C_U \cdot s_k \cdot n_{k,i}^{u,v} \tag{6.1}$$

Note that the first part of the objective is the total cost of the transponders, the second part is the total cost of the regenerators, and the third part is the total cost of the shared infrastructure.

6.3.4 Constraints

$$z_{m,n,u,v} = r_{m,n} \cdot y_{m,u} \cdot y_{n,v}, \forall 1 \le m \le |\mathbf{N}|, 1 \le n \le |\mathbf{N}|, 1 \le u \le |\mathbf{V}|, 1 \le v \le |\mathbf{V}| \tag{6.2}$$

$$\sum_k l_k \cdot f_k^{u,v} \ge \sum_{m,n} z_{m,n,u,v} \cdot t_{m,n}, \forall 1 \le u \le |\mathbf{V}|, 1 \le v \le |\mathbf{V}| \tag{6.3}$$

Constraints 6.2 - 6.3 guarantee that the total traffic of optical channels starting from physical node u and ending at physical node v is at least the traffic demand of virtual link

$(m,\ n)$, when virtual node m is mapped to physical node u and virtual node n is mapped to physical node v.

$$\sum_{i} x_i^{u,v} = 2 \cdot \sum_{m,n} z_{m,n,u,v}, \forall 1 \leq u \leq |\mathbf{V}|, 1 \leq v \leq |\mathbf{V}| \tag{6.4}$$

Constraint 6.4 ensures that for every virtual link, two paths are found between the physical nodes to which the virtual nodes are mapped.

$$\begin{gathered} x_i^{u,v} \cdot p_{i,j}^{u,v} + x_l^{u,v} \cdot p_{l,j}^{u,v} \leq 1, \forall 1 \leq u \leq |\mathbf{V}|, 1 \leq v \leq |\mathbf{V}|, \\ 1 \leq l \leq L, 1 \leq j \leq |\mathbf{E}|, 1 \leq i \leq L, i \neq l \end{gathered} \tag{6.5}$$

Constraint 6.5 guarantees that the two paths found for a virtual link are link-disjoint.

$$f_k^{u,v} \cdot x_i^{u,v} = n_{k,i}^{u,v}, \forall 1 \leq u \leq |\mathbf{V}|, 1 \leq v \leq |\mathbf{V}|, 1 \leq k \leq K, 1 \leq i \leq L \tag{6.6}$$

Constraint 6.6 ensures that the two paths found for a virtual link have the same configuration's optical channels.

$$\sum_{u} y_{m,u} \cdot ca_{m,u} = 1, \forall 1 \leq m \leq |\mathbf{N}| \tag{6.7}$$

Constraint 6.7 ensures that every virtual node is mapped to a physical node defined in its set of candidate nodes.

$$\sum_{u} y_{m,u} = 1, \forall 1 \leq m \leq |\mathbf{N}| \tag{6.8}$$

Constraint 6.8 guarantees that every virtual node is mapped to a single physical node only.

$$\sum_{m} y_{m,u} \leq 1, \forall 1 \leq u \leq |\mathbf{V}| \tag{6.9}$$

Constraint 6.9 ensures that any physical node can be mapped by at most one virtual node.

6.4 Heuristic Approach

We develop a heuristic approach for the SIC-VONM problem consisting of three steps. The first step is to calculate two link-disjoint paths with the shortest total distance between every s-d pair in the physical topology. The second step is node mapping. In this step, we map the end nodes of one virtual link at a time, until all the virtual links have been checked. The third step is the configuration selection, in which we select a set of optical channels with the lowest cost configurations to satisfy every virtual link. We name this approach the Minimum Cost Survivable Virtual Optical Network Mapping Algorithm (MC-SVONM). In this section, we discuss the strategies for the above three steps and propose our heuristic approach based on these strategies. Also, we propose a baseline algorithm and a lower bound for comparison.

6.4.1 MC-SVONM

Calculate Distance Matrix

For each node pair in the physical topology, we run Suurballe's algorithm [125] to find two link-disjoint paths with the shortest total distance. We use $SP(u, v)$ to denote the shortest total distance of two link-disjoint paths between physical nodes u and v. When the end nodes of a virtual link (m, n) are mapped to u and v, the virtual link (m, n) is mapped to the two pre-calculated link-disjoint paths between u and v.

Node Mapping

We first develop a metric $Metric(m, u)$, which is used to evaluate the mapping of virtual node m to physical node u. Suppose we want to map a virtual link (m, n). The virtual nodes adjacent to virtual node m in the virtual topology can be categorized into three types: 1) $OtherEndNode$: the other end node of current virtual link (m, n); 2) M^m: the set of

virtual nodes that have already been mapped to physical nodes and that are adjacent to m, excluding the $OtherEndNode$; 3) UM^m: the set of virtual nodes that have not been mapped to physical nodes and that are adjacent to m, excluding the $OtherEndNode$. An example is shown in Figure 6.2. Suppose virtual link (A, B) has been mapped, and now we want to map virtual link (B, C). For virtual node C, $OtherEndNode = \{B\}$, $M^C = \{A\}$, $UM^C = \{D, E\}$. Let *MAP(m)* denote the mapped physical node of virtual node m. We introduce another two parameters: $Metric_M(m, u)$, which is the average value of $\alpha_i \cdot SP(u, MAP(M_i^m))$ over all i, $1 \leq i \leq |M^m|$, and $Metric_{UM}(m, u)$, which is the average value of $\beta_j \cdot SP(u, MAP(UM_j^m))$ over all j, $1 \leq j \leq |UM^m|$. Here M_i^m and UM_j^m are the i_{th} node and j_{th} node of M^m and UM^m, respectively. α_i is the relative weight of virtual link (m, M_i^m) compared to the virtual link (m, n). $\alpha_i = \frac{t_{m,M_i^m}}{t_{m,n}}$. Similarly, β_j is the relative weight of virtual link (m, UM_j^m) compared to the virtual link (m, n). $\beta_j = \frac{t_{m,UM_j^m}}{t_{m,n}}$. Note that since UM_j^m has not yet been mapped, we don't know exactly what $MAP(UM_j^m)$ is, so we calculate the average shortest total distance of two link-disjoint paths from node u to all the candidate nodes of UM_j^m, and take this average distance as $SP(u, MAP(UM_j^m))$. Finally we have $Metric(m, u) = Metric_M(m, u) + Metric_{UM}(m, u)$.

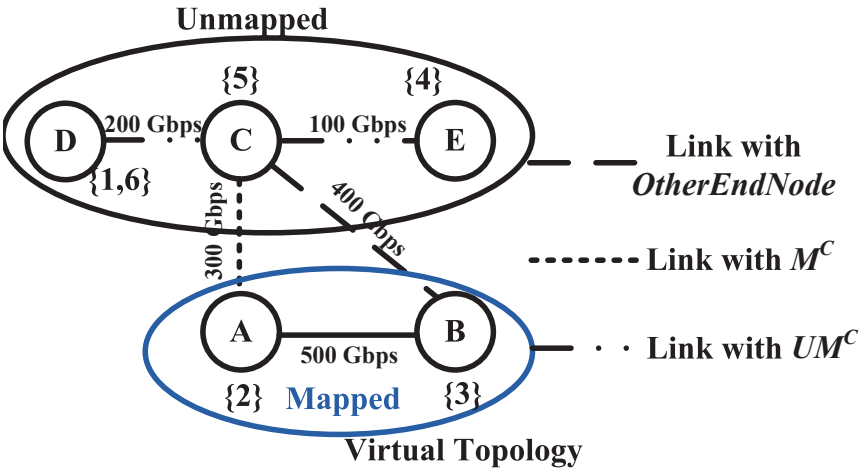

Figure 6.2. Example of *Metric(m, u)*

We show an example here for the calculation of $Metric(m, u)$. Suppose we want to map the virtual topology in Figure 6.2 to the physical topology shown in Figure 6.1. The candidate node set is labeled beside each virtual node. Suppose virtual node A has been mapped to physical node 2, virtual node B has been mapped to physical node 3, and we now want to map virtual link (B, C). Let's look at $Metric(C, 5)$. We can see that $MAP(M_1^C) = 2$, which is the physical node of virtual node A, so $SP(5, MAP(M_1^C)) = SP(5, 2) = 5100$ (total distance of path (5-3-2) and path (5-6-2)), $\alpha_1 = \frac{t_{C,A}}{t_{C,B}} = \frac{300}{400} = 0.75$. Since there is only one node in M^C, $Metric_M(C, 5) = \alpha_1 \cdot SP(5, MAP(M_1^C)) = 0.75 \cdot 5100 = 3825$. Now let's look at the set of $UM^C = \{$D, E$\}$. $SP(5, UM_1^C)$ is the average shortest distance taken from physical node 5 to all the candidate nodes of D, which are 1 and 6, so $SP(5, UM_1^C) = 6000$. $\beta_1 = \frac{200}{400} = 0.5$. Similarly, we have $SP(5, UM_2^C) = 2900$ and $\beta_2 = \frac{100}{400} = 0.25$. Then we have $Metric_{UM}(C, 5) = (0.5 \cdot 6000 + 0.25 \cdot 2900)/2 = 1862.5$. Overall, $Metric(C, 5) = 3825 + 1862.5 = 5687.5$.

Given a VON, we sort the virtual links in a descending order according to the amount of traffic on them. We start from the virtual link (m, n) with the largest traffic, where m has a set of candidate nodes $\{u_1, u_2, ..., u_x\}$, and n has a set of candidate nodes $\{v_1, v_2, ..., v_y\}$. Then we need to check whether the end nodes of this virtual link have been mapped or not.

If neither of these two end nodes have been mapped, we choose u_i and v_j with the smallest value of *Metric(m, u_i) + Metric(n, v_j) + SP(u_i, v_j)*, $1 \leq i \leq x, 1 \leq j \leq y$. Then virtual node m is mapped to physical node u_i, and n is mapped to v_j. We then proceed to the next virtual link until all the virtual nodes are mapped.

If either end node of virtual link (m, n) has been mapped, suppose m is mapped to node u while n has not been mapped yet, then we choose the v_j with the smallest value of *Metric(n, v_j) + SP(u, v_j)*, $1 \leq j \leq y$. Virtual node n is then mapped to physical node v_j, and we proceed to the next virtual link.

If both end nodes of virtual link (m, n) have been mapped, then we do nothing and proceed to the next virtual link.

Note that occasionally, a virtual node can not be mapped to physical nodes, since all of its candidates have been assigned to earlier mapped virtual nodes. Under this situation, we need to change the node mapping of earlier mapped virtual node to have a valid node mapping.

The node mapping algorithm is shown in Algorithm 7. In Algorithm 7, the *valid(u_i, v_j)* is to check if the two end nodes of a virtual link can be mapped to u_i and v_j. u_i and v_j are valid if they satisfy the following two requirements. First, u_i can not be the same physical node as v_j. Second, neither u_i nor v_j has been assigned to the earlier mapped virtual nodes, since we assume that no two virtual nodes can be mapped to the same physical node.

Configuration Selection

After the node mapping and the routing are decided, we can determine the cost of a $conf_k$'s optical channel using the cost model defined in Section II.A. Given a virtual link, its node mapping, and its routing, we let c_k denote the combined cost of the working path and the backup path of this virtual link under $conf_k$, i.e., $c_k = 2{*}ct_k + (NR(WP) + NR(BP)){*}cr_k + C_U{*}(Dist(WP) + Dist(BP)){*}f_k$, where WP denotes the working path and BP denotes the backup path. The combined cost of the working path and the backup path is calculated, since we assume the working path and the backup path of a virtual link share the same set of transponders. Given a virtual link with the traffic demand T, together with costs and line rates of different configurations' optical channels, the configuration selection problem is to minimize $\sum_k a_k c_k$, subject to $\sum_k a_k l_k \geq T$, where a_k is the number of $conf_k$'s optical channels.

The configuration selection problem can be solved in polynomial time, given that the number of configurations is fixed. In our solution, we start by finding the $\mathbf{Cost}(k, a_k)$ for all possible k and a_k, where $\mathbf{Cost}(k, a_k) = a_k \times c_k$. Then we tour around all possible combinations of line rates to achieve the traffic demand T, and select the line rate combination which gives the minimum total cost. Checking all possible line rate combinations requires a running time

Algorithm 7 getNodeMapping

Input: a physical optical network G_P(**V**, **E**), a VON G_V(**N**, **T**, **C**), set of sorted virtual links **VL**
Output: $MAP(G_V)$, which is node mapping of G_V(**N**, **T**, **C**)
//Main procedure
Begin
if **VL** == $\emptyset$ **then**
  return $MAP(G_V)$
end if
currentVL(m, n) ← the first virtual link in **VL**
Check whether m and n have been mapped
if both m and n have been mapped **then**
  VL ← **VL** – currentVL(m, n)
  getNodeMapping(G_P, G_V, **VL**)
else if neither end nodes have been mapped **then**
  for all m's candidate nodes u_i **do**
    for all n's candidate nodes v_j **do**
      if *valid*(u_i, v_j) **then**
        CM(u_i, v_j) ← *NodeMetric*(m, u_i) + *NodeMetric*(n, v_j) + *SP*(u_i, v_j)
      end if
    end for
  end for
else if end node m is mapped to node u while n is not mapped **then**
  for all n's candidate nodes v_j **do**
    if *valid*(u, v_j) **then**
      CM(u, v_j) ← *NodeMetric*(n, v_j) + *SP*(u, v_j)
    end if
  end for
end if
CM ← sort **CM** in an ascending order
for all (u_i, v_j) in **CM** **do**
  m is mapped to u_i, n is mapped to v_j
  VL ← **VL** – currentVL(m, n)
  getNodeMapping(G_P, G_V, **VL**)
  if all virtual nodes have been mapped **then**
    return $MAP(G_V)$
  end if
end for
End

of $O(\lceil \frac{T}{l_1} \rceil^K)$, where l_1 is the lowest line rate. Since the number of configurations is given, K is fixed, and thus the algorithm runs in polynomial time. This algorithm is shown in Algorithm 8. In Algorithm 8, $\boldsymbol{A_k}$ denotes the line rate combination, $a_k \in \boldsymbol{A_k}$, $1 \leq k \leq K$.

Algorithm 8 getConfigurations

Input: $\mathbf{C} = \{c_k\}$, $k = 1, 2, ..., K$, line rate set $\mathbf{L} = \{l_k\}$, $k = 1, 2, ..., K$, traffic demand T
Output: $minCost$, which is the minimum cost of line rate selection to accommodate T
BEGIN
for all $k = 1$ to K **do**
  $a_k = 0$
  while *true* **do**
    if $T - (a_k - 1) \times l_k \leq 0$ **then**
      break
    end if
    $\mathbf{Cost}(k, a_k) \leftarrow a_k \times c_k$
    $a_k \leftarrow a_k + 1$
  end while
end for
for all $a_1 = 0$ to $\lceil \frac{T}{l_1} \rceil$ **do**
  for all $a_2 = 0$ to $\lceil \frac{T}{l_2} \rceil$ **do**
    ...
    for all $a_{K-1} = 0$ to $\left\lceil \frac{T}{l_{K-1}} \right\rceil$ **do**
      $a_K = \left\lceil \frac{T - \sum_{k=0}^{K-1} a_k \cdot l_k}{l_K} \right\rceil$
      if $\sum_k \boldsymbol{Cost(k, a_k)} < minCost$ **then**
        $minCost \leftarrow \sum_k \boldsymbol{Cost(k, a_k)}$
      end if
    end for
    ...
  end for
end for
return $minCost$
END

6.4.2 Baseline Algorithm

The baseline algorithm is different from MC-SVONM in the steps of calculating distance matrix and node mapping. When calculating the distance matrix, for each s-d pair, the baseline algorithm finds one shortest path first using Dijkstra's algorithm. The edges of this path are then deleted from the physical topology, and the baseline algorithm finds the second shortest path using Dijkstra's algorithm. The total distance of these two paths are recorded as *SP(s, d)*. When mapping nodes, the baseline algorithm doesn't calculate $Metric(m, u)$, but considers only *SP(u, v)*. For example, if neither of a virtual link's end nodes have been mapped, then instead of choosing the u_i and v_j with the smallest value of *Metric(m,* u_i*)* + *Metric(n,* v_j*)* + *SP(*u_i*,* v_j*)*, the baseline algorithm chooses the u_i and v_j with the smallest value of *SP(*u_i*,* v_j*)*. The other steps of the baseline algorithm are the same as those of MC-SVONM.

6.4.3 Lower Bound

For comparison with the heuristic approach, we find a lower bound, which is, for every virtual link (m, n), where m can be mapped to $\{u_1, u_2, ..., u_x\}$, and n can be mapped to $\{v_1, v_2, ..., v_y\}$, we map (m, n) to the (u_i, v_j) with the smallest value of $SP(u_i, v_j)$, whether or not u_i or v_j has been mapped by other virtual nodes. Then we use the same routing and configuration selection as that of our heuristic approach for every virtual link. Note that this lower bound may not be achievable, since it allows multiple virtual nodes to be mapped to the same physical node, and allows a virtual node to be mapped to multiple physical nodes. For example, if every virtual node can be mapped to any physical node in G_P, then all the virtual links will be mapped to the same pair of link-disjoint paths with the shortest total distance in G_P.

6.5 Numerical Results

In this section, we present the simulation results of the ILP model on a small-scale network and our algorithms on both small-scale and large-scale networks. The ILP model was solved using IBM ILOG OPL $v12.2$, and the algorithms were implemented in Java. The simulation was run on a server with 16×2.4 GHz processors and 12 GB memory. We use two line rates: 40/100 Gbps, and each line rate has two possible modulation formats. The reachabilities, channel width, transponder costs and regenerator costs are shown in Table. 6.1. The unit SI cost is set to 10^{-5}/km·GHz referring to [124]. In our simulation, given a VON, each virtual node is assigned a unique physical node as central location, and the physical nodes within a certain diameter are included as the candidate nodes of this virtual node. We can increase the diameter to increase the number of candidate nodes.

Experiment 1. In the first experiment, we compare the performance of the ILP model with our heuristic algorithms. The experiment is conducted on the 6-node network shown in Figure 6.1. In the first part, we compare the total cost under different number of VONs. The average number of candidate nodes per virtual node is 3.5. The average number of virtual links per VON is 3.6, while the average nodal degree per virtual node is 2.0. The simulation results are averaged over more than 100 simulation runs. From Figure 6.3, we can see that the performance of MC-SVONM is almost the same as that of the ILP model and the difference is only 0.9%. Since the lower bound may not be achievable, its total cost is even lower than the ILP. The performance of the baseline algorithm is worse than the MC-SVONM, showing that the mapping strategy of MC-SVONM leads to lower cost.

In the second part, we compare the total cost under different average number of candidate nodes per virtual node. The number of VONs is 10. The average number of virtual links per VON is 3.8, while the average nodal degree per virtual node is 2.1. The simulation results are averaged over more than 100 simulation runs. Figure 6.4 shows that the total cost obtained by ILP, MC-VONM, the baseline algorithm, and the lower bound all decrease

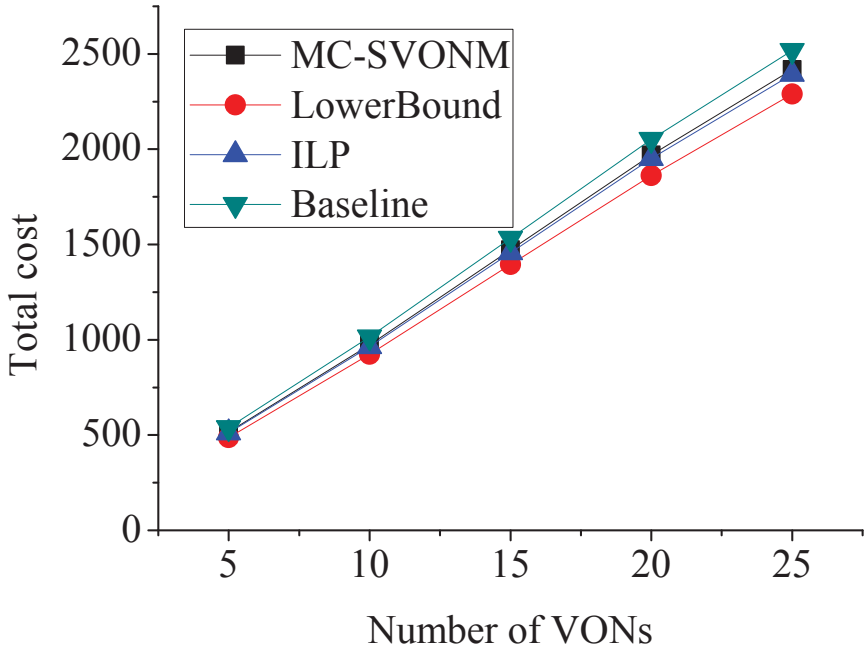

Figure 6.3. Total cost vs. number of VONs for 6-node network

along with the increase of average number of candidate nodes, since virtual links are more likely to be mapped to a shorter path. Again, we can see that the MC-SVONM results in a cost increase of only 5.8% compared to the ILP. The baseline algorithm is not too much different from the MC-SVONM due to the small network size. There is a huge decrease in the total cost for all the algorithms when the average number of candidate nodes increases from 3 to 4, because of a huge decrease in the regenerator cost.

Experiment 2. In the second experiment, we investigate the performance of our heuristic algorithm under a large-scale network, and study how the total cost changes along with increasing number of VONs. The experiment is conducted on the 75-node CORONET [1]. The average number of virtual links per VON is 11.4 and the average nodal degree per virtual node is 3.6. The results are averaged over more than 100 simulation runs. Figure 6.5 shows the total cost under different number of VONs. "MC-SVONM-i" refers to the MC-SVONM algorithm with the average number of candidate nodes per virtual node as i. This notation applies to the baseline algorithm and the lower bound as well.

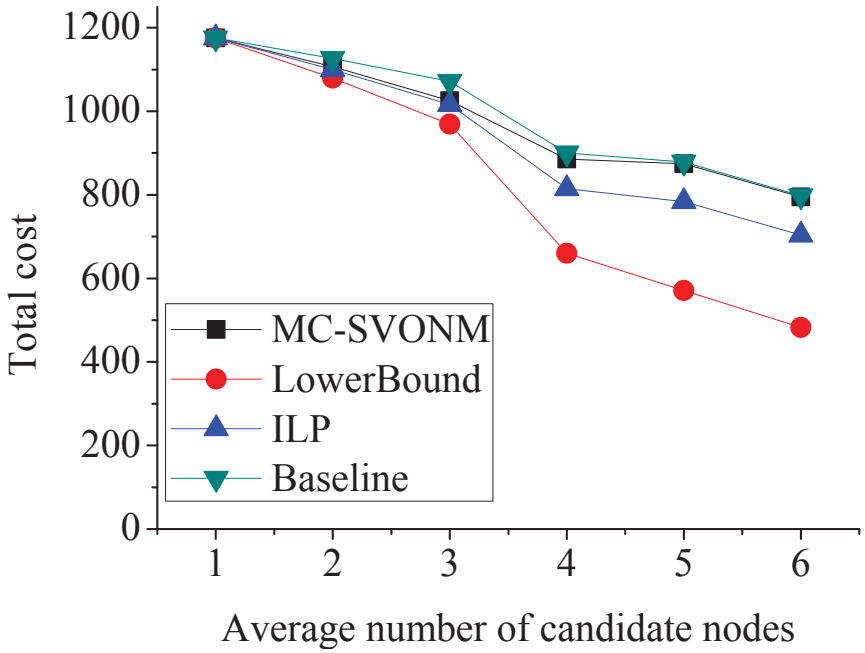

Figure 6.4. Total cost vs. average number of candidate nodes for 6-node network

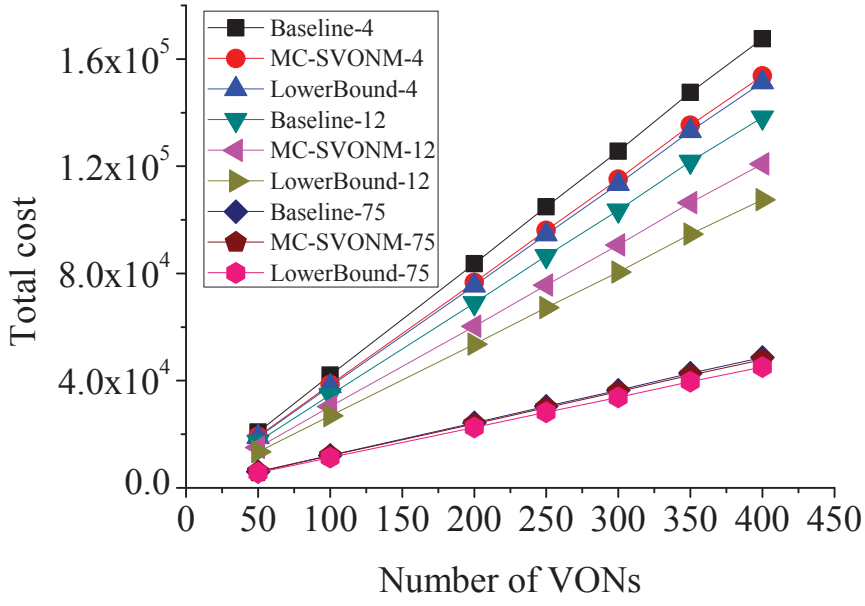

Figure 6.5. Total cost vs. number of VONs for 75-node CORONET

From Figure 6.5, we can see that the MC-SVONM algorithm is very close to the lower bound. The differences in the total cost are 1.6%, 11.1%, and 5.8%, respectively, when the average number of candidate nodes are 4, 12, and 75. Since the total cost of lower bound is even lower than the ILP, the results show that the MC-SVONM has near-optimal performance. The baseline algorithm has worse performance than the MC-SVONM algorithm under all simulation settings, and the baseline algorithm increases the total cost by 9.0%, 14.4%, and 1.6%, respectively, compared to MC-SVONM under 4, 12, and 75 candidate nodes, showing that the mapping strategy of MC-SVONM has good performance. When the number of candidate nodes is 75, the difference between MC-SVONM and the baseline algorithm is small, because under such high flexibility in node mapping, even the simple node mapping strategy as the baseline algorithm can achieve low cost.

Experiment 3. In the third experiment, we study the total cost, different equipment's cost, the number of transponders, and the number of regenerators under different number of candidate nodes in a large-scale network. The experiment is conducted on the 75-node CORONET [1]. The total number of VONs is 200. The average number of virtual links per VON is 11.4 and the average nodal degree per virtual node is 3.6. The results are averaged over more than 800 simulation runs.

From Figure 6.6, we can see that the total cost decreases when a virtual node has more mapping choices. The difference between the MC-SVONM algorithm and the lower bound becomes larger at first, and then becomes smaller. The reason is that the lower bound ignores the connectivity of the VON, so it can quickly eliminate regenerators by choosing the shortest paths for each virtual link when the number of candidate nodes increases; however, when the number of candidate nodes further increases, less regeneration is required, and only a few regenerators can be eliminated, so the line of the lower bound is almost flat after 40 candidate nodes. MC-SVONM only increases the total cost by 15.0%, on average, compared to the lower bound. The difference between MC-SVONM and the baseline in total cost is 24.6% on average.

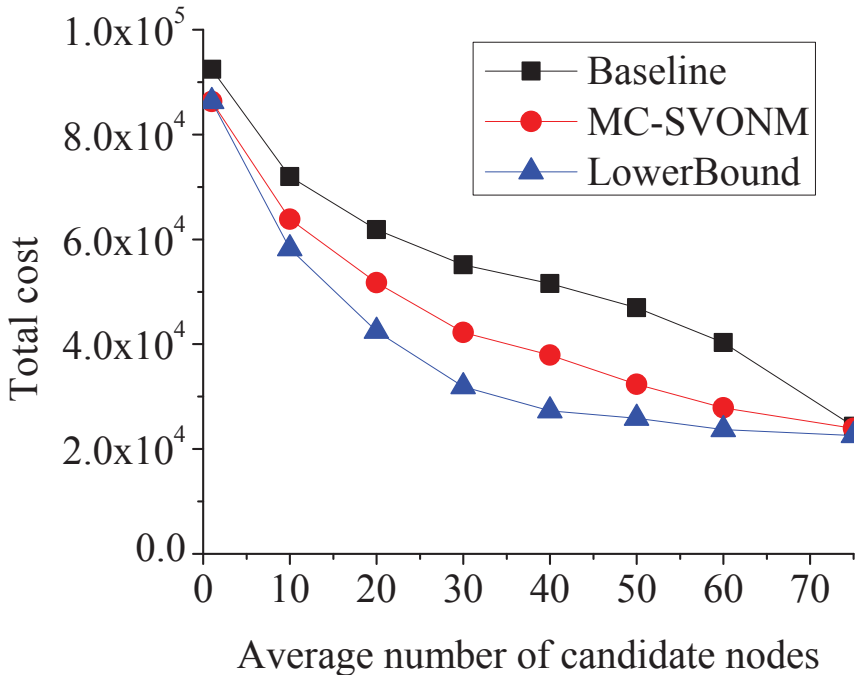

Figure 6.6. Total cost vs. average number of candidate nodes for 75-node network

Figure 6.7, Figure 6.8, and Figure 6.9 show different equipment's cost, number of transponders of each type, and the number of regenerators of each type, respectively, under different number of candidate nodes using the MC-SVONM algorithm. From Figure 6.7, we can see that the transponder cost hardly changes, showing that the transponder cost is almost unaffected by the length of the paths to which virtual links are mapped. The SI cost and the regenerator cost decrease significantly, since they are closely related to the path length. Figure 6.8 shows that the number of 100 Gbps transponders increases while the number of 40 Gbps transponders decreases when the number of candidate nodes increases. The reason is that a virtual link has a greater chance to be mapped to a shorter path when the number of candidate nodes increases, and the higher line rate is more cost-effective than the lower line rate in short distance transmission when fewer regenerators are needed. For the same reason, the ratio of the number of 40 Gbps transponders with 25 GHz channel width in the total number of 40 Gbps transponders becomes larger when the number of candidate nodes increases. From Figure 6.9, we can see that the number of regenerators decreases quickly at

the beginning, and then this decreasing slows down when the number of candidate nodes is large enough. This is why the total cost doesn't decrease linearly.

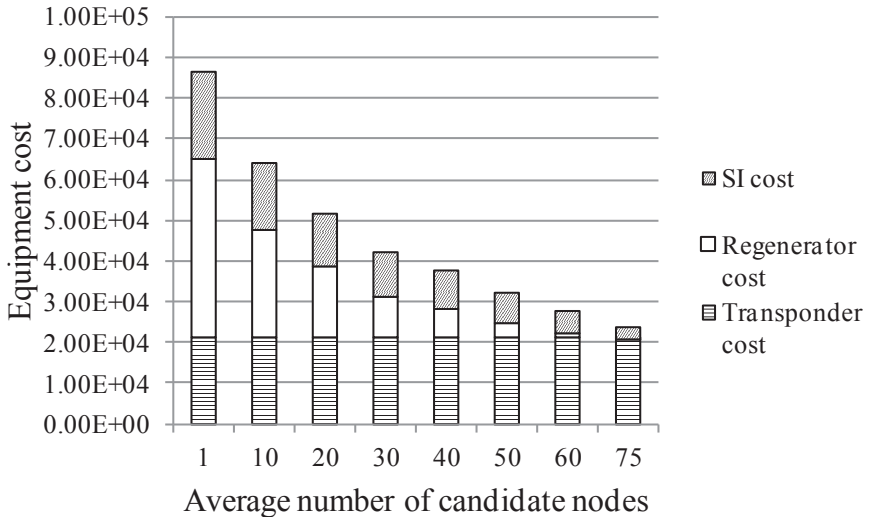

Figure 6.7. Equipment costs vs. average number of candidate nodes for 75-node network

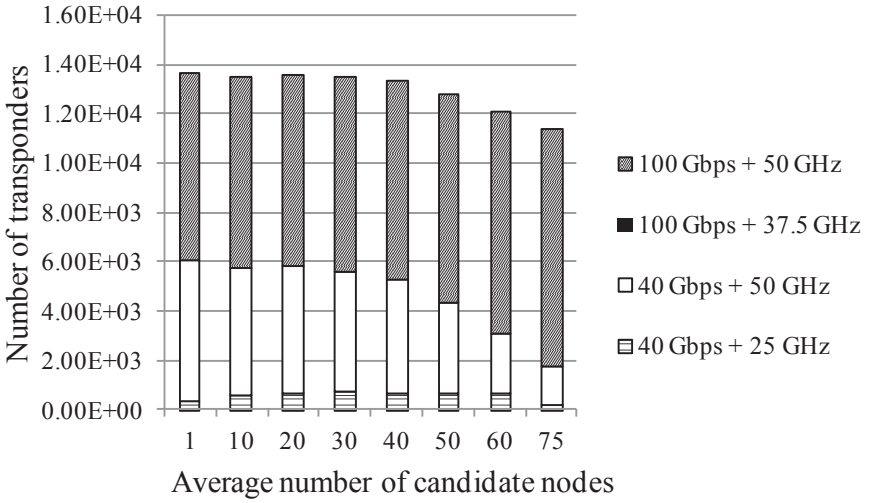

Figure 6.8. Number of transponders vs. average number of candidate nodes for 75-node network

Experiment 4. In the fourth experiment, we compare the total cost of using shared transponders or dedicated transponders for working and backup paths. The simulation settings are the same as those of Experiment 2. MC-SVONM-Dedicate uses separate sets of

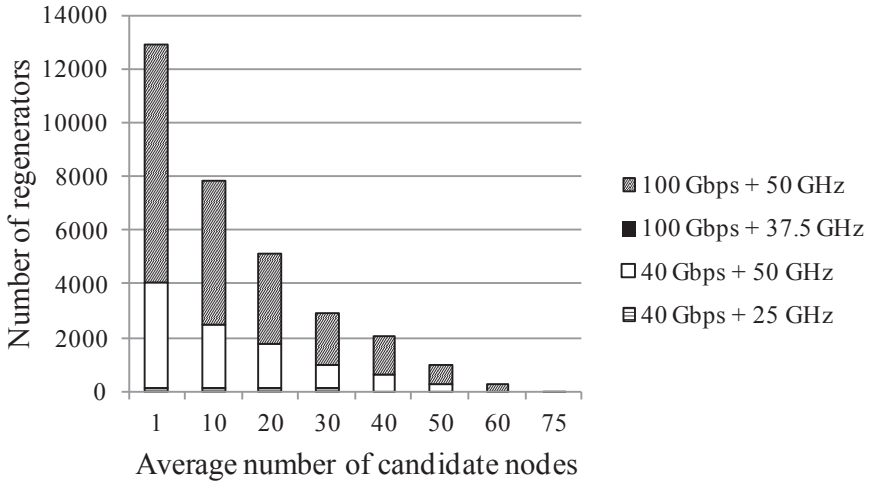

Figure 6.9. Number of regenerators vs. average number of candidate nodes for 75-node network

transponders for working and backup paths. The working and backup paths may use different configurations' optical channels. On the contrary, MC-SVONM-Share uses the same set of transponders for working and backup paths, but they must use the same configurations' optical channels.

From Figure 6.10, we can see that shared transponders always leads to lower cost. The total cost obtained by using dedicated transponders increases by 23.0%, 33.2%, and 87.7%, respectively, compared to shared transponders, when the number of candidate nodes are 1, 12, and 75.

6.6 Conclusion

In this chapter, we focus on the problem of survivable impairment-constrained virtual optical network mapping in flexible-grid optical networks (SIC-VONM), which aims to minimize the combined cost of working and backup optical network equipment, which include transponders, regenerators, and shared infrastructure. An ILP is formulated for SIC-VONM. We also propose a three-step heuristic algorithm MC-SVONM to solve large scale cases, and compare it with a baseline algorithm and a lower bound. The numerical results show that

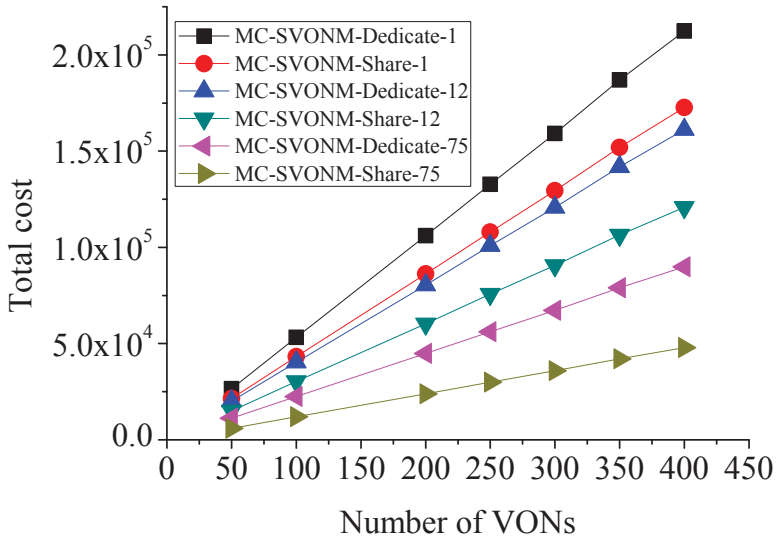

Figure 6.10. Shared transponders vs. dedicated transponders

the ILP can solve small scale problems properly and that the total cost obtained by our heuristic algorithm is very close to that of the ILP model. Also, MC-SVONM achieves results that are only slightly higher than the lower bound, showing near-optimal performance. The comparison of MC-SVONM with the baseline algorithm shows that our novel mapping strategy leads to lower cost. One possible area of future research work is to consider the survivable impairment-aware VON mapping problem in flexible-grid optical networks with shared protection.

CHAPTER 7

COST-OPTIMIZED DESIGN OF FLEXIBLE-GRID OPTICAL NETWORKS CONSIDERING RS SELECTION

In this chapter, we aim to minimize the total network cost in flexible-grid optical networks with multiple line rates.[1] Besides transponder cost, regenerator cost, and shared infrastructure cost, the cost of RSs is also considered. We first provide the problem definition and formulate the problem as an ILP. We also propose a heuristic algorithm considering both selection and placement of equipment to minimize the total network cost. Simulation results show the heuristic algorithm results in up to 28% cost saving, with no significant increase in spectrum usage.

7.1 Introduction

The optical backbone network is now evolving towards flexible-grid optical networks, where optical channels may be assigned different number of spectrum slots according to their transmission parameters [11]. Flexible-grid networks not only provide a more efficient spectrum utilization through tighter channel spacing, but also serve as an enabler to data rates beyond 100 Gbps (e.g., 400 Gbps, 1000 Gbps). Similar to MLR optical networks, physical layer impairments also exist in flexible-grid optical networks, and there are also great benefits in concentrating the RSs. Thus, we study the problem of concentrating RSs in flexible-grid optical networks, in order to achieve minimum network cost.

[1] ©2013 IEEE. Reprinted, with permission, from Weisheng Xie, Jason P. Jue, Xi Wang, Qiong Zhang, Qingya She, Paparao Palacharla, Motoyoshi Sekiya, "Cost-Optimized Design of Flexible-Grid Optical Networks Considering Regenerator Site Selection," *IEEE Global Communications Conference (GLOBECOM)*, December 2013

In this chapter, we consider RS selection for flexible-grid optical networks under impairment constraints that are represented as the reachability for each line rate. For a given set of connection requests, we need to find a path (or multiple paths) for each connection request, decide the line rate of each path, and place regenerators along each path if the distance is longer than the reachability for the chosen line rate. The objective of our problem is to minimize the total network cost, which includes the cost of transponders, regenerators, RSs, and the other shared infrastructure. We make the following assumptions: 1) the links in the optical network are bidirectional; 2) all requests are bidirectional; 3) sufficient link resources (e.g. spectrum) and node resources (e.g. transponders and regenerators) are available in the optical network, which means that no connection request will be blocked.

The rest of this chapter is organized as follows. In Section 7.2, a detailed problem description is provided. In Section 7.3, we propose an ILP formulation of the problem. In Section 7.4, a heuristic algorithm is presented. In Section 7.5, we show some numerical results for both ILP and the heuristic algorithm. Finally, we give a summary of our work in Section 7.6.

7.2 Problem Description

7.2.1 Network Model and Cost Model

The optical network can be represented as a graph $G(\mathbf{V}, \mathbf{E}, \mathbf{D})$, where $\mathbf{V}$ is a set of nodes, $\mathbf{E} = [e_{i,j}]$ is an adjacency matrix representing edges of $\mathbf{G}$, and $\mathbf{D} = [d_{i,j}]$ is the set of distances corresponding to the edge set $\mathbf{E}$, where $d_{i,j}$ is the link length of $e_{i,j}$. For each connection request, the requested traffic is broken down into multiple optical channels of different line rates. These optical channels are reserved along paths, and regenerators are placed at the RSs along the paths if needed.

In this chapter, we use reachability in actual distance (km) to measure the effect of impairments. The reachabilities of different line rates vary due to different physical impair-

ments. Thus, we use a set of reachabilities **A** to denote the reachabilities for different line rates.

The total network cost consists of the following four elements:

1. The transponders of different line rates;

2. The 3-R regenerators of different line rates;

3. RSs;

4. The other shared infrastructure (SI) such as the fiber, inline optical amplifiers, and ROADMs. The unit SI cost is the average cost of all shared infrastructure for 1 km of transmission distance and for consuming 1 GHz of optical bandwidth, i.e., \$/(km*GHz) [124].

Given an optical channel of certain line rate l_k and its path P, the cost of this optical channel is $2{*}ct_k + NR(P){*}cr_k + C_U{*}Dist(P){*}f_k$, where ct_k is the cost of line rate l_k's transponder, $NR(P)$ is the number of required line rate l_k's regenerators along the path P, cr_k is the cost of line rate l_k's regenerator, C_U is the unit SI cost, $Dist(P)$ is the distance of P, and f_k is the channel width of line rate l_k. The total network cost is the summation of all the optical channels' costs plus the cost of RSs.

7.2.2 Problem Statement

Given physical topology $G(\mathbf{V}, \mathbf{E}, \mathbf{D})$, where **V** is a set of nodes, **E** is a set of edges, **D** is a set of distance according to the edge set **E**, a set of line rates **L**, $l_k \in \mathbf{L}$, $1 \leq k \leq |\mathbf{L}|$, a reachability set **A**, $a_k \in \mathbf{A}$, $1 \leq k \leq |\mathbf{L}|$, where a_k is the reachability of line rate l_k, a set of transponder costs **CT**, $ct_k \in \mathbf{CT}$, $1 \leq k \leq |\mathbf{L}|$, where ct_k is the cost of a line rate l_k's transponder, a set of regenerator costs **CR**, $cr_k \in \mathbf{CR}$, $1 \leq k \leq |\mathbf{L}|$, where cr_k is the cost of a line rate l_k's regenerator, a set of channel width **F**, $f_k \in \mathbf{F}$, $1 \leq k \leq |\mathbf{L}|$, where f_k is the channel width of a line rate l_k's optical channel, the cost of a RS C_{RS}, the unit SI cost C_U, and a set of traffic demands **R**, $r_{s,t} \in \mathbf{R}$, where $r_{s,t}$ is the requested aggregated traffic from s to t.

Find: (1) the line rate selection for each connection request; (2) the routing for each optical channel; (3) the regenerator placement and RS selection.

Our objective is to minimize the total network cost, subject to the following constraints:

1. traffic constraint: every connection request is assigned one or several line rates, and the combined traffic of these assigned line rates is not smaller than that of the connection request;

2. impairment constraint: along any path, the length of each segment without regenerators does not exceed the corresponding line rate l_k's reachability limit a_k.

An example is shown in Figure 7.1. Suppose we have a traffic demand of 500 Gbps from Node 1 to Node 5. The available line rates, their corresponding costs, and corresponding channel width are shown in Table I. The cost of a RS is assumed to be 10. The unit SI cost is assumed to be 10^{-5}/km*GHz. As shown in Figure 7.1(b), We can choose two 400 Gbps channels along Path 1 with a total cost of 63.5, and select Node 6 as a RS. Or we can choose five 100 Gbps channels along Path 1 with a total cost of 55.5 by selecting Node 6 as a RS, as shown in Figure 7.1(c). Now we consider the case where both 400 Gbps and 100 Gbps are used. As Figure 7.1(d) shows, if we choose one 400 Gbps channel along Path 2, and one 100 Gbps channel along Path 1, the total cost is 55.85. Node 2 and Node 6 are selected as RSs. The cost can be decreased by choosing Path 1 for both 400 Gbps and 100 Gbps channels, as shown in Figure 7.1(e). The total cost is 45.85, and only Node 6 is selected as a RS. This is the optimal solution for this case. Thus, different line rate selection, routing, and regenerator placement will lead to different total cost.

7.3 ILP Formulation

The ILP model is based on a reachability graph in which a pair of directed auxiliary links are constructed between node pairs whose shortest path distance is shorter than or equal to the reachability. Figure 7.2 shows an example of the reachability graphs of the physical topology

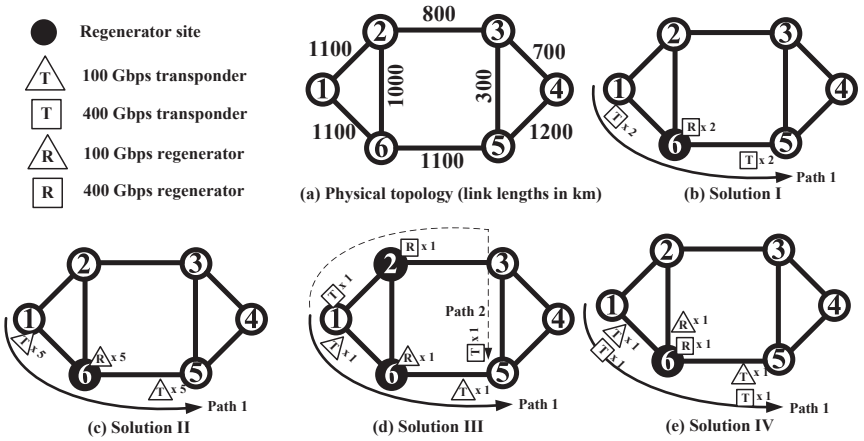

Figure 7.1. Example of the problem (link lengths in km)

shown in Figure 7.1, when the reachabilities are 1200 km and 2000 km, respectively. Under different reachability a_k, a given physical topology can have different reachability graphs. A shortest path in this auxiliary graph is a min-regenerator path in the network.

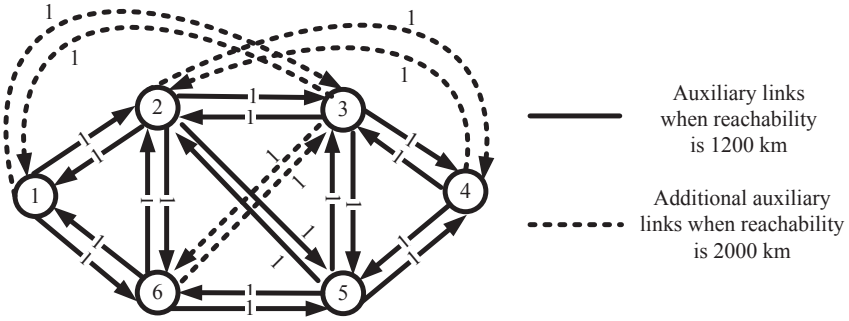

Figure 7.2. Reachability graphs

Next, we present the ILP formulation for the problem. First, we define some useful notations and variables.

7.3.1 Input Parameters

- $\mathbf{L} = [l_k]_{|\mathbf{L}|}$: set of line rates;
- $\mathbf{R} = [r_{s,t}]_{|\mathbf{V}|\times|\mathbf{V}|}$: set of connection requests;

• **E'** = $[e'_{k,i,j}]_{|\mathbf{L}|\times|\mathbf{V}|\times|\mathbf{V}|}$: $e'_{k,i,j}$ equals to 1 if there is an auxiliary link between i and j in the auxiliary graph corresponding to line rate l_k, otherwise 0;

• **D** = $[d_{i,j}]_{|\mathbf{V}|\times|\mathbf{V}|}$: shortest distance between i and j in the physical topology;

• **CT** = $[ct_k]_{|\mathbf{L}|}$: set of costs of transponders;

• **CR** = $[cr_k]_{|\mathbf{L}|}$: set of costs of regenerators;

• **F** = $[f_k]_{|\mathbf{L}|}$: set of channel width;

• C_{RS}: cost of a RS;

• C_U: unit SI cost;

• P: maximum number of paths for a connection request;

• VL: a pre-defined very large number.

7.3.2 Variables of ILP

• **X** = $[x^{s,t,p}_{k,i,j}]^{|\mathbf{V}|\times|\mathbf{V}|\times P}_{|\mathbf{L}|\times|\mathbf{V}|\times|\mathbf{V}|}$: $x^{s,t,p}_{k,i,j}$ equals to 1 if edge $e'_{k,i,j}$ is along the path p from s to t on line rate l_k's reachability graph, otherwise 0;

• **Y** = $[y^{s,t,p}_{k,i}]^{|\mathbf{V}|\times|\mathbf{V}|\times P}_{|\mathbf{L}|\times|\mathbf{V}|}$: $y^{s,t,p}_{k,i}$ equals to 1 if a line rate l_k's regenerator is placed at node i on the path p from s to t, otherwise 0;

• **Z** = $[z^{s,t}_k]^{|\mathbf{V}|\times|\mathbf{V}|}_{|\mathbf{L}|}$: number of required line rate l_k's transponder pairs from s to t;

• **S** = $[s_i]_{|\mathbf{V}|}$: equals to 1 if node i is selected as a RS, otherwise 0.

7.3.3 Objective

The objective is to minimize the following function:

$$min\ obj = \sum_{k,s,t} 2 \cdot ct_k \cdot z^{s,t}_k + \sum_{s,t,p,k,i} cr_k \cdot y^{s,t,p}_{k,i} + \sum_i C_{RS} \cdot s_i + \sum_{s,t,p,k,i,j} C_U \cdot f_k \cdot x^{s,t,p}_{k,i,j} \cdot d_{i,j} \quad (7.1)$$

Note that the first part of the objective is the total cost of the transponders; the second part is the total cost of the regenerators; the third part is the total cost of RSs; and the fourth part is the total cost of other shared infrastructure.

7.3.4 Constraints

$$\sum_{p,k,j} l_k \cdot (x_{k,s,j}^{s,t,p} - x_{k,j,s}^{s,t,p}) \geq r_{s,t}, \forall 1 \leq s \leq |\mathbf{V}|, 1 \leq t \leq |\mathbf{V}| \tag{7.2}$$

$$\sum_{p,k,j} l_k \cdot (x_{k,j,t}^{s,t,p} - x_{k,t,j}^{s,t,p}) \geq r_{s,t}, \forall 1 \leq s \leq |\mathbf{V}|, 1 \leq t \leq |\mathbf{V}| \tag{7.3}$$

$$\begin{gathered} \sum_{i} x_{k,i,j}^{s,t,p} = \sum_{i} x_{k,j,i}^{s,t,p}, \forall 1 \leq s \leq |\mathbf{V}|, 1 \leq t \leq |\mathbf{V}|, \\ 1 \leq p \leq P, 1 \leq k \leq |\mathbf{L}|, 1 \leq j \leq |\mathbf{V}|, j \neq s, t \end{gathered} \tag{7.4}$$

Constraint 7.2 guarantees that the source node generates a traffic flow greater than or equal to the requested traffic. Constraint 7.3 guarantees that the destination receives the same amount of data generated at the source node. Constraint 7.4 guarantees that for any intermediate node, the incoming and outgoing flows should be the same.

$$\begin{gathered} x_{k,i,j}^{s,t,p} \leq e'_{k,i,j}, \forall 1 \leq s \leq |\mathbf{V}|, 1 \leq t \leq |\mathbf{V}|, 1 \leq p \leq P, \\ 1 \leq k \leq |\mathbf{L}|, 1 \leq i \leq |\mathbf{V}|, 1 \leq j \leq |\mathbf{V}| \end{gathered} \tag{7.5}$$

Constraint 7.5 ensures that the route of line rate l_k's channel is on the reachability graph of line rate l_k.

$$\begin{gathered} y_{k,i}^{s,t,p} \geq x_{k,i,j}^{s,t,p}, \forall 1 \leq s \leq |\mathbf{V}|, 1 \leq t \leq |\mathbf{V}|, 1 \leq p \leq P, \\ 1 \leq k \leq |\mathbf{L}|, 1 \leq j \leq |\mathbf{V}|, 1 \leq i \leq |\mathbf{V}|, i \neq s \end{gathered} \tag{7.6}$$

Constraint 7.6 guarantees that a regenerator is placed for every hop of a path p, excluding the source and destination of path p, on the reachability graph.

$$z_k^{s,t} = \sum_{p,j} x_{k,s,j}^{s,t,p}, \forall 1 \leq s \leq |\mathbf{V}|, 1 \leq t \leq |\mathbf{V}|, 1 \leq k \leq |\mathbf{L}| \tag{7.7}$$

Constraint 7.7 is to calculate how many line rate l_k's transponder pairs are needed between each s-t pair.

$$s_i \geq \frac{\sum_{s,t,p,k} y_{k,i}^{s,t,p}}{VL}, \forall 1 \leq i \leq |\mathbf{V}| \tag{7.8}$$

Constraint 7.8 ensures that a node is selected as a RS when there is regenerator placed in this node.

7.4 Heuristic Approach

Our heuristic algorithm is based on three steps: (1) line rate selection; (2) routing and regenerator placement; (3) post processing.

7.4.1 Line Rate Selection

Given a connection request, we can obtain the cost of a line rate l_k's channel between the source and destination of this connection request by the following formula: $TC_{s,t,k} = 2{*}ct_k + (LHP_{s,t,k} - 1){*}cr_k + C_U{*}SP_{s,t}{*}f_k$, where $TC_{s,t,k}$ is the total cost of a line rate l_k's channel from s to t, $LHP_{s,t,k}$ is the least hop count from s to t in the reachability graph corresponding to line rate l_k, and $SP_{s,t}$ is the shortest path distance from s to t in the physical topology. Based on the traffic demand and the cost of each line rate's channel, we can determine the number of lightpaths together with the proper line rate for each path so that the total cost for the traffic demand is minimized. If the number of rates is given, this process can be done and achieve the optimal solution in polynomial time through dynamic programming, using Algorithm 8.

7.4.2 Routing and Regenerator Placement

After line rates are selected, we create $|\mathbf{L}|$ matrices $[T_k]_{|\mathbf{L}|}$, where $T_k = [t_{s,d}]_k$ contains the number of channels from s to d using line rate l_k. We start from the highest line rate's

matrix. In a matrix, we start from the largest demand. If a node is not a RS, the weights of all egress links of this node in line rate l_k's auxiliary graph are set to $t_{s,d}$ * cr_k + C_{RS}. If a node is already selected as a RS, the weights of its egress links are set to $t_{s,d}$ * cr_k. Then we run shortest path algorithm to find a path on line rate l_k's auxiliary graph for the channels from s to d using line rate l_k. All the internal nodes in this shortest path are selected as RSs. Regenerators of corresponding line rate are placed along this path in RS. The same procedure is applied to the next set of channels, and the weights of the links in the auxiliary graph are updated according to number of channels and the existing RSs.

7.4.3 Post Processing

The above routing and regenerator placement step only adds RSs without deleting any of them. However, it is possible that some earlier selected RS v may become unnecessary when one or several later selected RSs can cover the source-destination pairs that v originally covered with an even lower cost. An example is shown in Figure 7.3. Suppose we have two sets of optical channels: Set 1 from Node 1 to Node 4 with two 400 Gbps channels and Set 2 from Node 2 to Node 4 with one 400 Gbps channel. Suppose the costs and the reachabilities are the same as that in Section II.B. Using the routing and regenerator placement approach presented above, the results will be choosing Path 1 for Set 1 and choosing Path 2 for Set 2, while Node 5 and Node 3 are selected as RSs with a total cost of 100.125, as shown in Figure 7.3(a). However, as Figure 7.3(b) shows, if we change Set 1 from Path 1 to Path 3, the total cost will be reduced to 90.375, so choosing Node 5 as a RS becomes less cost-efficient.

Thus we propose a post processing approach to improve our solutions. For every RS v in the output of the routing and regenerator placement step, we delete v and check the lightpaths passing through v. These lightpaths have to be switched to other paths. The new lightpaths are found through the routing step described in Section IV. B, except that the weights of the egress links of a RS are set to a very small number, while the weights of the

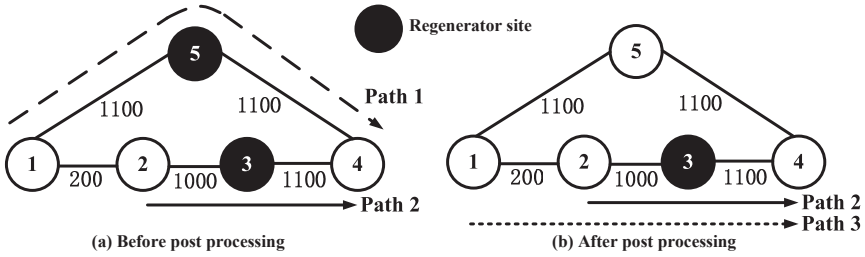

Figure 7.3. Post processing

egress links of an non-RS node are set to a very large number. After the new lightpaths are found, the total cost is re-calculated. If the new lightpaths have lower cost and no additional RS is added, then v is deleted, otherwise v remains in the set of RSs. This process is repeated for every RS.

7.4.4 Complete Heuristic Approach

Our heuristic approach follows the three-step process: line rate selection, routing and regenerator placement, and post processing. We name this approach the FlexGrid-MinCost (FG-MC) algorithm. The full FG-MC algorithm is shown in Algorithm 9.

For comparison with our heuristic, we have the FlexGrid-ShortestPath (FG-SP) algorithm, which uses the same line rate selection and post processing approaches as our heuristic, but always uses shortest paths in the physical topology to route the optical channels. We also compare with a SLR algorithm that does not consider line rate selection. In our simulation, the SLR algorithm uses either all 400 Gbps line rate (SLR-400G) or all 100 Gbps line rate (SLR-100G), and the routing is always shortest path in the physical topology. The FG-MC, FG-SP, SLR-400G, and SLR-100G algorithms allow regenerators to be placed anywhere. Any node with regenerators placed becomes a RS.

Algorithm 9 FlexGrid-MinCost (FG-MC)

Input: physical topology $G(\mathbf{V}, \mathbf{E}, \mathbf{D})$, the reachability set $\mathbf{A}$, the connection request set $\mathbf{R}$, regenerator cost set $\mathbf{CR}$, transponder cost set $\mathbf{CT}$, RS cost C_{RS}, and unit SI cost C_U
Output: total cost TC
//Main procedure
Begin
$[T_k]_{|\mathbf{L}|} = \mathbf{0}$
//Line rate selection
for all $r_{s,t} \in \mathbf{R}$ **do**
  Calculate $TC_{s,t,k}$ for all $1 \leq k \leq |\mathbf{L}|$
  Use dynamic programming to determine the line rate set $\boldsymbol{LR} = [lr_k]_{|\mathbf{L}|}$ with minimum cost
  for all $1 \leq k \leq |\mathbf{L}|$ **do**
    $[t_{s,t}]_k = [t_{s,t}]_k + lr_k$
  end for
end for
//Routing and regenerator placement
for all T_k from T_1 (highest rate) to $T_{|\mathbf{L}|}$ (lowest rate) **do**
  Pick the maximum $[t_{s,t}]_k$
  Update the reachability graph corresponding to line rate l_k
  Run shortest path algorithm on the reachability graph corresponding to line rate l_k
  The intermediate nodes of the path found are selected as RSs
  $[t_{s,t}]_k = 0$
end for
Post processing
Calculate total cost TC
End

7.5 Numerical Results

In this section, we present some numerical examples to show that the ILP can solve small-scale problems very well, while our heuristic algorithm can achieve good performance for both small-scale and large-scale networks. The ILP model was solved using IBM ILOG OPL v12.2. We use two line rates: 100/400 Gbps. The reachabilities, transponder costs, regenerator costs, and channel width are shown in Table 7.1, which are referred to [110]. The unit SI cost is 10^{-5}/GHz*km, which is referred to [124].

Table 7.1. Simulation parameters

Line Rate (Gbps)	**Reach (km)**	**Transponder Cost**	**Regenerator Cost**	**Channel Width (GHz)**
100	2000	2	4	50
400	1200	6	12	125

Experiment 1. In the first experiment, we compare the performance of the ILP model with our heuristic algorithm. The experiment is conducted on the 14-node NSFNet topology shown in Figure 7.4. The total costs of ILP and heuristic algorithm are compared under different network load, and under different costs of a RS. The average traffic between each node pair grows from 100 Gbps to 600 Gbps. The costs of a RS are 0.01, 1, and 100, respectively.

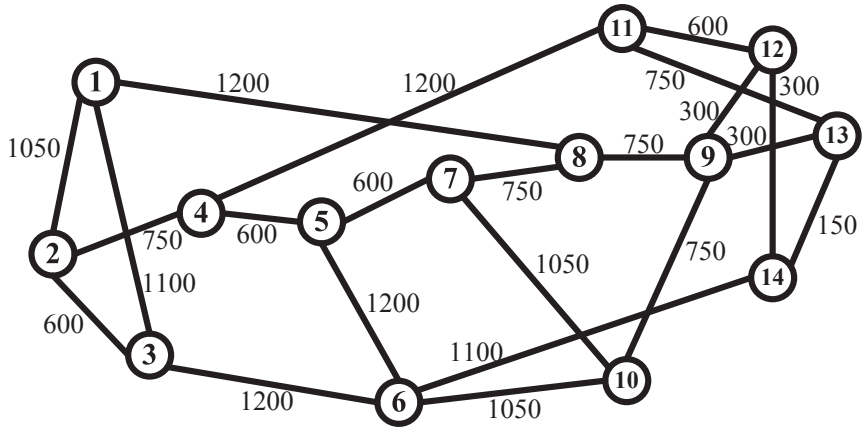

Figure 7.4. 14-node NSFNet (link lengths in km)

From Table 7.2, we can see that when the cost of a RS is low, the total costs obtained by our algorithm are almost the same as those of the ILP. When the cost of a RS is 100, the difference between the total costs of our heuristic algorithm and the ILP becomes bigger, but the difference is only 8.3% on average. Figure 7.5 shows different network equipment's costs under different cost of a RS, when the average node-pair traffic is 600 Gbps. From Figure 7.5, we can see that when the cost of a RS is 100, compared to our heuristic, the ILP

decreases the RS cost while slightly increases the transponder and regenerator costs. This is the reason why ILP outperforms the heuristic when the cost of a RS is high.

Table 7.2. Total cost vs. average traffic (Gbps) between each node pair under different per RS cost

Traffic	Per RS cost = 0.01		Per RS cost = 1		Per RS cost = 100	
	ILP	FG-MC	ILP	FG-MC	ILP	FG-MC
100	768.2	772.4	774.8	777.4	989.5	1080.6
200	1306.2	1319.2	1316.7	1324.1	1544.3	1634.3
300	1712.2	1726.0	1722.0	1730.9	2019.7	2109.5
400	2119.7	2124.6	2127.6	2132.5	2476.9	2837.7
500	2663.4	2669.8	2671.3	2677.8	3034.8	3383.5
600	3201.4	3215.1	3209.3	3223.0	3589.6	3929.3

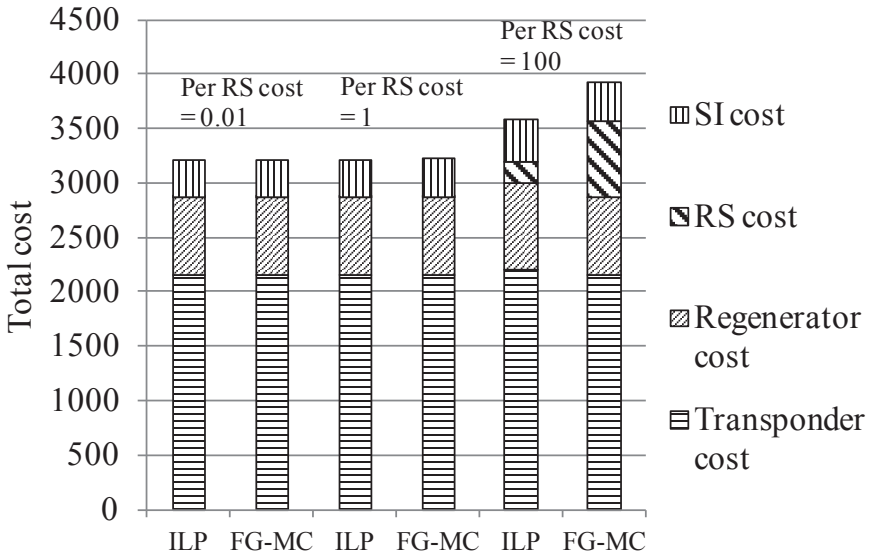

Figure 7.5. Network equipment costs for 14-node network

Experiment 2. In the second experiment, we investigate the performance of our heuristic algorithm under a large-scale network, and study how the total cost changes when the cost of a RS changes. The experiment is conducted on the 75-node CORONET CONUS topology [1]. The average traffic between each node pair is 600 Gbps.

From Figure 7.6, we can see that the FG-MC algorithm has the best performance, while FG-SP has better performance than the SLR-100G and SLR-400G algorithms. When the

cost of a RS is low, since the cost of a regenerator is much higher than that of a RS, FG-MC uses shortest path routing, and thus the performance of FG-MC and FG-SP are very close. However, along with the increase of the RS cost, the total cost obtained by FG-MC increases much slower than the other three approaches. The FG-MC algorithm can concentrate regenerators to form fewer RSs when the RS cost is high. The cost saving is around 22.0% when the cost of a RS is 1000.

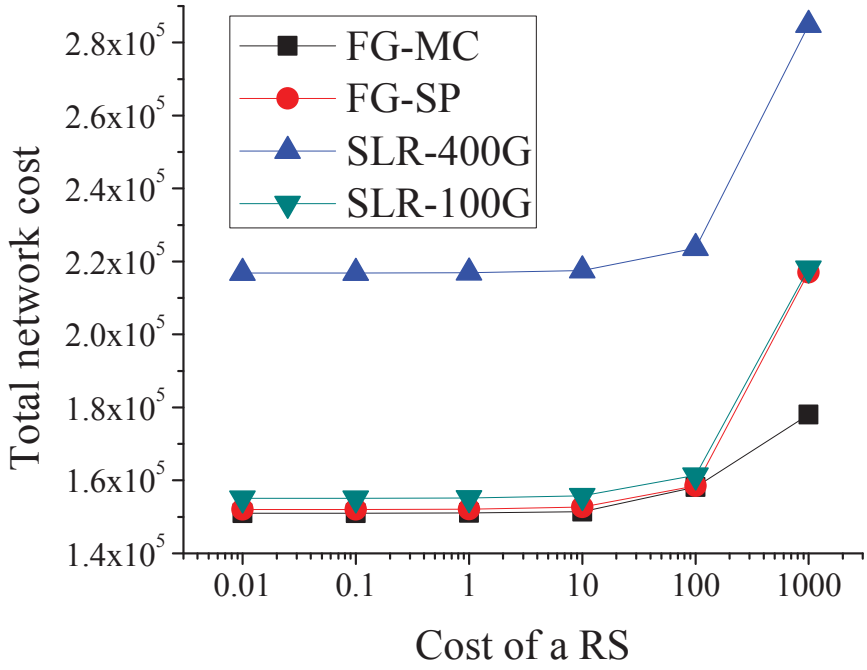

Figure 7.6. Total network cost vs. cost of a RS

Figure 7.7 shows different equipments' costs when the costs of a RS are 1 and 1000, respectively. When the cost of a RS is 1, the cost of RSs is low compared to other costs. The regenerator cost and transponder cost of the FG-MC are almost the same as those of the FG-SP, showing that FG-MC mostly chooses shortest paths under this situation. When the cost of a RS is 1000, FG-MC has a slight increase in the regenerator cost but saves a lot in RS cost compared to the FG-SP, showing that in order to be cost-efficient, the FG-MC selects fewer RSs by slightly increasing the path lengths.

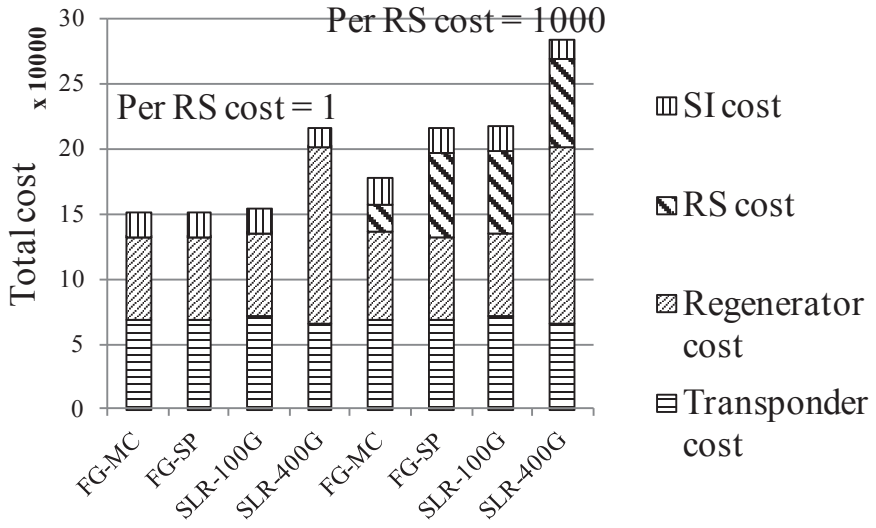

Figure 7.7. Network equipment costs for 75-node network

Experiment 3. In the third experiment, we study the total cost under different network load in a large-scale network. The experiment is conducted on the 75-node CORONET CONUS topology [1]. The average traffic between each node pair ranges from 100 Gbps to 700 Gbps. The cost of a RS is 1000.

Figure 7.8 shows that FG-MC has the best performance. Compared to the FG-SP algorithm, the average saving is around 28.5%. The SLR-400G approach has a stair-stepping increase in the total cost. The reason is that when the average traffic between each node pair increases by 100 Gbps, the 400 Gbps channel may still have vacant space for the increased traffic, thus no additional 400 Gbps channels are needed and the total cost remains the same.

Figure 7.9 shows the spectrum usage of the network under different network load. Each link's spectrum usage is the total occupied channel width on the link times this link's distance. The spectrum usage of the network is the summation of all the links' spectrum usage. We can see that the SLR-400G approach has the least spectrum usage in most cases, since 400 Gbps is more spectrum-efficient than 100 Gbps in high network load. However, considering the extreme high costs as shown in previous figures, the SLR-400G approach is not practical. We can also see that our heuristic only increases the spectrum usage of the

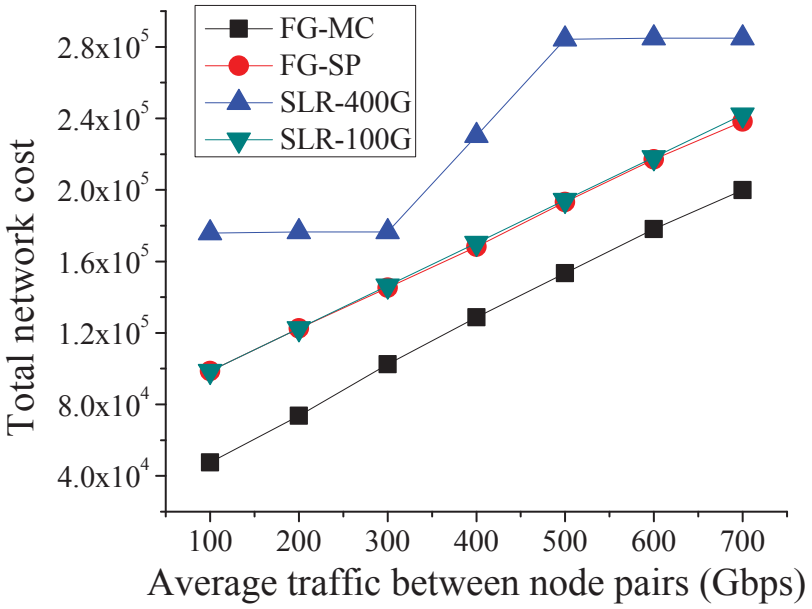

Figure 7.8. Total cost vs. network load

FG-SP algorithm by averagely 7.2%. Thus, our heuristic can save cost while not significantly increasing the spectrum usage.

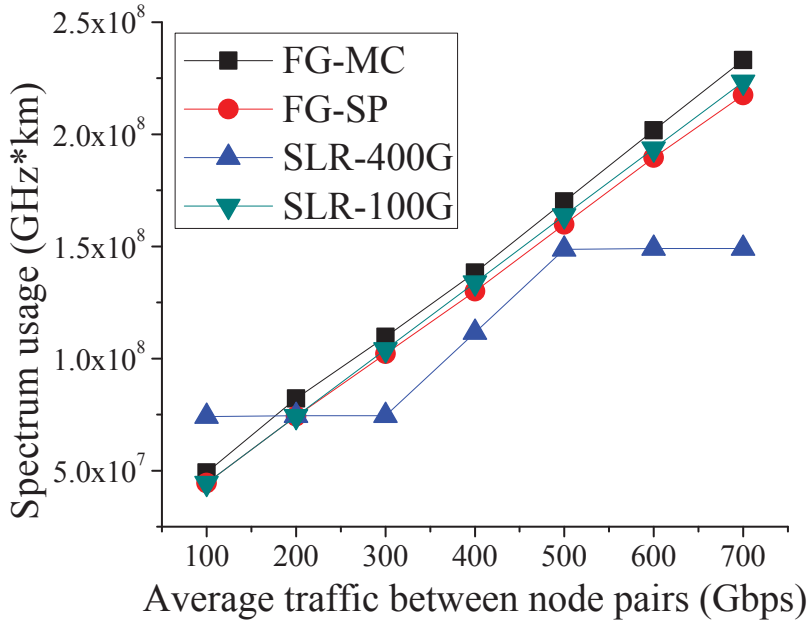

Figure 7.9. Spectrum usage vs. network load

7.6 Conclusion

In this chapter, we focus on the problem of designing a cost-efficient flexible-grid optical network, which aims to minimize the total network cost including transponder cost, regenerator cost, RS cost, and the other shared infrastructure cost. The problem is formulated as an ILP model. We also propose a heuristic approach, named FG-MC, to solve large-scale cases. The numerical results show that the ILP can solve small-scale problems properly and that the total cost obtained by FG-MC is only slightly higher than that of the ILP model. Furthermore, we show that RS selection also plays an important role in designing economical flexible-grid optical networks. Selecting the RSs properly can save up to 28% in total network cost, while the spectrum usage is not significantly increased. One possible area of future work is to consider the problem together with protection.

CHAPTER 8

CONCLUSION

With the emergence of heterogeneous applications, future telecommunication networks are expected to be more heterogeneous in the underlying transmission technologies. In MLR optical networks, different lightpaths can be assigned different line rates according to their bandwidth requirements and reachabilities. Also, traditional fixed-grid optical networks are expected to evolve into flexible-grid optical networks, where optical channels have flexible channel spacing and central frequency. The physical layer impairments impact the signal reachability in both MLR and flexible-grid optical networks, and require regenerator placement to restore the signal quality. In this dissertation, we have studied multiple network design problems with impairment constraints for both MLR and flexible-grid optical networks.

In Chapter 1 and Chapter 2, we introduce the background, motivations, and related papers of our dissertation. In Chapter 3, we focus on the problem of RS selection for MLR optical networks (MLR-RSS), which aims to minimize the number of RSs when routing is given with a request. We show that MLR-RSS is NP-complete, and then formulate an ILP model to solve the problem. Two heuristic algorithms and two approximation algorithms are proposed, named Independent algorithm, Sequential algorithm, MLR-combined algorithm, and Weighted MLR-combined algorithm. The numerical results show the performance comparison of these algorithms and show that the Weighted MLR-combined algorithm outperforms other algorithms. The Weighted MLR-combined algorithm requires not more than one RS than the ILP, showing near optimal performance. It is shown that the MLR approach can save more than 20% compared to using SLR approach for each line rate independently

and then combining them. The RS distribution shows that certain nodes in the network are more likely to be selected as RSs than the other nodes, under both uniform traffic and non-uniform traffic. It suggests a way for selecting RSs, that is, selecting the nodes with high SDPE first, and then adding extra RSs when necessary.

In Chapter 4, we focus on the problems of RS selection for MLR optical networks, when routing is flexible and not given with each connection request. We study two related problems: MLR-RSSFR and MLR-RSSRP. The objective of MLR-RSSFR is to minimize the number of RSs, while the objective of MLR-RSSRP is to minimize the combined cost of RSs and regenerators. The MLR-RSSFR and the MLR-RSSRP problems are shown to be NP-hard, so we formulate the ILP models and develop heuristic approaches to solve the problems. The heuristic approaches follow three steps: ordering of the requests, routing of the requests, and post processing. For the ordering strategies, we invent a novel metric called flexibility to decide which request to be routed first. The numerical results show the performance comparison of these algorithms and show that the heuristic algorithms utilizing the flexibility-based ordering strategy outperform the other heuristic algorithms in both MLR-RSSFR and MLR-RSSRP. The performance of our heuristic approaches are close to that of ILP, showing near-optimal performance. The results also shows that, by selecting a set of RSs wisely, we can save around 20% cost in RSs and regenerators.

In Chapter 5, we focus on the energy-efficient impairment-constrained regenerator placement (EIRP) problem, which aims to minimize the total energy consumption in the optical network with mixed line rates. We show that EIRP is NP-complete, and then formulate an ILP model for it. We also propose two heuristic approaches, named HLRF and RO, to solve large scale cases. The numerical results show that the ILP can solve small scale problems properly and that the energy consumption obtained by HLRF is only slightly higher than the lower bound and the ILP model. The numerical results also demonstrate that HLRF outperforms RO, in terms of energy efficiency. One possible area of future work is to consider

the EIRP problem in flexible-grid optical networks, where the spectrum amount is not only determined by the line rates, but also determined by the modulation formats, making the problem more complex.

In Chapter 6, we focus on the problem of survivable impairment-constrained virtual optical network mapping in flexible-grid optical networks (SIC-VONM), which aims to minimize the combined cost of working and backup optical network equipment, which include transponders, regenerators, and shared infrastructure. An ILP is formulated for SIC-VONM. We also propose a three-step heuristic algorithm MC-SVONM to solve large scale cases, and compare it with a baseline algorithm and a lower bound. The numerical results show that the ILP can solve small scale problems properly and that the total cost obtained by our heuristic algorithm is very close to that of the ILP model. Also, MC-SVONM achieves results that are only slightly higher than the lower bound, showing near-optimal performance. The comparison of MC-SVONM with the baseline algorithm shows that our novel mapping strategy leads to lower cost. One possible area of future research work is to consider the survivable impairment-aware VON mapping problem in flexible-grid optical networks with shared protection. While dedicated protection enables fast switching from primary path to backup path, shared protection is more efficient in resources.

In Chapter 7, we focus on the problem of designing a cost-efficient flexible-grid optical network, which aims to minimize the total network cost including transponder cost, regenerator cost, RS cost, and the other shared infrastructure cost. The problem is formulated as an ILP model. We also propose a heuristic approach, named FG-MC, to solve large-scale cases. The numerical results show that the ILP can solve small-scale problems properly and that the total cost obtained by FG-MC is only slightly higher than that of the ILP model. Furthermore, we show that RS selection also plays an important role in designing economical flexible-grid optical networks. Selecting the RSs properly can save up to 28% in total network cost, while the spectrum usage is not significantly increased. One possible

area of future work is to consider the problem together with protection, since survivability is an important issue in optical networks.

REFERENCES

[1] "DARPA CORONET Program on Dynamic Multi-Terabit Core Optical Networks, Sample Optical Network Topology Files," http://www.monarchna.com/topology.html.

[2] "Internet2, ESnet Complete First Transcontinental 100G Network Deployment," http://www.internet2.edu/news/pr/2011.10.11.100G.html, Oct. 2011.

[3] D. Qian, M.-F. Huang, E. Ip, Y.-K. Huang, Y. Shao, J. Hu, and T. Wang, "101.7-Tb/s PDM-128 QAM-OFDM Transmission over 3x55-km SSMF using Pilot-based Phase Noise Mitigation," in *Proceedings, Optical Fiber Communication Conference (OFC)*, Los Angeles, CA, March 2011.

[4] K. Christodoulopoulos, K. Manousakis, and E. Varvarigos, "Reach Adapting Algorithms for Mixed Line Rate WDM Transport Networks," *IEEE/OSA Journal of Lightwave Technology*, vol. 29, no. 21, pp. 3350–3363, Nov. 2011.

[5] A. Nag, M. Tornatore, and B. Mukherjee, "Optical Network Design with Mixed Line Rates and Multiple Modulation Formats," *IEEE/OSA Journal of Lightwave Technology*, vol. 28, no. 4, pp. 466–475, 2010.

[6] A. Nag and M. Tornatore, "Transparent Optical Network Design with Mixed Line Rates," in *Proceedings, International Conference on Advanced Networks and Telecommunication Systems (ANTS)*, Dec. 2008.

[7] K. Christodoulopoulos, K. Manousakis, and E. Varvarigos, "Adapting the Transmission Reach in Mixed Line Rates WDM Transport Networks," in *Proceedings, International Conference on Optical Network Design and Modeling (ONDM)*, Feb. 2011.

[8] M. Batayneh, D. Schupke, M. Hoffmann, A. Kirstadter, and B. Mukherjee, "Optical Network Design for a Multiline-Rate Carrier-Grade Ethernet Under Transmission-Range Constraints," *IEEE/OSA Journal of Lightwave Technology*, vol. 26, no. 1, pp. 121–130, 2008.

[9] "Spectral grids for WDM applications: DWDM frequency grid," in *ITU-T Recommendation Rec.G.694.1.*

[10] T. Xia, G. A. Wellbrock, Y. K. Huang, E. Ip, M. F. Huang, Y. Shao, T. Wang, Y. Aono, T. Tajima, S. Murakami, and M. Cvijetic, "Field Experiment with Mixed Line-Rate Transmission (112-Gb/s, 450-Gb/s, and 1.15-Tb/s) over 3,560 km of Installed Fiber Using Filterless Coherent Receiver and EDFAs Only," in *Proceedings, Optical Fiber Communication Conference (OFC)*, 2011.

[11] M. Jinno, H. Takara, B. Kozicki, Y. Tsukishima, Y. Sone, and S. Matsuoka, "Spectrum-Efficient and Scalable Elastic Optical Path Network: Architecture, Benefits, and Enabling Technologies," *IEEE Communications Magazine*, vol. 47, no. 11, pp. 66–73, Nov. 2009.

[12] M. Jinno, B. Kozicki, H. Takara, A. Watanabe, Y. Sone, T. Tanaka, and A. Hirano, "Distance-adaptive spectrum resource allocation in spectrum-sliced elastic optical path network," *IEEE Communications Magazine*, vol. 48, pp. 138–145, 2010.

[13] M. Jinno, T. Ohara, Y. Sone, A. Hirano, O. Ishida, and M. Tomizawa, "Elastic and Adaptive Optical Networks: Possible Adoption Scenarios and Future Standardization Aspects," *IEEE Communications Magazine*, vol. 49, no. 10, pp. 164–172, 2011.

[14] O. Gerstel, M. Jinno, A. Lord, and S. Yoo, "Elastic Optical Networking: A New Dawn for the Optical Layer?" *IEEE Communications Magazine*, vol. 50, no. 2, pp. s12 – s20, 2012.

[15] G. Zhang, M. Leenheer, A. Morea, and B. Mukherjee, "A Survey on OFDM-Based Elastic Core Optical Networking," *IEEE Communications Surveys and Tutorials*, vol. 15, no. 1, pp. 65–87, 2013.

[16] M. Jinno, H. Takara, Y. Sone, K. Yonenaga, and A. Hirano, "Multiflow Optical Transponder for Efficient Multilayer Optical Networking," *IEEE Communications Magazine*, vol. 53, no. 7, pp. 926–944, May 2009.

[17] F. Chang and M. Salmanian, "Routing Requirements in Photonic Networks," in *Proceedings, Optical Fiber Communication Conference (OFC)*, 2003.

[18] S. Azodolmolky, M. Klinkowski, E. Marin, D. Careglio, J. Pareta, and I. Tomkos, "A Survey on Physical Layer Impairments Aware Routing and Wavelength Assignment Algorithms in Optical Networks," *The International Journal of Computer and Telecommunications Networking*, vol. 50, no. 5, pp. 56–65, 2012.

[19] C. Saradhi and S. Subramaniam, "Physical Layer Impairment Aware Routing (PLIAR) In WDM Optical Networks: Issues and Challenges," *IEEE Communications Surveys and Tutorials*, vol. 11, pp. 109–130, 2009.

[20] S. Woodward, M. Feuer, I. Kim, P. Palacharla, X. Wang, and D. Bihon, "Service Velocity: Rapid Provisioning Strategies in Optical ROADM Networks," *IEEE/OSA Journal of Optical Communications and Networking*, vol. 4, no. 2, pp. 92–98, 2012.

[21] M. Feuer, S. Woodward, I. Kim, P. Palacharla, X. Wang, D. Bihon, B. Bathula, W. Zhang, R. Sinha, G. Li, and A. Chiu, "Simulations of a Service Velocity Network Employing Regenerator Site Concentration," in *Proceedings, Optical Fiber Communication Conference (OFC)*, 2012.

[22] N. Chowdhury and R. Boutaba, "A Survey of Network Virtualization," *Elsevier Computer Networks*, vol. 54, no. 5, pp. 862–876, Apr. 2010.

[23] ——, "Network virtualization: state of the art and research challenges," *IEEE Communications Magazine*, vol. 47, no. 7, pp. 20–26, 2009.

[24] A. Belbekkouche, M. M. Hasan, and A. Karmouch, "Resource Discovery and Allocation in Network Virtualization," *IEEE Communications Surveys and Tutorials*, vol. 14, no. 4, pp. 1114–1128, Feb. 2012.

[25] R. Nejabati, E. Escalona, S. Peng, and D. Simeonidou, "Optical Network Virtualization," in *Proceedings, International Conference on Optical Network Design and Modeling (ONDM)*, Feb. 2011.

[26] J. Elbers and A. Autenrieth, "Extending Network Virtualization into the Optical Domain," in *Proceedings, Optical Fiber Communication Conference (OFC)*, 2013, pp. 1–3.

[27] N. McKeown, T. Anderson, H. Balakrishnan, G. Parulkar, L. Peterson, J. Rexford, S. Shenker, and J. Turner, "OpenFlow: Enabling Innovation in Campus Networks," in *ACM SIGCOMM Computer Communication Review*, vol. 38, no. 2, 2008, pp. 69–74.

[28] S. Azodolmolky, R. Nejabati, S. Peng, A. Hammad, M. Channegowda, N. Efstathiou, A. Autenrieth, P. Kaczmarek, and D. Simeonidou, "Optical FlowVisor: An OpenFlow-based Optical Network Virtualization Approach," *Proceedings, Optical Fiber Communication Conference (OFC)*, 2012.

[29] "OpenFlow Switch Specification Version 1.4.0," https://www.opennetworking.org/images/stories/downloads/sdn-resources/onf-specifications/openflow/openflow-spec-v1.4.0.pdf, Oct. 2013.

[30] "Software-Defined Networking: The New Norm for Networks," https://www.opennetworking.org/images/stories/downloads/sdn-resources/white-papers/wp-sdn-newnorm.pdf, Apr. 2012.

[31] M. Flammini, A. Marchetti-Spaccamela, G. Monaco, L. Moscardelli, and S. Zaks, "On the Complexity of the Regenerator Placement Problem in Optical Networks," *IEEE/ACM Transactions on Networking*, vol. 19, no. 2, Apr. 2011.

[32] L. Chiaraviglio, M. Mellia, and F. Neri, "Reducing Power Consumption in Backbone Networks," in *Proceedings, IEEE International Conference on Communications (ICC)*, 2009.

[33] S. Nedevschi, L. Popa, G. Iannaccone, S. Ratnasamy, and D. Wetherall, "Reducing Network Power Consumption via Sleeping and Rate-adaptation," in *Proceedings of the 5th USENIX Symposium on Networked Systems Design and Implementation (NSDI)*, 2008.

[34] G. Mertzios, I. Sau, M. Shalom, and S. Zaks, "Placing Regenerators in Optical Networks to Satisfy Multiple Sets of Requests," *IEEE/ACM Transactions on Networking*, vol. 20, no. 6, pp. 1870–1879, 2012.

[35] S. Pachnicke, T. Paschenda, and P. M. Krummrich, "Physical Impairment based Regenerator Placement and Routing in Translucent Optical Networks," in *Proceedings, Optical Fiber Communication Conference (OFC)*, 2008, pp. 1–3.

[36] X. Yang and B. Ramamurthyn, "Sparse Regeneration in Translucent Wavelength-routed Optical Networks: Architecture, Network design and Wavelength Routing," *Photonic Network Communications*, vol. 10, no. 1, pp. 39–53, 2005.

[37] Y. Zhu, X. Gao, W. Wu, and J. Jue, "Efficient Impairment-Constrained 3R Regenerator Placement for Light-Trees in Optical Networks," *IEEE/OSA Journal of Optical Communications and Networking*, vol. 3, no. 4, pp. 359–371, Apr. 2011.

[38] G. Shen, Y. Shen, and H. Sardesai, "Impairment-Aware Lightpath Routing and Regenerator Placement in Optical Transport Networks With Physical-Layer Heterogeneity," *IEEE/OSA Journal of Lightwave Technology*, vol. 29, no. 18, pp. 2853–2860, Sept. 2011.

[39] C. Gao, H. Cankaya, A. Patel, J. Jue, X. Wang, Q. Zhang, P. Palacharla, and M. Sekiya, "Survivable Impairment-Aware Traffic Grooming and Regenerator Placement With Connection-Level Protection," *IEEE/OSA Journal of Optical Communications and Networking*, vol. 4, no. 3, pp. 259–270, Mar. 2012.

[40] W. Xie, Y. Zhu, and J. Jue, "Energy-Efficient Impairment-Constrained 3R Regenerator Placement in Optical Networks," in *Proceedings, Optical Fiber Communication Conference (OFC)*, Jun. 2012, pp. 3020–3024.

[41] Z. Zhu, X. Chen, F. Ji, L. Zhang, F. Farahmand, and J. Jue, "Energy-Efficient Translucent Optical Transport Networks With Mixed Regenerator Placement," *IEEE/OSA Journal of Lightwave Technology*, vol. 30, no. 19, pp. 3147–3156, Oct. 2012.

[42] X. Chen, F. Ji, Y. Wu, and Z. Zhu, "Energy-Efficient Resilience in Translucent Optical Networks With Mixed Regenerator Placement," *IEEE/OSA Journal of Optical Communications and Networking*, vol. 5, no. 7, pp. 741–750, Jul. 2013.

[43] A. Patel, P. Ji, A. Nag, Y. Huang, E. Ip, R. Chandrasekaran, and J. Jue, "Optimal Placement of Combined 2R/3R Regenerators in WDM Networks," in *Proceedings, OptoElectronics and Communications Conference (OECC)*, Jul. 2012, pp. 2348–2352.

[44] S. Chen, I. Ljubic, and S. Raghavan, "The regenerator location problem," *Networks*, vol. 55, no. 3, pp. 205–220, May 2010.

[45] B. Bathula, R. Sinha, A. Chiu, M. Feuer, G. Li, S. Woodward, W. Zhang, K. Bergman, I. Kim, and P. Palacharla, "On Concentrating Regenerator Sites in ROADM Networks," in *Proceedings, Optical Fiber Communication Conference (OFC)*, 2012.

[46] B. Bathula, R. Sinha, A. Chiu, M. Feuer, G. Li, S. Woodward, W. Zhang, R. Doverspike, P. Magill, and K. Bergman, "Cost Optimization Using Regenerator Site Concentration and Routing in ROADM Networks," in *Proceedings, International Conference on Design of Reliable Communication Networks (DRCN)*, March 2013, pp. 154–162.

[47] C. V. Saradhi, R. Fedrizzi, A. Zanardi, E. Salvadori, G. M. Galimberti, A. Tanzi, G. Martinelli, and O. Gerstel, "Traffic independent heuristics for regenerator site selection for providing any-to-any optical connectivity," in *Proceedings, Optical Fiber Communication Conference (OFC)*, 2010.

[48] C. V. Saradhi, A. Zanardi, R. Fedrizzi, E. Salvadori, G. M. Galimberti, A. Tanzi, G. Martinelli, and O. Gerstel, "A Framework for Regenerator Site Selection Based on Multiple Paths," in *Proceedings, Optical Fiber Communication Conference (OFC)*, 2010.

[49] C. V. Saradhi, R. Fedrizzi, A. Zanardi, E. Salvadori, G. M. Galimberti, A. Tanzi, G. Martinelli, and O. Gerstel, "Regenerator Sites Selection based on Multiple Paths Considering Impairments and Protection Requirements," in *Proceedings, European Conference on Networks and Optical Communications (NOC)*, 2011, pp. 84–87.

[50] M. Youssef, S. Zahr, and M. Gagnaire, "Traffic-Driven vs. Topology-Driven Strategies for Regeneration Sites Placement," in *Proceedings, IEEE International Conference on Communications (ICC)*, 2010.

[51] ——, "Cross Optimization for RWA and Regenerator Placement in Translucent WDM Networks," in *Proceedings, International Conference on Optical Network Design and Modeling (ONDM)*, 2010, pp. 1–6.

[52] S. Varma and J. Jue, "Regenerator Site Selection in Mixed Line Rate Waveband Optical Networks," *IEEE/OSA Journal of Optical Communications and Networking*, vol. 5, no. 3, pp. 198–209, 2013.

[53] F. Idziowski, S. Orlowski, C. Raack, H. Woesner, and A. Wolisz, "Saving Energy in IP-over-WDM Networks by Switching Off Line Cards in Low-Demand Scenarios," in *Proceedings, International Conference on Optical Network Design and Modeling (ONDM)*, 2010, pp. 1–6.

[54] C. Lange and A. Gladisch, "Energy Efficiency Limits of Load Adaptive Networks," in *Proceedings, Optical Fiber Communication Conference (OFC)*, Mar. 2010.

[55] Y. Wu, L. Chiaraviglio, M. Mellia, and F. Neri, "Power-Aware Routing and Wavelength Assignment in Optical Networks," in *Proceedings, European Conference and Exhibition on Optical Communication (ECOC)*, Sept. 2009.

[56] L. Chiaraviglio, M. Mellia, and F. Neri, "Energy-aware Backbone Networks: a Case Study," in *IEEE International Workshop on Green Communications (GreenComm)*, 2009.

[57] M. M. Hasan, F. Farahmand, A. Patel, and J. P. Jue, "Traffic Grooming in Green Optical Networks," in *Proceedings, IEEE International Conference on Communications (ICC)*, 2010, pp. 1–5.

[58] E. Yetginer and G. N. Rouskas, "Power efficient traffic grooming in optical WDM networks," in *Proceedings, IEEE Globecom*, 2009.

[59] S. Huang, D. Seshadri, and R. Dutta, "Traffic Grooming: a Changing Role in Green Optical Networks," in *Proceedings, IEEE Globecom*, 2009.

[60] G. Shen and R. S. Tucker, "Energy-Minimized Design for IP over WDM networks," *IEEE/OSA Journal of Optical Communications and Networking*, vol. 1, no. 1, pp. 176–186, Jun. 2009.

[61] J. Chabarek, J. Sommers, P. Barford, C. Estan, D. Tsiang, and S. Wright, "Power Awareness in Network Design and Routing," in *Proceedings, IEEE INFOCOM*, 2008.

[62] P. Chowdhury, M. Tornatore, and B. Mukherjee, "On the Energy Efficiency of Mixed-Line-Rate Networks," in *Proceedings, Optical Fiber Communication Conference (OFC)*, Mar. 2010.

[63] F. Musumeci, F. Vismara, V. Grkovic, M. Tornatore, and A. Pattavina, "On the Energy Efficiency of Optical Transport with Time Driven Switching," in *Proceedings, IEEE International Conference on Communications (ICC)*, 2011.

[64] N. Chowdhury, M. Rahman, and R. Boutaba, "Virtual Network Embedding with Coordinated Node and Link Mapping," in *Proceedings, IEEE INFOCOM*, 2009, pp. 783–791.

[65] J. Lischka and H. Karl, "A Virtual Network Mapping Algorithm based on Subgraph Isomorphism Detection," in *Proceedings, ACM Workshop on Virtualized Infrastructure Systems and Architectures (VISA)*, 2009, pp. 81–88.

[66] M. Yu, Y. Yi, J. Rexford, and M. Chiang, "Rethinking Virtual Network Embedding: Substrate Support for Path Splitting and Migration," *ACM SIGCOMM Computer Communication Review*, vol. 38, no. 2, pp. 17–29, 2008.

[67] H. Yu, V. Anand, C. Qiao, and H. Di, "Migration Based Protection for Virtual Infrastructure Survivability for Link Failure," in *Proceedings, Optical Fiber Communication Conference (OFC)*, 2011.

[68] B. Guo, C. Qiao, Y. He, Z. Chen, A. Xu, S. Huang, and H. Yu, "A Novel Virtual Node Migration Approach to Survive a Substrate Link Failure," in *Proceedings, Optical Fiber Communication Conference (OFC)*, 2012.

[69] X. Liu, C. Qiao, and T. Wang, "Robust Application Specific and Agile Private (ASAP) Networks Withstanding Multi-layer Failures," in *Proceedings, Optical Fiber Communication Conference (OFC)*, 2009, pp. 1–3.

[70] H. Yu, C. Qiao, V. Anand, X. Liu, H. Di, and G. Sun, "Survivable Virtual Infrastructure Mapping in a Federated Computing and Networking System under Single Regional Failures," in *Proceedings, IEEE Globecom*, 2010, pp. 1–6.

[71] S. Peng, R. Nejabati, S. Azodolmolky, E. Escalona, and D. Simeonidou, "An Impairment-aware Virtual Optical Network Composition Mechanism for Future Internet," in *Proceedings, European Conference and Exhibition on Optical Communication (ECOC)*, Sept. 2011.

[72] ——, "Virtual Optical Network Composition over Single-Line-Rate and Mixed-Line-Rate WDM Optical Networks," in *Proceedings, Optical Fiber Communication Conference (OFC)*, Mar. 2011.

[73] S. Peng, R. Nejabati, E. Escalona, and D. Simeonidou, "Virtual Optical Network Composition over Mixed-Line-Rate and Multiple-Modulation-Format WDM Networks," in *Proceedings, European Conference and Exhibition on Optical Communication (ECOC)*, Sept. 2012.

[74] A. Pages, J. Perello, and S. Spadaro, "Virtual Network Embedding in Optical Infrastructures," in *Proceedings, International Conference on Transparent Optical Networks*, 2012, pp. 1–4.

[75] A. Pages, J. Perello, S. Spadaro, and G. Junyent, "Strategies for Virtual Optical Network Allocation," *IEEE Communications Letters*, vol. 16, no. 2, pp. 268–271, 2012.

[76] Q. Zhang, W. Xie, Q. She, X. Wang, P. Palacharla, and M. Sekiya, "RWA for Network Virtualization in Optical WDM Networks," in *Proceedings, Optical Fiber Communication Conference (OFC)*, Mar. 2013.

[77] C. Gao and J. Jue, "Virtual Optical Network Embedding Considering Mixed Transparent and Translucent Virtual Links," in *Proceedings, Optical Fiber Communication Conference (OFC)*, 2013, pp. 1–3.

[78] W. Xie, F. Khandaker, J. Jue, Q. Zhang, X. Wang, Q. She, P. Palacharla, and M. Sekiya, "Impairment-Aware Virtual Optical Network Mapping in Mixed-Line-Rate Optical Networks," in *Proceedings, International Workshop on Optical networking (i-WON)*, Dec. 2013.

[79] C. Meixner, F. Dikbiyik, M. Tornatore, C. Chuah, and B. Mukherjee, "Disaster-Resilient Virtual-Network Mapping and Adaptation in Optical Networks," in *Proceedings, International Conference on Optical Network Design and Modeling (ONDM)*, 2013, pp. 107–112.

[80] A. Patel, P. Ji, Y. Huang, and T. Wang, "Distance-adaptive virtual network embedding in software-defined optical networks," in *Proceedings, OptoElectronics and Communications Conference (OECC)*, 2013, p. 1C2.

[81] S. Zhang, L. Shi, C. Vadrevu, and B. Mukherjee, "Network Virtualization over WDM and Flexible-Grid Optical Networks," *Elsevier Optical Switching and Networking (OSN)*, vol. 10, no. 4, pp. 291–300, 2013.

[82] A. Pages, J. Perello, S. Spadaro, J. Garcia-Espin, J. F. Riera, and S. Figuerola, "Optimal allocation of virtual optical networks for the future Internet," in *Proceedings, International Conference on Optical Network Design and Modeling (ONDM)*, Apr. 2012, p. 1C6.

[83] J. Zhao, S. Subramaniam, and M. Brandt-Pearce, "Virtual Topology Mapping in Elastic Optical Networks," in *Proceedings, IEEE International Conference on Communications (ICC)*, Jun. 2013, p. 1C5.

[84] L. Gong, W. Zhao, Y. Wen, and Z. Zhu, "Dynamic transparent virtual network embedding over elastic optical infrastructures," in *Proceedings, IEEE International Conference on Communications (ICC)*, Jun. 2013, p. 1C5.

[85] L. Gong and Z. Zhu, "Virtual Optical Network Embedding (VONE) Over Elastic Optical Networks," *IEEE/OSA Journal of Lightwave Technology*, vol. 32, no. 3, pp. 450–460, Feb. 2014.

[86] Z. Ye, A. Patel, P. Ji, C. Qiao, and T. Wang, "Virtual Infrastructure Embedding over Software-Defined Flex-Grid Optical Networks," in *Proceedings, IEEE Globecom*, Dec. 2013, p. 1C6.

[87] Q. Zhang, Q. She, Y. Zhu, X. Wang, P. Palacharla, and M. Sekiya, "Survivable Resource Orchestration for Optically Interconnected Data Center Networks," in *Proceedings, European Conference and Exhibition on Optical Communication (ECOC)*, 2013, p. 1C3.

[88] K. Christodoulopoulos, I. Tomkos, and E. Varvarigos, "Routing and Spectrum Allocation in OFDM-based Optical Networks with Elastic Bandwidth Allocation," in *Proceedings, IEEE Globecom*, 2010.

[89] A. N. Patel, P. N. Ji, J. P. Jue, and T. Wang, "Routing, Wavelength Assignment, and Spectrum Allocation in Transparent Flexible Optical WDM (FWDM) Networks," in *Proceedings, International Conference on Photonics in Switching*, 2010.

[90] W. Yang, C. Xiaojun, and P. Yi, "A Study of the Routing and Spectrum Allocation in Spectrum-Sliced Elastic Optical Path networks," in *Proceedings, IEEE INFOCOM*, 2011, pp. 1503–1511.

[91] M. Klinkowski and K. Walkowiak, "Routing and Spectrum Assignment in Spectrum Sliced Elastic Optical Path Network," *IEEE Communications Letters*, vol. 15, pp. 884–886, 2011.

[92] Y. Sone, A. Hirano, A. Kadohata, M. Jinno, and O. Ishida, "Routing and Spectrum Assignment Algorithm Maximizes Spectrum Utilization in Optical Networks," in *Proceedings, European Conference and Exhibition on Optical Communication (ECOC)*, 2011.

[93] L. Velasco, M. Klinkowsi, M. Ruiz, and J. Comellas, "Modeling the Routing and Spectrum Allocation Problem for Flexgrid Optical Networks," *Photonic Network Communications*, vol. 24, no. 3, pp. 177–186, Dec. 2012.

[94] Y. Zhao, J. Zhang, X. Shu, J. Wang, and W. Gu, "Routing and Spectrum Assignment (RSA) in OFDM-based Bandwidth-Variable Optical Networks," in *Proceedings, OptoElectronics and Communications Conference (OECC)*, 2011, pp. 543–544.

[95] Y. Wang, J. Zhang, Y. Zhao, J. Wang, and W. Gu, "Routing and Spectrum Assignment by Means of Ant Colony Optimization in Flexible Bandwidth Networks," in *Proceedings, Optical Fiber Communication Conference (OFC)*, 2012, pp. 1–3.

[96] Y. Wang, J. Zhang, Y. Zhao, J. Liu, and W. Gu, "Spectrum Consecutiveness based Routing and Spectrum Allocation in Flexible Bandwidth Networks," *Chinese Optics Letters*, vol. 10, pp. 1–4, 2012.

[97] K. Christodoulopoulos, I. Tomkos, and E. A. Varvarigos, "Elastic Bandwidth Allocation in Flexible OFDM-Based Optical Networks," *IEEE/OSA Journal of Lightwave Technology*, vol. 29, pp. 1354–1366, 2011.

[98] S. Yang and F. Kuipers, "Impairment-Aware Routing in Translucent Spectrum-Sliced Elastic Optical Path Networks," in *Proceedings, European Conference on Networks and Optical Communications (NOC)*, 2012.

[99] A. N. Patel, P. N. Ji, J. P. Jue, and T. Wang, "Dynamic Routing, Wavelength Assignment, and Spectrum Allocation in Transparent Flexible Optical WDM Networks," in *SPIE Optoelectronics and Photonics Conference*, 2011.

[100] X. Wan, L. Wang, N. Hua, H. Zhang, and X. Zheng, "Dynamic Routing and Spectrum Assignment in Flexible Optical Path Networks," in *Proceedings, Optical Fiber Communication Conference (OFC)*, 2011, pp. 1–3.

[101] S. Thiagarajan, M. Frankel, and D. Boertjes, "Spectrum Efficient Super-Channels in Dynamic Flexible Grid Networks - A Blocking Analysis," in *Proceedings, Optical Fiber Communication Conference (OFC)*, 2011, pp. 1–3.

[102] X. Wan, N. Hua, H. Zhang, and X. Zheng, "Study of Dynamic Routing and Spectrum Assignment in Bitrate Flexible Optical Networks," *Photonic Network Communications*, vol. 24, no. 3, pp. 219–227, Dec. 2012.

[103] T. Takagi, H. Hasegawa, K. Sato, Y. Sone, B. Kozicki, A. Hirano, and M. Jinno, "Dynamic routing and frequency slot assignment for elastic optical path networks that adopt distance adaptive modulation," in *Proceedings, Optical Fiber Communication Conference (OFC)*, 2011, pp. 1–3.

[104] N. Sambo and P. Castoldi, "Toward High-Rate and Flexible Optical Networks," *IEEE Communications Magazine*, vol. 50, pp. 66–72, 2012.

[105] A. N. Patel, P. N. Ji, J. P. Jue, and T. Wang, "Survivable transparent Flexible optical WDM (FWDM) networks," in *Proceedings, Optical Fiber Communication Conference (OFC)*, 2011, pp. 1–3.

[106] B. Chen, J. Zhang, Y. Zhao, H. Chen, S. Huang, W. Gu, and J. Jue, "Minimized Spectral Resource Consumption with Rescaled Failure Probability Constraint in Flexible Bandwidth Optical Networks ," in *Proceedings, Optical Fiber Communication Conference (OFC)*, 2013, pp. 1–3.

[107] J. Zhang, B. Chen, Y. Zhao, H. Chen, W. Zhang, X. Li, J. P. Jue, S. Huang, and W. Gu, "Minimized Spectrum Resource Consumption with Rescaled Failure Probability Constraint in Flexible Bandwidth Optical Networks," *IEEE/OSA Journal of Optical Communications and Networking*, vol. 5, no. 9, pp. 980–993, Sept. 2013.

[108] A. N. Patel, P. N. Ji, J. P. Jue, and T. Wang, "First Shared Path Protection Scheme for Generalized Network Connectivity in Gridless Optical WDM Networks," 2010.

[109] A. Eira, J. Pedro, and J. Pires, "Optimized Design of Shared Restoration in Flexible-Grid Transparent Optical Networks," in *Proceedings, Optical Fiber Communication Conference (OFC)*, 2011.

[110] A. Eira, J. Santos, J. Pedro, and J. Pires, "Design of Survivable Flexible-Grid DWDM Networks with Joint Minimization of Transponder Cost and Spectrum Usage," in *Proceedings, European Conference and Exhibition on Optical Communication (ECOC)*, Sept. 2012.

[111] B. Chen, J. Zhang, Y. Zhao, C. Lv, W. Zhang, Y. Gu, S. Huang, and W. Gu, "A Novel Recovery Algorithm for Multi-link Failures in Spectrum-Elastic Optical Path Networks ," 2011.

[112] Y. Sone, A. Watanabe, W. Imajuku, Y. Tsukishima, B. Kozicki, H. Takara, and M. Jinno, "Bandwidth Squeezed Restroration in Spectrum-Sliced Elastic Optical Path Networks (SLICE)," *IEEE/OSA Journal of Optical Communications and Networking*, vol. 3, pp. 223–233, 2011.

[113] B. Chen, J. Zhang, Y. Zhao, C. Lv, W. Zhang, S. Huang, X. Zhang, and W. Gu, "Multi-link failure restoration with dynamic load balancing in spectrum-elastic optical path networks," *Elsevier Optical Switching and Networking (OSN)*, vol. 18, no. 1, pp. 21–28, Jan. 2012.

[114] Y. Zhang, X. Zheng, Q. Li, N. Hua, Y. Li, and H. Zhang, "Traffic grooming in Spectrum-Elastic Optical Path Networks," in *Proceedings, Optical Fiber Communication Conference (OFC)*, 2011, pp. 1–3.

[115] A. N. Patel, P. N. Ji, J. P. Jue, and T. Wang, "Traffic grooming in flexible optical WDM (FWDM) networks," in *Proceedings, OptoElectronics and Communications Conference (OECC)*, 2011, pp. 405–406.

[116] M. Liu, M. Tornatore, and B. Mukherjee, "Survivable Traffic Grooming in Elastic Optical Networks - Shared Path Protection," in *Proceedings, IEEE International Conference on Communications (ICC)*, 2012.

[117] P. N. Ji, A. N. Patel, D. Qian, J. P. Jue, J. Hu, Y. Aono, and T. Wang, "Optical-Layer Traffic Grooming in Flexible Optical WDM (FWDM) Networks," in *Proceedings, European Conference and Exhibition on Optical Communication (ECOC)*, 2011.

[118] A. N. Patel, P. N. Ji, T. Wang, and J. P. Jue, "Optical-Layer Traffic Grooming in Fleixible Grid WDM Networks," in *Proceedings, IEEE Globecom*, 2011.

[119] G. Zhang, M. D. Leenheer, and B. Mukherjee, "Optical Traffic Grooming in OFDM-Based Elastic Optical Networks," *IEEE/OSA Journal of Optical Communications and Networking*, vol. 4, pp. 17–25, Nov. 2012.

[120] S. Zhang, M. Tornatore, G. Shen, and B. Mukherjee, "Evolution of Traffic Grooming from SDH/SONET to Flexible Grid," in *Proceedings, European Conference and Exhibition on Optical Communication (ECOC)*, 2013.

[121] S. Zhang, M. Tornatore, G. Shen, J. Zhang, and B. Mukherjee, "Evolving Traffic Grooming in Multi-Layer Flexible-Grid Optical Networks with Software-Defined Elasticity," *IEEE/OSA Journal of Lightwave Technology*, accepted for publication.

[122] V. Chvatal, "A greedy heuristic for the set-covering problem," *Mathematics of Operations Research*, vol. 4, no. 3, pp. 233–235, 1979.

[123] "Cisco 40-Channel Single-Module ROADM," http://www.cisco.com.

[124] X. Zhou, L. Nelson, and P. Magill, "Rate-adaptable Optics for Next Generation Long-haul Transport Networks," *IEEE Communications Magazine*, vol. 51, no. 3, pp. 41–49, Mar. 2013.

[125] J. W. Suurballe and R. E. Tarjan, "A Quick Method for Finding Shortest Pairs of Disjoint Paths," *Networks*, vol. 14, no. 2, pp. 325–336, 1984.

VITA

Weisheng Xie graduated from Beijing University of Posts and Telecommunications (BUPT) in 2010 with a Bachelor of Engineering degree in Information Engineering. He started his Ph.D. study in Telecommunications Engineering (TE) at The University of Texas at Dallas (UTD) from Fall 2010. He was a teaching assistant from Fall 2010 to Fall 2012, and he has been a research assistant thereafter. During Summer 2012, he was a full-time Research Intern with Fujitsu Laboratories of America, Richardson, TX. His work there yielded one published paper and one filed USA patent. During Summer 2013 and Fall 2013, he was a Research Intern at Huawei, Santa Clara, CA, where he produced three papers and two USA patent applications. He is a student member of IEEE. His research areas include impairment-constrained optical network design, software-defined networking (SDN), and network virtualization.

Publications Related to the Dissertation

(Journals)

1. **W. Xie**, J. Jue, X. Wang, Q. Zhang, Q. She, P. Palacharla, and M. Sekiya, "Regenerator Site Selection for Mixed Line Rate Optical Networks," IEEE/OSA Journal of Optical Communications and Networking (JOCN), Vol. 6, No. 3, pp. 291-302, March 2014.

2. **W. Xie**, J. Jue, X. Wang, Q. Zhang, Q. She, P. Palacharla, and M. Sekiya, "Regenerator Site Selection for Mixed Line Rate Optical Networks with Flexible Routing," IEEE/OSA Journal of Optical Communications and Networking (JOCN), under review, 2014.

3. **W. Xie**, J. Jue, Q. Zhang, X. Wang, Q. She, P. Palacharla, and M. Sekiya, "Survivable Impairment-Aware Virtual Optical Network Mapping in Flexible-Grid Optical Networks,"

IEEE/OSA Journal of Optical Communications and Networking (JOCN), under review, 2014.

(Conferences)

4. **W. Xie**, J. Jue, Q. Zhang, X. Wang, Q. She, P. Palacharla, and M. Sekiya, "Survivable Virtual Optical Network Mapping in Flexible-Grid Optical Networks," **(Invited paper)**, IEEE International Conference on Computing, Networking and Communications (ICNC), Honolulu, HI, Feb. 2014.

5. **W. Xie**, J. Jue, X. Wang, Q. Zhang, Q. She, P. Palacharla, and M. Sekiya, "Cost-Optimized Design of Flexible-Grid Optical Networks Considering Regenerator Site Selection," IEEE Global Communications Conference (GLOBECOM), Atlanta, GA, Dec. 2013.

6. **W. Xie**, F. Khandaker, J. Jue, Q. Zhang, X. Wang, Q. She, P. Palacharla, and M. Sekiya, "Impairment-Aware Virtual Optical Network Mapping in Mixed-Line-Rate Optical Networks," International Workshop on Optical networking (iWON), Atlanta, GA, Dec. 2013.

7. **W. Xie**, J. Jue, X. Wang, Q. Zhang, Q. She, P. Palacharla, and M. Sekiya, "Regenerator Site Selection and Regenerator Placement for Mixed Line Rate Optical Networks," IEEE International Conference on Computing, Networking and Communications (ICNC), San Diego, CA, Jan. 2013.

8. **W. Xie**, J. Jue, X. Wang, Q. Zhang, Q. She, P. Palacharla, and M. Sekiya, "Regenerator Pool Site Selection for Mixed Line Rate Optical Networks," IEEE International Conference on Communications (ICC), Ottawa, Canada, Jun. 2012.

9. **W. Xie**, Y. Zhu, and J. Jue, "Energy-Efficient Impairment-Constrained 3R Regenerator Placement in Optical Networks," IEEE International Conference on Communications (ICC), Ottawa, Canada, Jun. 2012.

10. **W. Xie**, J. Jue, X. Wang, Q. Zhang, Q. She, P. Palacharla, and M. Sekiya, "Regenerator Site Selection for Mixed Line Rate Optical Networks with Flexible Routing," International

Conference on Optical Networking Design and Modeling (ONDM), Colchester, UK, Apr. 2012.

Publications Not Related to the Dissertation

(Conferences)

1. **W. Xie**, J. Zhu, C. Huang, M. Luo, and W. Chou, "Network Virtualization with Dynamic Resource Pooling and Trading Mechanism," IEEE Global Communications Conference (GLOBECOM), accepted, 2014.

2. **W. Xie**, J. Zhu, C. Huang, M. Luo, and W. Chou, "Dynamic Resource Pooling and Trading Mechanism in Flexible-Grid Optical Network Virtualization," IEEE International Conference on Cloud Networking (CloudNet), under review, 2014.

3. B. Chen, **W. Xie**, J. Zhang, J. Jue, Y. Zhao, S. Huang, and W. Gu, "Energy and Spectrum Efficiency with Multi-Flow Transponders and Elastic Regenerators in Survivable Flexible Bandwidth Virtual Optical Networks," IEEE/OSA Optical Fiber Communication Conference (OFC), San Francisco, CA, Mar. 2014.

4. J. Zhu, **W. Xie**, L. Li, M. Luo, and W. Chou, "Software Service Defined Network: Centralized Network Information Service," IEEE Software Defined Networks for Future Networks and Services (SDN4FNS), Trento, Italy, Nov. 2013.

5. Q. Zhang, **W. Xie**, Q. She, X. Wang, P. Palacharla, and M. Sekiya, "RWA for Network Virtualization in Optical WDM Networks," IEEE/OSA Optical Fiber Communication Conference (OFC), Anaheim, CA, Mar. 2013.